
TESI DI DOTTORATO

GIOVANNI SCILLA

Variational motion of discrete interfaces

Dottorato in Matematica, Roma «La Sapienza» (2013).

<http://www.bdim.eu/item?id=tesi_2013_ScillaGiovanni_1>

L'utilizzo e la stampa di questo documento digitale è consentito liberamente per motivi di ricerca e studio. Non è consentito l'utilizzo dello stesso per motivi commerciali. Tutte le copie di questo documento devono riportare questo avvertimento.



SAPIENZA
UNIVERSITÀ DI ROMA

Variational motion of discrete interfaces

Scuola di dottorato Vito Volterra

Dottorato di Ricerca in Matematica – XXVI Ciclo

Candidate

Giovanni Scilla

ID number 1378175

Thesis Advisor

Prof. Andrea Braides

A thesis submitted in partial fulfillment of the requirements
for the degree of Doctor of Philosophy in Mathematics

October 2013

Thesis not yet defended

Variational motion of discrete interfaces

Ph.D. thesis. Sapienza – University of Rome

© 2013 Giovanni Scilla. All rights reserved

This thesis has been typeset by \LaTeX and the Sapthesis class.

Author's email: scilla@mat.uniroma1.it

Dedicated to my family

Contents

Introduction	vii
1 Preliminaries	1
1.1 Γ -convergence	1
1.2 Convergence of sets	2
1.3 Functions of bounded variation and sets of finite perimeter	3
2 Minimizing movements along a sequence of functionals	5
2.1 Minimizing movements: definition and basic properties	5
2.2 Minimizing movements along a sequence	7
2.3 Commutability along ‘fast-converging’ sequences	9
2.4 Homogenization of minimizing movements	10
2.5 A scaling of the energies is a time-scaling	14
2.6 Negative scaling and discrete approximation: backward motions	14
3 Geometric minimizing movements	17
3.1 Motion by mean curvature	17
3.2 A variational approach to curvature-driven motion	18
3.3 Motion by crystalline curvature	19
4 Motion of discrete interfaces in homogeneous media	23
4.1 Lattice energies as interfacial energies	23
4.2 Homogeneous ferromagnetic energies on discrete sets	24
4.3 A discrete-in-time minimization scheme	25
4.4 Motion of a rectangle	27
4.5 Motion of a polyrectangle	30
5 Motion of discrete interfaces in ‘high-contrast’ periodic media	33
5.1 Motivation and survey of the main results	33
5.2 Inhomogeneous ferromagnetic energies on discrete sets	34
5.3 Motion of a rectangle	36
5.3.1 A new pinning threshold	44
5.3.2 Definition of the effective velocity	45
5.3.3 Description of the homogenized limit motion.	49
5.4 Computation of the velocity function	50
5.4.1 The case $N_\beta = 1$	51
5.4.2 The case $N_\beta = 2$	53

6	Motion of discrete interfaces in ‘low-contrast’ periodic media	55
6.1	Motivation and results	55
6.2	Inhomogeneous ‘low-contrast’ ferromagnetic energies	57
6.3	Motion of a rectangle	58
6.3.1	Definition of the effective velocity	61
6.3.2	The effective pinning threshold	65
6.3.3	Computation of the velocity function	66
6.3.4	Description of the homogenized limit motion	68
6.4	The periodic case with K contrast parameters	69
6.4.1	The pinning threshold	70
6.4.2	The effective velocity function	71
6.4.3	Computation of the velocity function	72
7	Nucleation and backward motion of discrete interfaces	73
7.1	The crystalline case: motivation	73
7.2	A simple example: the ℓ^∞ -distance	74
7.3	Setting of the problem	77
7.4	The general case	79
7.4.1	The nucleation threshold	79
7.4.2	Discrete nucleation	81
7.4.3	The limit motion	83
7.5	Some examples of nucleation	84
7.5.1	The ℓ^1 -distance	85
7.5.2	An example of asymmetric distance	86
A	Variational problems with percolation: rigid spin systems	89
A.1	The model problem and the percolation approach	89
A.2	Notation and setting of the problem	92
A.3	Some results from percolation theory	93
A.4	The rigid percolation theorem	96
A.5	A continuity result	102
	Bibliography	109

Introduction

Geometric variational evolutions, in particular curvature-based motions, may be studied using an implicit-time scheme proposed by Almgren, Taylor and Wang [3]. Following the formal consideration that curvature can be seen as the variation of the perimeter, they defined a time-discrete trajectory E_k^τ , where τ is a time step, E_0^τ is an initial set and E_k^τ is a minimizer of

$$\min \left\{ P(E) + \frac{1}{\tau} \int_{E \Delta E_{k-1}^\tau} \text{dist}(x, \partial E_{k-1}^\tau) dx \right\}, \quad (1)$$

where P is the Euclidean perimeter and $\text{dist}(\cdot, \partial F)$ is the Euclidean distance from the boundary of F . We can read (1) as follows: the set E_k^τ “contracts” by minimizing the perimeter subject to a penalization of its “distance” from E_{k-1}^τ . After defining $E^\tau(t) = E_{\lfloor t/\tau \rfloor}^\tau$ for all $t \geq 0$, a suitable limit as $\tau \rightarrow 0$ of these time-discrete trajectories gives motion by mean curvature (Sections 3.1 and 3.2). Note that this scheme can be framed in the setting of *minimizing movements* (Section 2.1), after the identification of a set E with its characteristic function $u = \chi_E$ and by considering perimeter type energies (see Chapter 3).

The same scheme can be repeated taking P the crystalline perimeter

$$P^\alpha(E) = \alpha \int_{\partial^* E} \|\nu\|_1 d\mathcal{H}^1, \quad \alpha > 0 \quad (2)$$

to obtain *motion by crystalline curvature* in dimension two, as described by Almgren and Taylor [2].

In the case of initial datum a coordinate rectangle of side lengths L_1^0 and L_2^0 , the evolution by crystalline curvature is a rectangle with the same centre and sides of lengths $L_1(t), L_2(t)$ governed by the system of ordinary differential equations

$$\begin{cases} \dot{L}_1(t) = -\frac{4\alpha}{L_2(t)} \\ \dot{L}_2(t) = -\frac{4\alpha}{L_1(t)} \end{cases} \quad (3)$$

with $L_1(0) = L_1^0$ and $L_2(0) = L_2^0$ (see Section 3.3). This means that each side of the rectangle moves inwards with velocity equal to twice its crystalline curvature (i.e., the inverse of its length), so that the other side contracts with twice this velocity.

In a recent paper, Braides, Gelli and Novaga [14] (see Chapter 4 for a detailed presentation of this paper) used the Almgren, Taylor and Wang scheme coupled

with a homogenization procedure, by introducing a further parameter ε , interpreted as a space-scale, and considering $E_0^{\tau,\varepsilon}$ initial data, $E_k^{\tau,\varepsilon}$ as a minimizer of

$$\min \left\{ P_\varepsilon^\alpha(E) + \frac{1}{\tau} \int_{E \Delta E_{k-1}^{\tau,\varepsilon}} d_\infty^\varepsilon(x, \partial E_{k-1}^{\tau,\varepsilon}) dx \right\}, \quad (4)$$

with the constraint $E_0^{\tau,\varepsilon}, E \in \mathcal{D}_\varepsilon$, \mathcal{D}_ε being the class of finite unions of ε -squares.

The P_ε^α are discrete “ferromagnetic-type” energies, defined on subsets $E \subset \varepsilon\mathbb{Z}^2$ by

$$P_\varepsilon^\alpha(E) = \alpha \varepsilon \# \{ (i, j) \in \mathbb{Z}^2 \times \mathbb{Z}^2 : \varepsilon i \in E, \varepsilon j \notin E, |i - j| = 1 \}, \quad (5)$$

which Γ -converge to the crystalline perimeter P^α (see e.g., Alicandro, Braides and Cicalese [1]). The terminology used for these discrete energies is motivated as follows. We consider the simplest *lattice energy*, that is, depending on a discrete variable $u = \{u_i\}$ indexed by the nodes i of the standard lattice $\varepsilon\mathbb{Z}^2$, given by

$$P_\varepsilon^\alpha(u) = \frac{1}{4} \alpha \sum_{|i-j|=\varepsilon} \varepsilon (u_i - u_j)^2, \quad (6)$$

where u_i takes only the two values $+1$ and -1 (*spin systems*). Note that its density only differs by constants from the usual ferromagnetic energy density $-u_i u_j$. After identifying a function u with the set E obtained as the union of all closed unit squares with centers i such that $u_i = 1$, the energy P_ε^α can be rewritten (with a slight abuse of notation) as a perimeter functional

$$P_\varepsilon^\alpha(u) = P_\varepsilon^\alpha(E) = \alpha \mathcal{H}^1(\partial E), \quad (7)$$

and hence can be interpreted as an interfacial energy.

The discrete distance d_∞^ε in (4) is defined, for $E \in \mathcal{D}_\varepsilon$, as

$$d_\infty^\varepsilon(x, \partial E) = d_\infty(i, \partial E) + \frac{\varepsilon}{2}, \quad \text{if } x \in Q_\varepsilon(i) = i + \varepsilon[-1/2, 1/2]^2, \quad (8)$$

where $d_\infty(x, A) = \min\{\|x - y\|_\infty : y \in A\}$.

The scheme (4) is applied at fixed τ with $\varepsilon = \varepsilon(\tau)$, so that the discrete trajectories $E_k^{\tau,\varepsilon}$ depend on the interaction between the two scales, and hence also their limits. This problem can be cast in the general framework of *minimizing movements along a Γ -converging sequence* (Chapter 2, Section 2.3). If $\varepsilon \ll \tau$, then the limit motion is the crystalline flow (3), while if $\tau \ll \varepsilon$, then $E_k^{\tau,\varepsilon} \equiv E_0^{\tau,\varepsilon}$ and the motion is “pinned” (i.e., it coincides identically with the initial limit set). This observation highlights the existence of a critical ε - τ regime (namely, $\tau \sim \varepsilon$) which captures the most interesting features of the motion connected to these energies. Hence, we assume $\tau = \gamma\varepsilon$ for $\gamma > 0$ and denote $E_k^\varepsilon = E_k^{\tau,\varepsilon}$.

Let $E_0^{\tau,\varepsilon}$ be a coordinate rectangle in \mathcal{D}_ε . If E_{k-1}^ε is a coordinate rectangle, then also E_k^ε defined by minimization of energy (4) is a coordinate rectangle contained in E_{k-1}^ε and containing the center of E_{k-1}^ε . The main steps of the proof are the following:

- each connected component of E_k^ε is a coordinate rectangle contained in E_{k-1}^ε , by considering the smallest rectangle containing its intersection with E_{k-1}^ε (‘rectangularization’);

- actually, there is only one connected component, since each connected component can be translated in direction of the center of E_{k-1}^ε without increasing its energy;
- E_k^ε contains the center of E_{k-1}^ε , otherwise we can construct a competitor which contradicts the connectedness of E_k^ε .

The resulting limit evolution is still a rectangle. In case of a unique evolution, the side lengths $L_1(t), L_2(t)$ of this rectangle are governed by a system of ‘degenerate’ ordinary differential equations

$$\begin{cases} \dot{L}_1(t) = -\frac{2}{\gamma} \left\lfloor \frac{2\alpha\gamma}{L_2(t)} \right\rfloor \\ \dot{L}_2(t) = -\frac{2}{\gamma} \left\lfloor \frac{2\alpha\gamma}{L_1(t)} \right\rfloor \end{cases} \quad (9)$$

for almost every t , with initial conditions $L_1(0) = L_1^0$ and $L_2(0) = L_2^0$.

Note some new features with respect to the crystalline motion (3), as follows.

(a) *Degenerate equations.* The motion is described by a system of degenerate ordinary differential equations (9), whose right-hand sides are discontinuous. In fact, the discrete motion is obtained by overcoming some energy barriers in a ‘quantized’ manner. Moreover, we may read in the equations the effect of the Γ -limit energy (through the crystalline form of the evolution and the coefficient α) and of the interplay between the time and space scales (through the scaling γ).

(b) *A pinning threshold.* If both the initial side-lengths are above the *pinning threshold* $\tilde{L} = 2\alpha\gamma$, then the right-hand sides of equations (9) are zero and the motion is pinned. This threshold is obtained by computing the values for which a side of length L may not move inwards of ε by decreasing the energy in (4). The corresponding variation of the energy is given by

$$-2\alpha\varepsilon + \frac{1}{\gamma}L\varepsilon, \quad (10)$$

which is positive if and only if $L \geq \tilde{L} = 2\alpha\gamma$.

(c) *Inhomogeneity of the motion.* The limit motion (9) cannot be obtained following the Almgren-Taylor-Wang approach for any perimeter functional. It can be regarded as a non-homogeneous crystalline motion, with a velocity depending on a function of the curvature: if the curvature κ of a side is identified with the inverse of its length, then the law for the velocity v of that side is

$$v = f(\kappa)\kappa,$$

where $f(\kappa) = \frac{1}{\gamma} \lfloor 2\alpha\gamma\kappa \rfloor \frac{1}{\kappa}$. Note that f is always less or equal than 2, the coefficient in the continuous case, which shows how an additional discreteness effect is to slow down the crystalline motion.

Scope of the first part of this thesis is to show that the Γ -limit of the discrete energies P_ε^α is not sufficient to completely describe at the critical regime the effective

limit motion, which is also affected by microscopic geometric properties not detected in the limit. The main result is described in Chapter 5 (which forms the content of a joint work with A. Braides [19]). We introduce a further inhomogeneity in the perimeters P_ε^α by considering, for any subset $E \subset \varepsilon\mathbb{Z}^2$,

$$P_\varepsilon^{\alpha,\beta}(E) = \frac{1}{2}\varepsilon \sum \{c_{ij} : (i,j) \in \mathbb{Z}^2 \times \mathbb{Z}^2, \varepsilon i \in E, \varepsilon j \notin E, |i-j|=1\},$$

(we use the notation $\sum\{x_a : a \in A\} = \sum_{a \in A} x_a$), where the coefficients c_{ij} equal $\alpha > 0$ except for some well-separated periodic square inclusions of size N_β where $c_{ij} = \beta > \alpha$ (*high-contrast* medium). The periodicity cell is pictured in Fig. 1. These

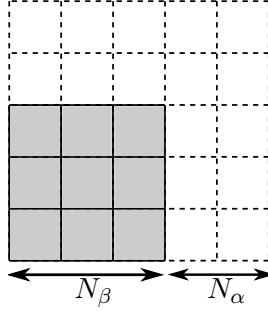


Figure 1. Periodicity cell. Continuous lines represent β -bonds, dashed lines α -bonds.

inclusions are not energetically favorable and can be neglected in the computation of the Γ -limit, which is still the crystalline perimeter P^α as in (2), with the same coefficient α (Remark 5.2.1). For this, we note that $P_\varepsilon^{\alpha,\beta} \geq P_\varepsilon^\alpha$ (from which we deduce the lower bound $\Gamma\text{-}\liminf_{\varepsilon \rightarrow 0} P_\varepsilon^{\alpha,\beta} \geq P^\alpha$) and that recovery sequences for the Γ -limit of $P_\varepsilon^{\alpha,\beta}$ can be constructed at a scale $N_{\alpha\beta}\varepsilon$, $N_{\alpha\beta} := N_\alpha + N_\beta$, thus ‘avoiding’ the β -connections.

We restrict our analysis to the case of initial data coordinate rectangles at the critical regime $\tau = \gamma\varepsilon$ (which also in this case is the most interesting), and we apply the Almgren, Taylor and Wang approach as in (4) to the energies

$$\mathcal{F}_{\varepsilon,\tau}^{\alpha,\beta}(E, F) = P_\varepsilon^{\alpha,\beta}(E) + \frac{1}{\tau} \int_{E \Delta F} d_\infty^\varepsilon(x, \partial F) dx. \quad (11)$$

More precisely, given an initial set $E_0^\varepsilon \in \mathcal{D}_\varepsilon$ which is a coordinate rectangle, we define recursively a sequence $E_k^{\varepsilon,\tau}$ in \mathcal{D}_ε by requiring the following:

- (i) $E_0^{\varepsilon,\tau} = E_0^\varepsilon$;
- (ii) $E_{k+1}^{\varepsilon,\tau}$ is a minimizer of the functional $\mathcal{F}_{\varepsilon,\tau}^{\alpha,\beta}(\cdot, E_k^{\varepsilon,\tau})$.

The *discrete flat flow* associated to functionals $\mathcal{F}_{\varepsilon,\tau}^{\alpha,\beta}$ is thus defined by

$$E^{\varepsilon,\tau}(t) = E_{\lfloor t/\tau \rfloor}^{\varepsilon,\tau}, \quad t \geq 0. \quad (12)$$

Assuming that the initial data E_0^ε tend, in the Hausdorff sense (see Section 1.2), to a coordinate rectangle E_0 , we are interested in identifying the motion described by any converging subsequence of $E^{\varepsilon,\tau}(t)$ as $\varepsilon, \tau \rightarrow 0$.

The presence of the inclusions is felt in the minimization procedure since they may influence the choice of $E_k^{\tau, \varepsilon}$. In fact, we show that the evolute of a coordinate rectangle by minimization of the energy is an α -type coordinate rectangle, that is, a rectangle whose sides intersect only α -bonds, thus avoiding the inclusions. Contrary to the case treated in Chapter 4, it is not simple to show that the minimizers are actually rectangles: this is a technical point contained in Proposition 5.3.5. In particular, rectangularization and translation of a connected component may increase the perimeter term $P_\varepsilon^{\alpha, \beta}$ in the energy, so that they cannot be performed in a periodic environment.

Here we just give a brief overview of the proof. The evolute F is connected (Step 1) and, if not α -type, it is an α -type rectangle R^α with some protrusions intersecting β -bonds, as in Fig. 2 (Step 2). The optimal profile of a protrusion (Step 3) on a single β -square, if non-empty, is horizontal; we can substitute protrusions on consecutive β -squares with a single horizontal protrusion, and also join different protrusions by translations toward one of the corner β -squares, if energetically convenient. At this point, we are in one of the two situations pictured in Fig. 3. We can remove all the β -connections inside the border β -squares (Step 4), so that the evolute is the union of an α -type rectangle R and possibly one to four rectangles \tilde{R}_i intersecting the corner β -squares of side length at most $N_{\alpha\beta}\varepsilon$ (Fig. 4). These small rectangles are actually not there (Step 5), so that, finally, F is an α -type rectangle.

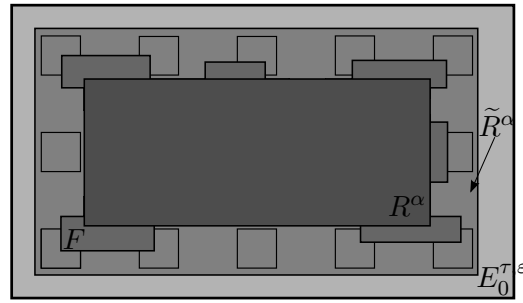


Figure 2. α -rectangularization.

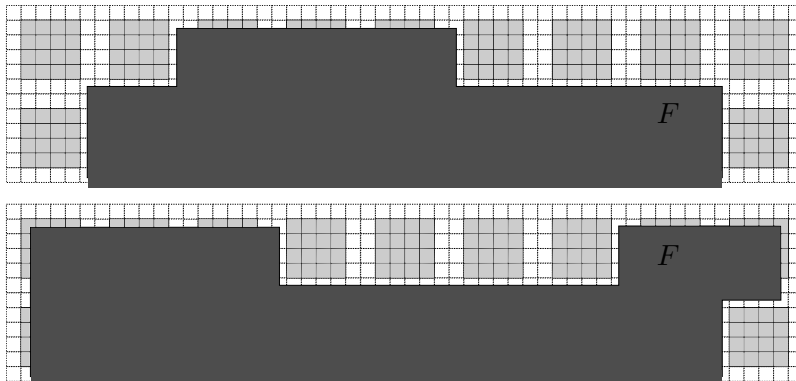


Figure 3. Profiles of the upper side of candidate minimal F .

As shown by Braides, Gelli and Novaga (see Section 4.4), the motion of each side of $E_k^\varepsilon = E_k^{\varepsilon, \tau}$ can be studied separately, since the constraint of being an α -type

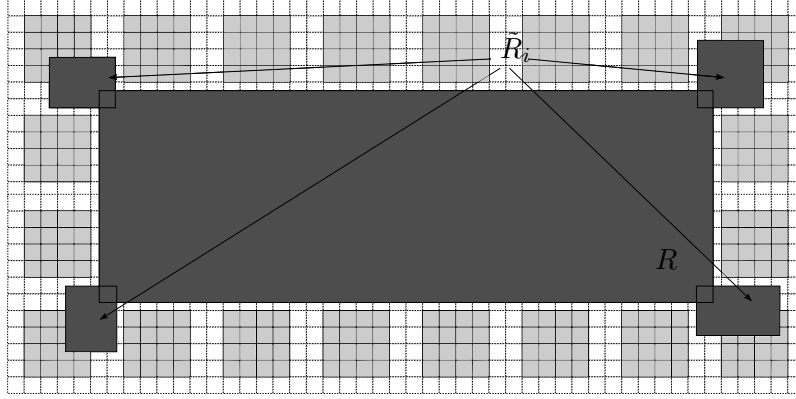


Figure 4. The set obtained in Step 4.

rectangle does not influence the argument therein, which consists in remarking that the bulk term due to the small corner rectangles in Fig. 5 is negligible. As a consequence, we can describe the motion in terms of the length of the sides of E_k^ε .

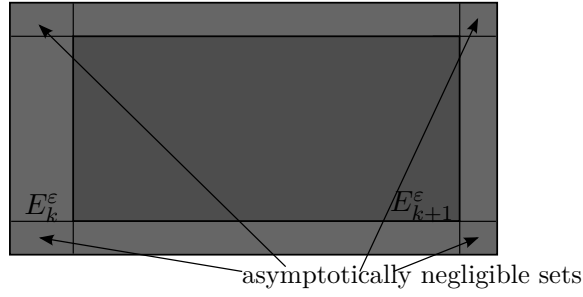


Figure 5. Picture of E_{k+1}^ε inside E_k^ε .

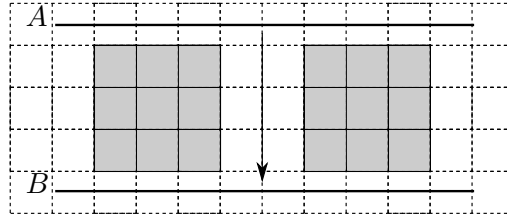


Figure 6. Motion is possible if the side can move at least by $(N_\beta + 1)\varepsilon$.

We first compute the new pinning threshold (Section 5.3.1). By the condition that E_k^ε be an α -type rectangle, we have to impose that it is not energetically favorable for a side to move inwards by $(N_\beta + 1)\varepsilon$ (see Fig. 6). We then write the variation of the energy functional $\mathcal{F}_{\varepsilon, \tau}^{\alpha, \beta}$ from configuration A to configuration B in Fig. 6, regarding a side of length L . If we impose it to be positive, we obtain the pinning threshold

$$\bar{L} := \frac{4\alpha\gamma}{N_\beta + 2}. \quad (13)$$

Note that this threshold depends on N_β and not on the value $\beta > \alpha$ and that, if

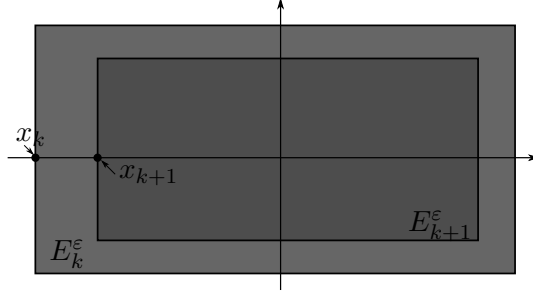


Figure 7. Reduction to a one-dimensional problem.

$N_\beta = 0$ (or, otherwise, $\alpha = \beta$), we recover the previous threshold $\tilde{L} = 2\alpha\gamma$.

As remarked above, up to an error vanishing as $\varepsilon \rightarrow 0$, the motion of each side is independent of the other ones. As a consequence, its description can be reduced to a one-dimensional problem, where the unknown represents, e.g., the location of the left hand vertical side of E_k^ε . Let x_k represents the projection of this side of E_k^ε on the horizontal axis, as in Fig. 7. The location of x_{k+1} depends on a minimization argument involving x_k and the length L_k of the corresponding side of E_k^ε . However, this latter dependence is locally constant, except for a discrete set of values of γ/L_k . This *singular set* depends on N_β (not on β) and it is given by

$$S_{N_\beta} = \frac{1}{2\alpha} \left(\mathbb{Z} \cup \left(\frac{1}{2} + \mathbb{Z} \right) \right) \quad (14)$$

(see Section 5.3.2, Definition 5.3.6).

We examine the iterated minimizing scheme for $\gamma/L_k = \gamma/L \in (0, +\infty) \setminus S_{N_\beta}$ fixed, which reads

$$\begin{cases} x_{k+1}^L = x_k^L + \bar{N}_k, & k \geq 0 \\ x_0^L = x^0 \end{cases} \quad (15)$$

with $x^0 \in \{0, 1, \dots, N_{\alpha\beta} - 1\}$ and $\bar{N}_k \in \mathbb{N}$ the minimizer of

$$\min \left\{ -2\alpha N + \frac{1}{\gamma} \frac{N(N+1)}{2} L : N \in \mathbb{N}, \quad [x_k^L + N]_{N_{\alpha\beta}} \in \mathbb{Z}_{N_\alpha} \right\}, \quad (16)$$

$\mathbb{Z}_{N_\alpha} = \{[0]_{N_{\alpha\beta}}, \dots, [N_\alpha - 1]_{N_{\alpha\beta}}\}$, which is unique by the requirement that $\gamma/L \notin S_{N_\beta}$. Note that the function to be minimized on the integers in (16) represents the variation of the energy $\mathcal{F}_{\varepsilon, \tau}^{\alpha, \beta}$ corresponding to the removal of N ε -stripes, and the constraint is due to the fact that, as showed before, the side may stay only on α -connections.

After at most N_α steps, $\{x_k^L\}_{k \geq 0}$ is *periodic modulo* $N_{\alpha\beta}$ (Proposition 5.3.7), that is, there exist integers $\bar{k} \leq N_\alpha$, $M \leq N_\alpha$ and $n \geq 1$ such that

$$x_{k+M}^L = x_k^L + n N_{\alpha\beta} \quad \text{for all } k \geq \bar{k}. \quad (17)$$

Moreover, the quotient n/M depends only on γ/L ; in particular, it does not depend on the starting point x^0 .

We can define the velocity of a side as a *mean velocity* averaging on a period; that is,

$$v = \frac{n N_{\alpha\beta} \varepsilon}{M \tau}. \quad (18)$$

In (18) the velocity is the ratio between the minimal (periodic) displacement of the side and the product of the time-scale τ and the number of steps necessary to describe the minimal period, each of which considered as a 1-time step.

Correspondingly, we define the *effective velocity function* $f : (0, +\infty) \setminus S_{N_\beta} \rightarrow [0, +\infty)$ by setting

$$f(Y) = \frac{nN_{\alpha\beta}}{M}, \quad (19)$$

with M and n in (17) defined by L and γ such that $Y = \gamma/L$. By Proposition 5.3.7, this is a good definition. The function f is non-decreasing and piecewise-constant, independent of β but depends on N_β and $f(Y) = 0$ if $Y < \gamma/\bar{L}$, \bar{L} the pinning threshold (see Remark 5.3.10 for the proof of these and other properties of f).

It may be not easily described for generic N_α and N_β . We compute it, by means of algebraic formulas, in the simpler cases $N_\beta = 1$ and $N_\beta = 2$, with varying N_α (Section 5.4). These are prototypes for the cases N_β odd and N_β even, respectively. In particular, if $N_\alpha = N_\beta = 1$, then the velocity function is given by

$$\bar{f}(\gamma/L) = 2 \left\lfloor \frac{\alpha\gamma}{L} + \frac{1}{4} \right\rfloor, \quad (20)$$

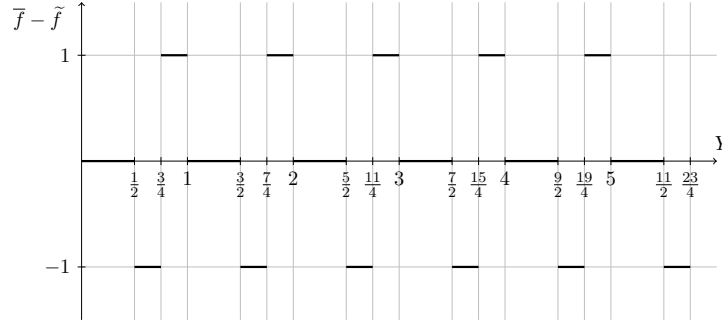


Figure 8. Difference between inhomogeneous-homogeneous velocity function ($\alpha = \gamma = 1$).

while if $N_\alpha = 1$ and $N_\beta = 2$, then it is given by

$$\bar{\bar{f}}(\gamma/L) = 3 \left\lfloor \frac{2}{3} \frac{\alpha\gamma}{L} + \frac{1}{3} \right\rfloor. \quad (21)$$

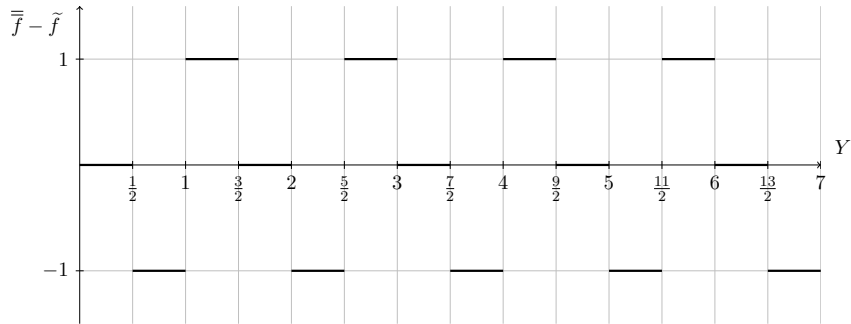


Figure 9. Difference between inhomogeneous-homogeneous velocity function ($\alpha = \gamma = 1$).

In Fig. 8 and Fig. 9 we compare (20) and (21), respectively, with the velocity function of the homogeneous case $\tilde{f}(\gamma/L) = \lfloor 2\alpha\gamma/L \rfloor$, showing that the inhomogeneities in the lattice may accelerate or decelerate the motion.

The limit motion (Theorem 5.3.13) can still be represented through a system of degenerate ordinary differential equations of the form

$$\begin{cases} \dot{L}_1(t) = -\frac{2}{\gamma} f\left(\frac{\gamma}{L_2(t)}\right) \\ \dot{L}_2(t) = -\frac{2}{\gamma} f\left(\frac{\gamma}{L_1(t)}\right) \end{cases} \quad (22)$$

for almost every t , with initial conditions $L_1(0) = L_1^0$ and $L_2(0) = L_2^0$, where f is given by (19).

We also extend these results to more general initial sets (see Remark 5.3.14), in particular *polyrectangles* (Section 4.5).

In Chapter 6 (which forms the content of the paper by myself [44]), we give another example of the fact that the microstructure can affect the limit evolution without changing the Γ -limit. To this end, we perform a multi-scale analysis by introducing a *contrast parameter* δ_ε and considering a *low-contrast* medium, that is a periodic mixture of two homogeneous materials whose propagating properties are close to each other. One of them can be considered as a fixed background medium (described by α -connections) and the other as a small (vanishing) perturbation from that one, that is with $\beta = \beta_\varepsilon = \beta(\varepsilon)$ and $\beta_\varepsilon - \alpha = \delta_\varepsilon \rightarrow 0$ as $\varepsilon \rightarrow 0$. With the same notation as in Chapter 5, we restrict ourselves to the case $N_\alpha = N_\beta = 1$; despite of its simplicity, the choice of this particular geometry will suffice to show new features of the motion. The main result is the existence of a threshold value of the contrast parameter below which we have a new homogenized effective velocity, which takes into account the propagation velocities in both the connections α and β ; above this threshold, instead, it is independent of the value of β and the motion is obtained by considering only the α -connections.

A heuristic computation suggests that the correct scaling for δ_ε is

$$\beta_\varepsilon - \alpha = \delta_\varepsilon = \delta\varepsilon$$

for some constant $\delta > 0$.

As before, we assume that $\tau = \gamma\varepsilon$ and restrict the description of the motion to the case of initial data coordinate rectangles. The evolute of a coordinate rectangle by minimization of the energy is again a coordinate rectangle (Proposition 6.3.1). We show that there exists a threshold $\tilde{\delta} = \frac{1}{2\gamma}$ such that if $\delta < \tilde{\delta}$ (subcritical regime) then the evolute rectangles may have some *β -type side* (that is, a side intersecting only β -connections), while if $\delta \geq \tilde{\delta}$ (supercritical regime) the β -connections are avoided as in the case $\beta > \alpha$ (Proposition 6.3.4). Note that this result gives information also for more general choices of the vanishing rate of δ_ε : if $\delta_\varepsilon \ll \varepsilon$, we reduce to the subcritical case, while if $\delta_\varepsilon \gg \varepsilon$, we are in the supercritical case.

The limit motion can still be described through a system of degenerate ordinary differential equations as in (22) with a new effective velocity function f_δ depending

on δ , given by

$$f_\delta(Y) = \begin{cases} 0 & \text{if } Y < \frac{C_{\delta,\gamma} + 1}{2\alpha}, \\ 2k & \text{if } Y \in \left(\frac{2k - C_{\delta,\gamma}}{2\alpha}, \frac{2k + 1 + C_{\delta,\gamma}}{2\alpha} \right), \\ 2k + 1 & \text{if } Y \in \left(\frac{2k + 1 + C_{\delta,\gamma}}{2\alpha}, \frac{2k + 2 - C_{\delta,\gamma}}{2\alpha} \right), \end{cases} \quad k \geq 0,$$

where $C_{\delta,\gamma} = \min\{\delta\gamma, 1/2\}$. Note that we recover the velocity function of the homogeneous case \tilde{f} computing f_δ for $\delta = 0$ (see Section 6.3.3). If we choose $\delta = 1/2\gamma$ (actually, for any $\delta \geq 1/2\gamma$), we recover the velocity function \bar{f} (20) which corresponds to the high-contrast case.

Contrary to the high-contrast case (14), the singular set (Definition 6.3.2) now depends also on β through δ and it is given by

$$S_\delta = \frac{1}{2\alpha} [(2\mathbb{Z} + 1 + \delta\gamma) \cup (2\mathbb{Z} - \delta\gamma)]. \quad (23)$$

We have a new effective pinning threshold (Section 6.3.2) given by

$$\bar{L}_\delta = \max \left\{ \frac{2\alpha\gamma}{\delta\gamma + 1}, \frac{4}{3}\alpha\gamma \right\}.$$

(see Fig. 10).

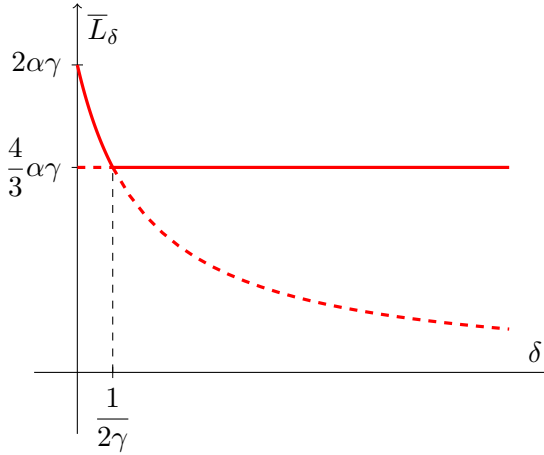


Figure 10. Effective pinning threshold (represented by the continuous line).

The same problem as before is treated also in the case of non-uniform inclusions distributed into periodic uniform layers (Section 6.4).

In the second part of the thesis (Chapter 7), which contains the results of joint works with A. Braides [20, 21], we consider the opposite problem of (1): defining a motion when starting from the same discrete schemes for sets which “expand”

by *maximizing* the perimeter subject to a penalization of their distance from the previous set. Formally, this involves considering problems of the form

$$\min \left\{ -P(E) + \frac{1}{\tau} \int_{E \Delta E_{k-1}^\tau} \text{dist}(x, \partial E_{k-1}^\tau) dx \right\}, \quad (24)$$

which can be seen as a “backward” version of the previous ones (see Section 2.6) if the index k is considered as parameterizing negative time. Unfortunately, this problem is ill-posed, giving the trivial infimum $-\infty$ at the first step (Remark 7.1.1).

Following a suggestion by J.W. Cahn, we consider a discrete approximation of P in the crystalline case, and use it to define a backward crystalline-curvature motion with prescribed extinction point (or, equivalently, *nucleation* of the motion defined for positive times). To this end, we introduce a suitable scaling of the energies which can be interpreted as a time-scaling of the discrete trajectories (Section 2.5).

In Section 7.2 we treat a simple example. We introduce a new parameter $\lambda > 0$, consider initial data $E_0^{\tau, \varepsilon, \lambda} = Q_\varepsilon = \varepsilon Q = \varepsilon \left[-\frac{1}{2}, \frac{1}{2} \right]^2$ (which, in the discrete setting, all correspond to the singleton $\{0\}$), and define iteratively $E_k^{\tau, \varepsilon, \lambda} \in \mathcal{D}_\varepsilon$ as a minimizer of

$$\min \left\{ -\frac{1}{\lambda} P_\varepsilon(E) + \frac{1}{\tau} \int_{E \Delta E_{k-1}^{\tau, \varepsilon, \lambda}} d_\infty^\varepsilon(x, \partial E_{k-1}^{\tau, \varepsilon, \lambda}) dx \right\}, \quad (25)$$

where $P_\varepsilon(E) = \mathcal{H}^1(\partial E)$ (i.e., the discrete energy (5) computed for $\alpha = 1$), and d_∞^ε is defined by (8).

Contrary to the forward case, in which crystalline motion has been described only in dimension two, due to its simpler form the limit can be described in all dimensions $d \geq 2$ (the definitions of P_ε and d_∞^ε are modified accordingly).

We first determine the correct scaling for λ and τ in terms of ε in order to have a non-trivial limit. To this end, we note that the minimal variation of the energy in (25) from the set $E_{k-1}^{\tau, \varepsilon, \lambda}$ corresponds to the addition of an ε -cube with no side in common with $E_{k-1}^{\tau, \varepsilon, \lambda}$. The variation is

$$-\frac{2d}{\lambda} \varepsilon^{d-1} + \frac{1}{\tau} K \varepsilon^{d+1} \quad (26)$$

with $0 \neq K \in \mathbb{N}$. This quantity may be negative if and only if

$$1 \leq \frac{2d\tau}{\lambda \varepsilon^2}. \quad (27)$$

The relative scaling of ε, τ and λ must be such that this condition be satisfied. We treat the case

$$\tau/\varepsilon = \gamma \in (0, +\infty), \quad \lambda \varepsilon = \alpha \in (0, +\infty), \quad (28)$$

so that (27) corresponds to

$$\frac{1}{2d} \leq \frac{\gamma}{\alpha}. \quad (29)$$

First note that if (29) is not satisfied, then every competing set E in the definition of $E_1^{\tau, \varepsilon, \lambda}$ gives a strictly larger value than the set $E_0^{\tau, \varepsilon, \lambda}$; hence, each discrete trajectory is trivial, and so is their limit: $E(t) = \{0\}$.

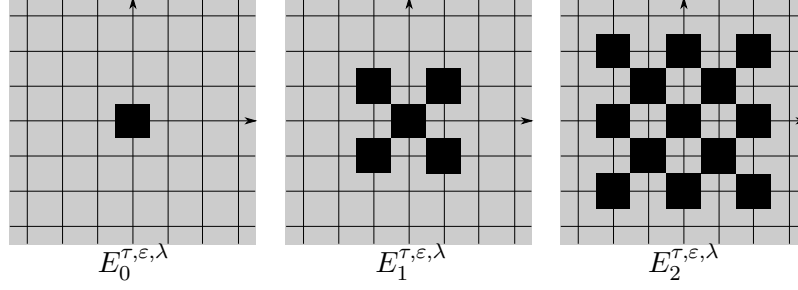


Figure 11. Some steps of the discrete evolution in dimension two.

Suppose now that (29) is satisfied. We then prove that $E_k^{\tau, \varepsilon, \lambda}$ is a (even) checkerboard structure containing εQ (see Fig. 11); i.e., it is the union of cubes $\varepsilon(i + Q)$ with $i \in \mathbb{Z}^d$ and $\|i\|_1 = |i_1| + \dots + |i_d|$ even (for short, we say that i is even). Moreover,

$$\{i \in \mathbb{Z}^d : \varepsilon i \in E_k^{\tau, \varepsilon, \lambda}\} = \left\{i \in \mathbb{Z}^d \text{ even}, \|i\|_\infty \leq \left\lfloor \frac{2d\gamma}{\alpha} \right\rfloor k\right\}. \quad (30)$$

The statement above can be proved inductively by showing that

$$\{i \in \mathbb{Z}^d : \varepsilon i \in E_k^{\tau, \varepsilon, \lambda}\} = \left\{i \in \mathbb{Z}^d \text{ even}, d_\infty\left(i, \frac{1}{\varepsilon} E_{k-1}^{\tau, \varepsilon, \lambda}\right) \leq \left\lfloor \frac{2d\gamma}{\alpha} \right\rfloor\right\}. \quad (31)$$

If we define $E^\tau(t) = E_{\lfloor t/\tau \rfloor}^{\tau, \varepsilon, \lambda}$, then, for all fixed t , the Kuratowski limit of the family $E^\tau(t)$ as $\tau \rightarrow 0$ is a cube of centre 0 and side length $2 \left\lfloor \frac{2d\gamma}{\alpha} \right\rfloor t$. Moreover, if $\frac{2d\gamma}{\alpha} \notin \mathbb{N}$, then the motion is given by a family of expanding cubes whose sides move with constant velocity $\left\lfloor \frac{2d\gamma}{\alpha} \right\rfloor$. If $\frac{2d\gamma}{\alpha} \in \mathbb{N}$, then we obtain that the sets E are contained in the cubes moving with velocity $\frac{2d\gamma}{\alpha}$, and contain the cubes moving with velocity $\frac{2d\gamma}{\alpha} - 1$, but need not be cubes themselves. This is due to the non-uniqueness of the minimal sets in (25).

The problem can be set for different distances d_φ (induced by a norm φ) in place of the ∞ -distance we used before (Section 7.4), under the same assumptions (28) on τ, λ and in dimension $d = 2$. In this case, the *nucleation threshold* (Section 7.4.1) depends on the norm φ and can be estimated as

$$\frac{\gamma}{\alpha} \geq \frac{1}{4} \min\left\{\varphi_{-1,1}, \varphi_{1,1}, 2 \min\{\varphi_{1,0}, \varphi_{0,1}\} + \min\{\varphi_{0,1}, \varphi_{1,0}, \varphi_{1,1}, \varphi_{-1,1}\}\right\}, \quad (32)$$

where $\varphi_{x,y} := \varphi(x, y)$. Note that, if $\varphi = \|\cdot\|_\infty$ and $d = 2$, we recover (29).

In this general framework, however, it is not trivial to show that the minimizers are checkerboard (actually, we assume this fact as a technical hypothesis). Moreover, we might not have that the minimal sets $E_k^\varepsilon = E_k^{\tau, \varepsilon, \lambda}$ correspond to the same checkerboard structure (even or odd); in particular, we might have that they ‘oscillate’ between even or odd checkerboards. This may happen only for a finite number of indices k ; eventually, they stabilize and after some \bar{k} correspond to the same parity (Proposition 7.4.4).

In order to define a non-trivial limit motion, we consider a suitable ‘convexification’ of the minimal sets. More precisely, if $\mathcal{I}_{k,\varepsilon} \subseteq \varepsilon\mathbb{Z}^2$ is the set of the centers of the ε -squares contained in E_k^ε , we define $F_k^\varepsilon = \text{conv}(\mathcal{I}_{k,\varepsilon})$, $\text{conv}(\mathcal{I})$ being the smallest

convex polygon containing \mathcal{I} . We then have two cases (Theorem 7.4.7):

(i) if the *nucleus* E_1^ε (Definition 7.4.2) corresponds to the even checkerboard (see Fig. 12 for an example), then F_k^ε and F_1^ε are homothetic with center 0, for all $k \geq 1$ (Remark 7.4.6). In this case, if we define $F_\varepsilon(t) = F_{\lfloor t/\tau \rfloor}^\varepsilon$, $t \geq 0$, then for all fixed t the Kuratowsky limit of the family $F_\varepsilon(t)$ as $\varepsilon \rightarrow 0$ is a polygon $F(t)$ given by

$$F(t) = \frac{1}{\gamma} t F_1, \quad (33)$$

where $F_1 = \frac{1}{\varepsilon} F_1^\varepsilon$ and $\gamma = \tau/\varepsilon$.

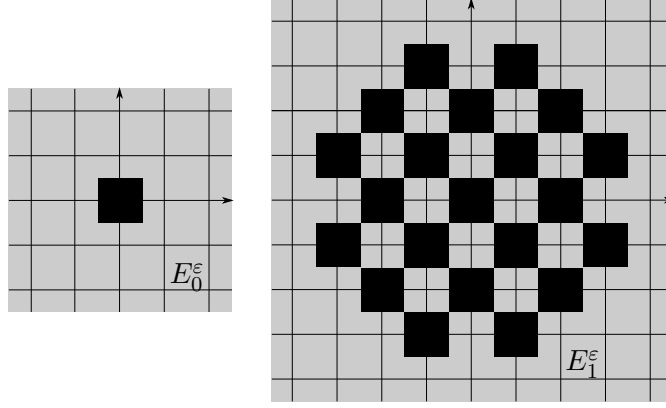


Figure 12. An example of nucleus E_1^ε .

(ii) if E_1^ε corresponds to the odd checkerboard, then E_k^ε oscillates between odd and even checkerboards, and after $\bar{k} = \bar{k}(\alpha, \gamma)$ steps it stabilizes on the same checkerboard. If we define $G_\varepsilon(t) = G_{\lfloor t/\tau \rfloor}^\varepsilon$, where $G_k^\varepsilon = \text{conv}(\mathcal{I}_{k,\varepsilon})$ (here we change notation to make a comparison with the case (i)), then for all fixed t the Kuratowsky limit of the family $G_\varepsilon(t)$ as $\varepsilon \rightarrow 0$ is a polygon $G(t)$ satisfying the inclusion

$$G(t) \subseteq F(t), \quad (34)$$

where $F(t)$ is given by (33). Hence, the limit motion in (ii) is slower than (i).

In Section 7.5.2, we give an example where the limit set is of dimension $d - 1$; more precisely, in dimension two, a linearly growing segment. For this, we consider the (sufficiently) asymmetric norm

$$\varphi(i) = \sqrt{\frac{33}{8}(i_1^2 + i_2^2) - \frac{31}{4}i_1i_2}, \quad i \in \varepsilon\mathbb{Z}^2. \quad (35)$$

We assume also that

$$\frac{\sqrt{2}}{8} \leq \frac{\gamma}{\alpha} < \frac{1}{8}\sqrt{\frac{33}{2}}. \quad (36)$$

In this case,

$$\begin{aligned} \mathcal{I}_{k,\varepsilon} &= \{i \in \varepsilon\mathbb{Z}^2 : i \in E_k^\varepsilon\} = \left\{i \in \varepsilon\mathbb{Z}^2 \text{ even}, \varphi(i) < \frac{4\gamma}{\alpha}\varepsilon k\right\} \\ &= \left\{i \in \varepsilon\mathbb{Z}^2 \text{ even}, |i_1| = |i_2| = 0, \dots, k\right\} \end{aligned} \quad (37)$$

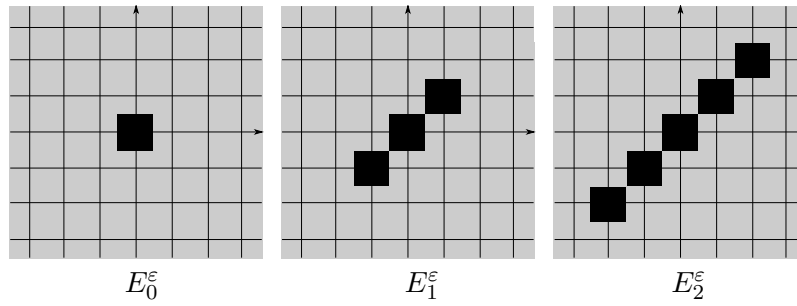


Figure 13. Some steps of the evolution.

and, for all fixed t , the Kuratowsky limit of the family $F_\varepsilon(t) = F_{\lfloor t/\tau \rfloor}^\varepsilon = \text{conv}(\mathcal{I}_{\lfloor t/\tau \rfloor, \varepsilon})$ as $\varepsilon \rightarrow 0$ is a segment $F(t)$ such that $F(0) = \{0\}$ and whose length $L(t)$ satisfies

$$L(t) = \frac{1}{\gamma} 2\sqrt{2}t \quad (38)$$

for almost every $t \geq 0$.

In view of the possible definition of variational motion in a *random* media (that is, with randomly distributed inclusions) motivated by finding at least an estimate for the pinning threshold, the Appendix A contains the results of the paper [45] by myself about the homogenization of the energies associated to a spin system with randomly distributed unbounded coefficients. The model problem that we have in mind is that of a crystalline two-dimensional solid subject to fracture. We suppose that the relevant scale is that of the surface fracture energy, so we may neglect the elastic energy of the lattice (this can be taken separately into account as in the paper by Braides and Piatnitski [16]). In this case, depending on the applied forces or boundary displacement of the sample, a fracture may appear, separating two regions where the displacement is constant. In the Griffith theory of Fracture (see Griffith [32]), the energy necessary for the creation of a crack is proportional to its area; in a discrete setting this is translated in the number of atomic bonds that are broken. In our model, at the atomistic level, there is a random distribution of ‘strong’ unbreakable bonds and ‘weak’ (ferromagnetic) breakable bonds. This model translates into a *rigid* spin problem, where the two values of the spin parametrize the two regions of constant displacement of the crystal. We note that in this problem the random distribution of rigid or weak bonds is considered as fixed and as characteristic of the crystalline material, so that we are interested in almost sure properties of the overall energies when the measure of the sample is large with respect to the atomic distance. The way we will describe the overall behavior of this system is by scaling the domain lattice by a small parameter ε and introducing the corresponding scaled energies, and then compute the variational limit (Γ -limit) of such energies, which is defined on the continuum and it can be considered as an effective energy.

The microscopic energy under examination can be written as

$$\sum_{ij} \sigma_{ij}^\omega (1 - u_i u_j), \quad (39)$$

where $u_i \in \{\pm 1\}$ is a spin variable indexed on the lattice \mathbb{Z}^2 , the sum runs on

nearest-neighbors (i.e. $|i - j| = 1$) in a given portion $\Omega \cap \mathbb{Z}^2$ of \mathbb{Z}^2 , the coefficients σ_{ij}^ω depend on the realization ω of an independent and identically distributed (i.i.d.) random variable and

$$\sigma_{ij}^\omega = \begin{cases} +\infty & \text{with probability } p \\ 1 & \text{with probability } 1 - p, \end{cases}$$

with $p \in [0, 1]$ fixed and the convention $+\infty \cdot 0 = 0$.

In order to describe the behavior as the size of Ω diverges we introduce a scaled problem, in which, on the contrary, Ω is kept fixed, but scaled energies are defined as follows. A small parameter $\varepsilon > 0$ is introduced, the lattice is scaled accordingly to $\varepsilon\mathbb{Z}^2$, and the energies (39) are scaled (after multiplying by 2) to

$$E_\varepsilon^\omega(u) := \sum_{ij} \varepsilon \sigma_{ij}^\omega (u_i - u_j)^2. \quad (40)$$

After this scaling, the sum is taken on nearest neighbors in $\Omega \cap \varepsilon\mathbb{Z}^2$.

The coarse graining of these energies corresponds to a general approach in the theory of Γ -convergence for lattice system where the discrete functions $u = \{u_i\}$ are identified with their piecewise-constant extensions, and the scaled lattice energies with energies on the continuum whose asymptotic behavior is described by taking L^1 -limits in the u variable and applying a mesoscopic homogenization process to the energies. A general theory for interfacial energies by Ambrosio and Braides [5] suggests the identification of limit energies with functionals of the form

$$\int_{\Omega \cap \partial\{u=1\}} \varphi(x, \nu) d\mathcal{H}^1,$$

with ν the normal to $\partial\{u = 1\}$.

Our analysis will be carried out by using results from Percolation theory. Percolation is a model for random media (see Grimmett [33] and Kesten [37]). We are interested in *bond percolation* on the square lattice \mathbb{Z}^2 : we view \mathbb{Z}^2 as a graph with edges between neighboring vertices, and all edges are, independently of each other, chosen to be ‘strong’ with probability p and ‘weak’ with probability $1 - p$. A weak path is a sequence of consecutive weak edges, a weak cluster is a maximal connected component of the collection of weak edges. Percolation exhibits a phase transition: there exists a critical value of probability p_c , the *percolation threshold*, such that if $p < p_c$ then with probability one there exist a unique infinite weak cluster, while if $p > p_c$ then all the weak clusters are finite almost surely. For bond percolation on \mathbb{Z}^2 , the percolation threshold is given by $p_c = \frac{1}{2}$.

Actually, the structure of the Γ -limit of the energies (40) depends on probability through the percolation threshold (Section A.4). Above the percolation threshold, the Γ -limit is $+\infty$ on the functions not identically equal to 1 or -1: this means that the solid almost surely is rigid and there is no fracture. Below the percolation threshold, instead, the coarse graining leads first to showing that indeed we may define a limit magnetization u taking values in $\{\pm 1\}$. This u is obtained as a L^1 -limit on the scaled infinite weak cluster, thus neglecting the values u_i on nodes i isolated from that cluster. The surface tension is obtained by optimizing the almost sure

contribution of the interfaces, and showing that it can be expressed as a first-passage percolation problem, so that the limit is of the form

$$\int_{\Omega \cap \partial\{u=1\}} \lambda_p(\nu) d\mathcal{H}^1. \quad (41)$$

In this case, a crack in the crystal may appear following a minimal path on the infinite weak cluster and the microscopical pattern of the lattice (this fact justifies the anisotropy of the fracture energy (41)). The value $\lambda_p(\nu)$ (Proposition A.3.7) is defined through the asymptotic behavior of the chemical distance (that is, the distance on the infinite weak cluster, Definition A.3.3) between a pair of points aligned with ν . Note that the Γ -liminf inequality is obtained by a blow-up argument; we perform a construction based on the Channel property (Theorem A.3.2) which allows to modify the test sets in order to get a ‘weak’ boundary, thus avoiding bonds with infinite energy. This is useful also for the construction of a recovery sequence.

In Section A.5 we show that the homogenization of rigid spin systems is actually a limit case of the *elliptic* random homogenization of spin systems (see Braides and Piatnitski [17]); that is, the behavior of a rigid spin system is approximated by that of an elliptic spin system with one of the interaction coefficients very large. The proof of this new “continuity” property of the surface tension (Proposition A.5.5) essentially relies on a percolation result (Lemma A.5.1).

Acknowledgments

I would like to express my sincere gratitude to my supervisor Andrea Braides for the opportunity he gave me: every result contained in this thesis is the fruit of interesting and illuminating discussions with him. I also thank him for his friendship, help, encouragement and his unlimited patience that have supported me during my course of study.

I am also grateful to Adriana Garroni for her support and advice from the first moment.

Chapter 1

Preliminaries

In this chapter we fix some notation and collect some preliminary results which will be useful in the sequel.

1.1 Γ -convergence

In this section we recall some basic definitions and properties of Γ -convergence. We refer to Braides [10] and Dal Maso [25] for more details on the computation and the topological properties of the Γ -limits.

Let X be a separable metric space and F_ε, F functionals defined on X .

Definition 1.1.1. *We say that F is the Γ -limit of the sequence (F_ε) if it satisfies the following conditions:*

(i) (lower bound) *for all $u \in X$,*

$$F(u) \leq \liminf_{\varepsilon \rightarrow 0} F_\varepsilon(u_\varepsilon) \quad \text{for all } u_\varepsilon \rightarrow u;$$

(ii) (upper bound) *for all $u \in X$, there exists $u_\varepsilon \rightarrow u$ such that*

$$F(u) \geq \limsup_{\varepsilon \rightarrow 0} F_\varepsilon(u_\varepsilon);$$

in this case, we write

$$F(u) = \Gamma\text{-}\lim_{\varepsilon \rightarrow 0} F_\varepsilon(u).$$

Remark 1.1.2 (alternate upper bound inequalities). If F is a lower bound then requiring that (ii) holds is equivalent to any of the following:

- (recovery sequence) there exists $u_\varepsilon \rightarrow u$ such that $F(u) = \lim_{\varepsilon \rightarrow 0} F_\varepsilon(u_\varepsilon)$;
- (approximate limsup inequality) for all $\eta > 0$ there exists $u_\varepsilon \rightarrow u$ such that $F(u) + \eta \geq \limsup_{\varepsilon \rightarrow 0} F_\varepsilon(u_\varepsilon)$.

From the definition it follows an important property of Γ -convergence, that is the stability under continuous perturbations.

Proposition 1.1.3 (stability under continuous perturbations). *Let F_ε Γ -converge to F and G_ε converge continuously to G (i.e., $G_\varepsilon(u_\varepsilon) \rightarrow G(u)$ if $u_\varepsilon \rightarrow u$); then $F_\varepsilon + G_\varepsilon$ Γ -converge to $F + G$.*

It is useful to define the lower and upper Γ -limits, so that the existence of a Γ -limit can be viewed as their equality.

Definition 1.1.4 (lower and upper Γ -limits). *We define*

$$\Gamma\text{-}\liminf_{\varepsilon \rightarrow 0} F_\varepsilon(u) = \inf \{ \liminf_{\varepsilon \rightarrow 0} F_\varepsilon(u_\varepsilon) : u_\varepsilon \rightarrow u \} \quad (1.1)$$

$$\Gamma\text{-}\limsup_{\varepsilon \rightarrow 0} F_\varepsilon(u) = \inf \{ \limsup_{\varepsilon \rightarrow 0} F_\varepsilon(u_\varepsilon) : u_\varepsilon \rightarrow u \}. \quad (1.2)$$

Remark 1.1.5. The Γ -limit exists at a point u if and only if

$$\Gamma\text{-}\liminf_{\varepsilon \rightarrow 0} F_\varepsilon(u) = \Gamma\text{-}\limsup_{\varepsilon \rightarrow 0} F_\varepsilon(u).$$

Then (i) of Definition 1.1.1 also reads $F(u) \leq \Gamma\text{-}\liminf_{\varepsilon \rightarrow 0} F_\varepsilon(u)$ and (ii) reads $F(u) \geq \Gamma\text{-}\limsup_{\varepsilon \rightarrow 0} F_\varepsilon(u)$.

The fundamental property of Γ -convergence is expressed by the following theorem.

Theorem 1.1.6 (Fundamental Theorem of Γ -convergence). *Let (F_ε) satisfy the ‘mild coerciveness’ property, i.e., there exists a precompact sequence (u_ε) with $F_\varepsilon(u_\varepsilon) = \inf F_\varepsilon + o(1)$, and Γ -converge to F . Then*

- (i) F admits minimum, and $\min F = \liminf_{\varepsilon \rightarrow 0} F_\varepsilon$;
- (ii) if (u_{ε_k}) is a minimizing sequence for some subsequence F_{ε_k} (i.e., is such that $F_{\varepsilon_k}(u_{\varepsilon_k}) = \inf F_{\varepsilon_k} + o(1)$) which converges to some \bar{u} , then its limit point is a minimizer for F .

1.2 Convergence of sets

(i) **Kuratowski convergence.** For the definition of Kuratowski convergence, we refer to Kuratowski [38].

Definition 1.2.1 (Kuratowski convergence). *A sequence of sets E_ε is said to converge in the sense of Kuratowski or K-converge to a set E , written $E = K\text{-}\lim_{\varepsilon \rightarrow 0} E_\varepsilon$, if*

$$\text{Ls}_{\varepsilon \rightarrow 0} E_\varepsilon \subset E \subset \text{Li}_{\varepsilon \rightarrow 0} E_\varepsilon \quad (1.3)$$

where

$$\text{Li}_{\varepsilon \rightarrow 0} E_\varepsilon = \{x \in \mathbb{R}^2 : x = \lim_{\varepsilon \rightarrow 0} x_\varepsilon, x_\varepsilon \in E_\varepsilon\} \quad (1.4)$$

is the *liminf* and

$$\text{Ls}_{\varepsilon \rightarrow 0} E_\varepsilon = \{x \in \mathbb{R}^2 : x = \lim_{j \rightarrow \infty} x_{\varepsilon_j}, x_{\varepsilon_j} \in E_{\varepsilon_j}, \varepsilon_j \searrow 0\}. \quad (1.5)$$

is the *limsup*.

(ii) **Hausdorff convergence.** The *Hausdorff distance* between two sets A and B , denoted by $d_{\mathcal{H}}(A, B)$, is defined as

$$d_{\mathcal{H}}(A, B) = \max\{\sup\{\text{dist}(x, B) | x \in A\}, \sup\{\text{dist}(x, A) | x \in B\}\}$$

unless both A and B are empty, in which case $d_{\mathcal{H}}(A, B) = 0$.

Definition 1.2.2 (Hausdorff convergence). A sequence $\{E_\varepsilon\}$ of closed subsets of \mathbb{R}^2 is said to Hausdorff converge to a closed set E if $\lim_{\varepsilon \rightarrow 0} d_{\mathcal{H}}(E_\varepsilon, E) = 0$.

Note that, on the class of closed subsets, the Hausdorff convergence implies the Kuratowski convergence.

1.3 Functions of bounded variation and sets of finite perimeter

For the general theory of functions of bounded variation and sets of finite perimeter we refer to Ambrosio, Fusco and Pallara [6], Braides [9]; we recall some definitions and results (here in dimension $d = 2$) necessary in the sequel.

Let Ω be an open subset of \mathbb{R}^2 . We say that $u \in L^1(\Omega)$ is a *function of bounded variation* if its distributional first derivatives $D_i u, i = 1, 2$ are Radon measures with finite total variation in Ω . We denote this space by $BV(\Omega)$ and we write $u \in BV(\Omega; \{\pm 1\})$ when the function u is of bounded variation in Ω and takes only the values -1 and $+1$.

Let $u : \Omega \rightarrow \mathbb{R}$ be a Borel function. We say that $z \in \mathbb{R}$ is the *approximate limit* of u at x if for every $\varepsilon > 0$

$$\lim_{\rho \rightarrow 0^+} \rho^{-2} \mathcal{L}^2(\{y \in B_\rho(x) \cap \Omega : |u(y) - z| > \varepsilon\}) = 0,$$

where we denote by $\mathcal{L}^2(E)$ the 2-dimensional Lebesgue measure of E . We define the *jump set* $S(u)$ of function u as the subset of Ω where the approximate limit of u does not exist. It turns out that $S(u)$ is a Borel set and $\mathcal{L}^2(S(u)) = 0$. If $u \in BV(\Omega)$, then $S(u)$ is *countably 1-rectifiable*; that is, $S(u) = N \cup (\bigcup_{i \in \mathbb{N}} K_i)$, where $\mathcal{H}^1(N) = 0$, $\mathcal{H}^1(N)$ is the 1-dimensional Hausdorff measure of N and (K_i) is a sequence of compact sets, each contained in a C^1 hypersurface Γ_i . A *normal unit vector* ν_u to $S(u)$ exists \mathcal{H}^1 -almost everywhere on $S(u)$, in the sense that, if $S(u)$ is represented as above, then $\nu_u(x)$ is normal to Γ_i for \mathcal{H}^1 -almost everywhere $x \in K_i$.

Let E be a Borel subset of \mathbb{R}^2 . The *essential boundary* $\partial^* E$ of E is defined as

$$\partial^* E = \left\{ x \in \mathbb{R}^2 : \limsup_{\rho \rightarrow 0} \frac{\mathcal{L}^2(B_\rho(x) \cap E)}{\rho^2} > 0, \limsup_{\rho \rightarrow 0} \frac{\mathcal{L}^2(B_\rho(x) \setminus E)}{\rho^2} > 0 \right\}.$$

The set E is of *finite perimeter* in Ω if the characteristic function χ_E is in $BV(\Omega)$. The total variation $|D\chi_E|(\Omega)$ is the *perimeter* of E in Ω , denoted by $P(E; \Omega)$ (simply $P(E)$ if $\Omega = \mathbb{R}^2$). For \mathcal{H}^1 -almost every $x \in \partial^* E$, the limit

$$\nu_E(x) = \lim_{\rho \rightarrow 0} \frac{D\chi_E(B_\rho(x))}{|D\chi_E|(B_\rho(x))}$$

exists and belongs to $S^1 = \{|x| = 1\}$; the vector ν_E is the generalized *inner normal* to ∂^*E . The set of points $x \in \text{supp}(D\chi_E) \cap \Omega$ where this property holds is called the *reduced boundary* of E . For any x in the reduced boundary of E , the sets $(E - x)/\rho$ locally converge in measure as $\rho \rightarrow 0$ to the half-space orthogonal to $\nu_E(x)$ and containing $\nu_E(x)$. The measure $D\chi_E$ can be represented as

$$D\chi_E = \nu_E \mathcal{H}^1 \llcorner \partial^*E.$$

In particular, for every set E of finite perimeter in Ω , $P(E; \Omega) = \mathcal{H}^1(\partial^*E \cap \Omega)$.

Chapter 2

Minimizing movements along a sequence of functionals

The main results of this thesis rely on the definition and the properties of *minimizing movements along a sequence of functionals*. In order to provide the necessary introductory preparation, we will follow Braides [11], Chapters 7-8 and 10, for definitions, examples and the proofs of the theorems contained in this chapter.

2.1 Minimizing movements: definition and basic properties

We introduce a notion of energy-based motion which generalizes an implicit-time scheme for the approximation of solutions of gradient flows to general (also non differentiable) energies. We use the terminology of *minimizing movements*, introduced by De Giorgi (see [26]) and revisited by Ambrosio [4], even though we will not follow the precise notation used in the literature.

Definition 2.1.1 (minimizing movements). *Let X be a separable Hilbert space and let $F : X \rightarrow [0, +\infty]$ be coercive and lower-semicontinuous. Given $u_0 \in X$ and $\tau > 0$ we define recursively $u_k, k \geq 1$, as a minimizer of the problem*

$$\min \left\{ F(v) + \frac{1}{2\tau} \|v - u_{k-1}\|^2 \right\}, \quad (2.1)$$

and the piecewise-constant trajectory $u^\tau : [0, +\infty) \rightarrow X$ given by

$$u^\tau(t) = u_{\lfloor t/\tau \rfloor}. \quad (2.2)$$

A minimizing movement for F from u_0 is any limit of a subsequence u^{τ_j} uniform on compact sets of $[0, +\infty)$.

Note that we are not focusing on the general topological assumptions on function spaces and convergences. In this definition we have taken $F \geq 0$ and X Hilbert space for simplicity. More in general, we can take X a metric space and the power of the distance in place of the squared norm. In addition, the topology on X with respect to which F is lower semicontinuous can be weaker than the one of the related distance (see Ambrosio, Gigli and Savaré [7] for a more general theory).

Remark 2.1.2. A heuristic explanation of the definition above is given when F is smooth. In this case, with the due notation, a minimizer for (2.1) solves the equation

$$\frac{u_k - u_{k-1}}{\tau} = -\nabla F(u_k); \quad (2.3)$$

i.e., u^τ solves the equation

$$\frac{u^\tau(t) - u^\tau(t - \tau)}{\tau} = -\nabla F(u^\tau(t)). \quad (2.4)$$

If we can pass to the limit in this equation, as $u^\tau \rightarrow u$, then we obtain

$$\frac{\partial u}{\partial t} = -\nabla F(u). \quad (2.5)$$

This is easily shown to hold if $X = \mathbb{R}^n$ and $F \in C^2(\mathbb{R}^n)$. In this case, by taking any $\varphi \in C_0^\infty((0, T); \mathbb{R}^n)$ we have

$$\begin{aligned} -\int_0^T \langle \nabla F(u^\tau(t)), \varphi \rangle dt &= \int_0^T \left\langle \frac{u^\tau(t) - u^\tau(t - \tau)}{\tau}, \varphi \right\rangle dt \\ &= -\int_0^T \left\langle u^\tau(t), \frac{\varphi(t) - \varphi(t + \tau)}{\tau} \right\rangle dt, \end{aligned}$$

from which, passing to the limit

$$\int_0^T \langle \nabla F(u), \varphi \rangle dt = \int_0^T \langle u, \varphi' \rangle dt;$$

i.e., (2.5) is satisfied in the sense of distributions, and hence in the classical sense.

Definition 2.1.3 (local minimizer). A function u_0 is said to be a local minimizer of F if there exists $\delta > 0$ such that

$$F(u_0) \leq F(u) \quad \text{if} \quad \|u - u_0\| < \delta.$$

Remark 2.1.4 (stationary solutions). Let u_0 be a local minimizer for F , then the only minimizing movement for F from u_0 is the constant function $u(t) = u_0$.

Indeed, if u_0 is a minimizer for F on the set of v such that $\|v - u_0\| \leq \delta$, then by the positiveness of F it is the only minimizer of $F(v) + \frac{1}{2\tau}\|v - u_0\|^2$ for $\tau < \delta^2/F(u_0)$ if $F(u_0) > 0$ (for any τ if $F(u_0) = 0$). So that $u_k = u_0$ for all k for these τ .

Proposition 2.1.5 (existence of minimizing movements). For all F and u_0 as in Definition 2.1.1 there exists a minimizing movement $u \in C^{1/2}([0, +\infty); X)$.

Proof. By the coerciveness and lower-semicontinuity of F we obtain that u_k are well-defined for all k . Moreover, since

$$F(u_k) + \frac{1}{2\tau}\|u_k - u_{k-1}\|^2 \leq F(u_{k-1}),$$

we have $F(u_k) \leq F(u_{k-1})$ and

$$\|u_k - u_{k-1}\|^2 \leq 2\tau(F(u_{k-1}) - F(u_k)),$$

so that for $t > s$

$$\begin{aligned}
\|u^\tau(t) - u^\tau(s)\| &\leq \sum_{k=\lfloor s/\tau \rfloor + 1}^{\lfloor t/\tau \rfloor} \|u_k - u_{k-1}\| \\
&\leq \sqrt{\lfloor t/\tau \rfloor - \lfloor s/\tau \rfloor} \sqrt{\sum_{k=\lfloor s/\tau \rfloor + 1}^{\lfloor t/\tau \rfloor} \|u_k - u_{k-1}\|^2} \\
&\leq \sqrt{\lfloor t/\tau \rfloor - \lfloor s/\tau \rfloor} \sqrt{2\tau \sum_{k=\lfloor s/\tau \rfloor + 1}^{\lfloor t/\tau \rfloor} (F(u_{k-1}) - F(u_k))} \\
&\leq \sqrt{\lfloor t/\tau \rfloor - \lfloor s/\tau \rfloor} \sqrt{2\tau (F(u_{\lfloor s/\tau \rfloor}) - F(u_{\lfloor t/\tau \rfloor}))} \\
&\leq \sqrt{2F(u_0)} \sqrt{\tau(\lfloor t/\tau \rfloor - \lfloor s/\tau \rfloor)} \\
&\leq \sqrt{2F(u_0)} \sqrt{t - s + \tau}.
\end{aligned}$$

This shows that the functions u^τ are almost equicontinuous and equibounded in $C([0, +\infty); X)$. Hence, up to a subsequence, they converge uniformly. Moreover, passing to the limit as $\tau \rightarrow 0$ we obtain

$$\|u(t) - u(s)\| \leq \sqrt{2F(u_0)} \sqrt{|t - s|}$$

so that $u \in C^{1/2}([0, +\infty); X)$. □

2.2 Minimizing movements along a sequence

As remarked in Section 2.1, the definition of minimizing movement is usually given for a single functional F . Now we will introduce a parameter ε (often interpreted as a space-scale) and give a notion of minimizing movement along a sequence of functionals $\{F_\varepsilon\}_{\varepsilon>0}$, which will depend in general on the interaction between the time scale τ and the parameter ε in the energies.

Definition 2.2.1 (minimizing movements along a sequence). *Let X be a separable Hilbert space, let $F_\varepsilon : X \rightarrow [0, +\infty]$ be equicoercive and lower-semicontinuous, $u_0^\varepsilon \rightarrow u_0$ with*

$$F_\varepsilon(u_0^\varepsilon) \leq C < +\infty, \quad (2.6)$$

and let $\tau_\varepsilon > 0$ converge to 0 as $\varepsilon \rightarrow 0$. With fixed $\varepsilon > 0$, we define u_k^ε recursively as a minimizer for the problem

$$\min \left\{ F_\varepsilon(v) + \frac{1}{2\tau} \|v - u_{k-1}^\varepsilon\|^2 \right\}, \quad (2.7)$$

and the piecewise-constant trajectory $u^\varepsilon : [0, +\infty) \rightarrow X$ given by

$$u^\varepsilon(t) = u_{\lfloor t/\tau_\varepsilon \rfloor}^\varepsilon. \quad (2.8)$$

A minimizing movement for F_ε from u_0^ε is any limit of a subsequence u^{ε_j} uniform on compact sets of $[0, +\infty)$.

After remarking that the Hölder continuity estimates in Proposition 2.1.5 only depend on the bound on $F_\varepsilon(u_0^\varepsilon)$, with the same proof we can show the following result.

Proposition 2.2.2 (existence of minimizing movements). *For every F_ε and u_0^ε as above, there exist minimizing movements for F_ε from u_0^ε in $C^{1/2}([0, +\infty); X)$.*

Remark 2.2.3. The limit minimizing movement may depend on the choice of the mutual behavior of ε and τ . For example, we consider the functions

$$F_\varepsilon(x) = \begin{cases} -x & \text{if } x \leq 0 \\ 0 & \text{if } 0 \leq x \leq \varepsilon \\ \varepsilon - x & \text{if } x \geq \varepsilon, \end{cases}$$

which converge uniformly to $F(x) = -x$. Let x_0 be a fixed initial datum.

If $x_0 > 0$, then for $\varepsilon < x_0$ we have $x_k^\varepsilon = x_{k-1}^\varepsilon + \tau$ for all $k \geq 0$.

If $x_0 \leq 0$, then we have $x_k^\varepsilon = x_{k-1}^\varepsilon + \tau$ if $x_{k-1}^\varepsilon \leq -\tau$. If $0 \geq x_{k-1}^\varepsilon > -\tau$, then $x_k^\varepsilon - x_{k-1}^\varepsilon$ is obtained by minimizing the function

$$f(y) = \begin{cases} -y + \frac{1}{2\tau}y^2 & \text{if } 0 \leq y \leq -x_{k-1}^\varepsilon \\ x_{k-1}^\varepsilon + \frac{1}{2\tau}y^2 & \text{if } -x_{k-1}^\varepsilon \leq y \leq -x_{k-1}^\varepsilon + \varepsilon \\ \varepsilon - y + \frac{1}{2\tau}y^2 & \text{if } y \geq -x_{k-1}^\varepsilon, \end{cases}$$

whose minimizer is always $y = \tau + x_{k-1}^\varepsilon$ if $\varepsilon - x_{k-1}^\varepsilon > \tau$. In this case, $x_k^\varepsilon = 0$. If, otherwise, $\varepsilon - x_{k-1}^\varepsilon \leq \tau$, the other possible minimizer is $y = \tau$. We then have to compare the values

$$f(-x_{k-1}^\varepsilon) = x_{k-1}^\varepsilon + \frac{1}{2\tau}(x_{k-1}^\varepsilon)^2, \quad f(\tau) = \varepsilon - \frac{1}{2}\tau.$$

We have three cases:

- (a) $\varepsilon - \frac{1}{2}\tau > 0$. In this case, we have $x_k^\varepsilon = 0$ (and this holds for all subsequent steps);
- (b) $\varepsilon - \frac{1}{2}\tau < 0$. In this case, we either have $f(\tau) < f(x_{k-1}^\varepsilon)$, in which case $x_k^\varepsilon = x_{k-1}^\varepsilon + \tau$ (and this then holds for all subsequent steps); otherwise $x_k^\varepsilon = 0$ and $x_{k+1}^\varepsilon = x_k^\varepsilon + \tau$ (and this holds for all subsequent steps);
- (c) $\varepsilon - \frac{1}{2}\tau = 0$. If $x_{k-1}^\varepsilon < 0$ then $x_k^\varepsilon = 0$ (otherwise we already have $x_{k-1}^\varepsilon = 0$).

Then, since we have the two solutions $y = 0$ and $y = \tau$, we have $x_j^\varepsilon = 0$ for $k \leq j \leq k_0$ for some $k_0 \in \mathbb{N} \cup \{+\infty\}$ and $x_j^\varepsilon = x_{j-1}^\varepsilon + \tau$ for $j > k_0$.

We can summarize the possible minimizing movements with initial datum $x_0 \leq 0$ as follows:

- (i) If $\tau < 2\varepsilon$, then the unique minimizing movement is $x(t) = \min\{x_0 + t, 0\}$;
- (ii) If $\tau > 2\varepsilon$, then the unique minimizing movement is $x(t) = x_0 + t$;
- (iii) If $\tau = 2\varepsilon$, then we have the family of minimizing movements (parametrized by $x_1 \leq x_0$) $x(t) = \max\{\min\{x_0 + t, 0\}, x_1 + t\}$.

For $x_0 > 0$ we always have the only minimizing movement $x(t) = x_0 + t$.

2.3 Commutability along ‘fast-converging’ sequences

We now show that, by suitably choosing the ε - τ regimes, the minimizing movement along the sequence F_ε from u_ε converges to a minimizing movement for the limit F from u_0 (‘fast-converging ε ’), while for other choices (‘fast-converging τ ’) the minimizing movement converges to a limit of minimizing movements for F_ε as $\varepsilon \rightarrow 0$. As an heuristic remark, we can say that minimizing movements for all other regimes are ‘trapped’ between these two extrema.

Theorem 2.3.1 (“extreme” asymptotic behaviours). *Let F_ε be a equi-coercive sequence of non-negative lower-semicontinuous functionals on a Hilbert space X Γ -converging to F , let $u_\varepsilon \rightarrow u_0$. Then*

- (i) *there exists a choice of $\varepsilon = \varepsilon(\tau)$ such that every minimizing movement along F_ε , with time-step τ and initial data u_ε , is a minimizing movement for F from u_0 on $[0, T]$ for all T ;*
- (ii) *there exists a choice of $\tau = \tau(\varepsilon)$ such that every minimizing movement along F_ε , with time-step τ and initial data u_ε , is the limit of a sequence of minimizing movements for F_ε (for ε fixed) from u_ε on $[0, T]$ for all T .*

Proof. (i) We first note that, if $u_\varepsilon \rightarrow u_0$, then the solutions of

$$\min \left\{ F_\varepsilon(u) + \frac{1}{2\tau} \|u - u_\varepsilon\|^2 \right\} \quad (2.9)$$

converge, as $\varepsilon \rightarrow 0$, to solutions of

$$\min \left\{ F(u) + \frac{1}{2\tau} \|u - u_0\|^2 \right\} \quad (2.10)$$

since we have a continuously converging perturbation of a Γ -converging sequence (see Proposition 1.1.3 and Theorem 1.1.6).

Let $u_\varepsilon \rightarrow u_0$ and $\tau > 0$ be fixed. We consider the sequence $\{u_k^{\tau, \varepsilon}\}$ defined by iterated minimization of F_ε with initial point u_ε , as in (2.9). Since $u_\varepsilon \rightarrow u_0$, up to subsequences we have $u_1^{\tau, \varepsilon} \rightarrow u_1^{\tau, 0}$, which minimizes

$$\min \left\{ F(u) + \frac{1}{2\tau} \|u - u_0\|^2 \right\}. \quad (2.11)$$

The points $u_2^{\tau, \varepsilon}$ converge to $u_2^{\tau, 0}$. Since they minimize

$$\min \left\{ F_\varepsilon(u) + \frac{1}{2\tau} \|u - u_1^{\tau, \varepsilon}\|^2 \right\} \quad (2.12)$$

and $u_1^{\tau,\varepsilon} \rightarrow u_1^{\tau,0}$, their limit is a minimizer of

$$\min \left\{ F(u) + \frac{1}{2\tau} \|u - u_1^{\tau,0}\|^2 \right\}. \quad (2.13)$$

This operation can be repeated iteratively, obtaining (upon subsequences) $u_k^{\tau,\varepsilon} \rightarrow u_k^{\tau,0}$ and $\{u_k^{\tau,0}\}$ iteratively minimizes F with initial point u_0 . Since, up to subsequences, the trajectories $\{u_k^{\tau,0}\}$ converge to a minimizing movement for F with initial datum u_0 , the thesis follows by a diagonal argument.

(ii) For fixed ε , the piecewise-constant functions $u^{\varepsilon,\tau}(t) = u_{\lfloor t/\tau \rfloor}^{\varepsilon,\tau}$ converge uniformly to a minimizing movement u^ε for F_ε with initial datum u_ε . By compactness, these u^ε converge uniformly to some function u as $\varepsilon \rightarrow 0$. Again, we conclude by a diagonal argument. \square

2.4 Homogenization of minimizing movements

We now examine minimizing movements along oscillating sequences (with many local minima), treating two model cases in the real line. These examples seem to be interesting in view of Chapters 4-6 about homogenization of geometric minimizing movements.

Example 2.4.1 (minimizing movements for piecewise-constant energies). We apply the minimizing-movement scheme (2.7)-(2.8) to the functions

$$F_\varepsilon(x) = - \left\lfloor \frac{x}{\varepsilon} \right\rfloor \varepsilon \quad (2.14)$$

converging to $F(x) = -x$. This is a prototype of a function with many local minimizers (actually, in this case all points are local minimizers) converging to a function with few local minimizers (actually, none).

Note that, with fixed ε , for any initial datum x_0 the minimizing movement for F_ε is trivial: $u(t) = x_0$, since all points are local minimizers (see Remark 2.1.4). Conversely, the corresponding minimizing movement for the limit is $u(t) = x_0 + t$.

We now fix an initial datum x_0 , the space-scale ε and the time-scale τ , and examine the successive-minimization scheme from x_0 . Note that it is not restrictive to suppose that $0 \leq x_0 < 1$, up to a translation in $\varepsilon\mathbb{Z}$.

The first minimization giving x_1 is

$$\min \left\{ F_\varepsilon(x) + \frac{1}{2\tau} (x - x_0)^2 \right\}; \quad (2.15)$$

note that the function to minimize equals $-x + \frac{1}{2\tau} (x - x_0)^2$ if $x \in \varepsilon\mathbb{Z}$.

Apart some singular cases that we deal separately below, we have two possibilities:

(i) If $\frac{\tau}{\varepsilon} < \frac{1}{2}$, then the motion is trivial. The value $1/2$ is the ‘pinning threshold’.

Indeed, after setting $x_0 = s\varepsilon$ with $0 \leq s < 1$, we have two sub-cases:

- (a) the minimizer x_1 belongs to $[0, \varepsilon)$. This occurs exactly if $F_\varepsilon(x) + \frac{1}{2\tau}(\varepsilon - x_0)^2 > 0$; i.e.,

$$\tau < \frac{(s-1)^2\varepsilon}{2}. \quad (2.16)$$

In this case, the only minimizer is the initial datum x_0 . This implies that we have $x_k = x_0$ for all k .

- (b) we have that $x_1 = \varepsilon$. This implies that, up to a translation, we are in the case $x_0 = 0$ with $s = 0$, and (2.16) holds since $\tau < \frac{\varepsilon}{2}$. Hence, $x_k = x_1$ for all $k \geq 1$;
- (ii) If $\frac{\tau}{\varepsilon} > \frac{1}{2}$, then for ε small the minimum is taken on $\varepsilon\mathbb{Z}$. So that again we may suppose that $x_0 = 0$.

Note that we are leaving out for the time being the case when $x_0 = 0$ and $\frac{\tau}{\varepsilon} = \frac{1}{2}$. In that case we have a double choice for the minimizer; such situations will be examined separately.

If $x_0 = 0$ then x_1 is computed by solving

$$\min \left\{ F_\varepsilon(x) + \frac{1}{2\tau}x^2 : x \in \varepsilon\mathbb{Z} \right\}, \quad (2.17)$$

and is characterized by

$$x_1 - \frac{1}{2}\varepsilon \leq \tau \leq x_1 + \frac{1}{2}\varepsilon. \quad (2.18)$$

We then have

$$x_1 = \left\lfloor \frac{\tau}{\varepsilon} + \frac{1}{2} \right\rfloor \varepsilon \quad \text{if } \frac{\tau}{\varepsilon} + \frac{1}{2} \notin \mathbb{Z} \quad (2.19)$$

(note again that we have two solutions for $\frac{\tau}{\varepsilon} + \frac{1}{2} \in \mathbb{Z}$, which also includes the case $\frac{\tau}{\varepsilon} = \frac{1}{2}$ already set aside, and we examine those cases separately). The same computation is repeated at each k giving

$$\frac{x_k - x_{k-1}}{\tau} = \left\lfloor \frac{\tau}{\varepsilon} + \frac{1}{2} \right\rfloor \frac{\varepsilon}{\tau}. \quad (2.20)$$

We can now choose τ and ε tending to 0 simultaneously and pass to the limit. The behaviour of the limit minimizing movements is governed by the quantity

$$w = \lim_{\varepsilon \rightarrow 0} \frac{\tau}{\varepsilon}, \quad (2.21)$$

which we may suppose exists, up to subsequences. If $w + \frac{1}{2} \notin \mathbb{Z}$ then the minimizing movement along F_ε from x_0 is uniquely defined by

$$u(t) = x_0 + vt, \quad \text{with } v = \left\lfloor w + \frac{1}{2} \right\rfloor \frac{1}{w}, \quad (2.22)$$

so that the whole sequence converges if the limit in (2.21) exists. Note that

- **(pinning)** we have $v = 0$ when $\frac{\tau}{\varepsilon} < \frac{1}{2}$ for ε small. In particular, this holds for $\tau \ll \varepsilon$ (i.e., for $w = 0$);

- **(limit motion for slow times)** if $\varepsilon \ll \tau$ then the motion coincides with the gradient flow of the limit, with velocity 1;
- **(discontinuous dependence of the velocity)** the velocity is a discontinuous function of w at points of $\frac{1}{2} + \mathbb{Z}$. Note, moreover, that it may be actually greater than the limit velocity 1;
- **(non-uniqueness at $w \in \frac{1}{2} + \mathbb{Z}$)** in these exceptional cases we may have either of the two velocities $1 + \frac{1}{2w}$ or $1 - \frac{1}{2w}$ in the cases $\frac{\varepsilon}{\tau} + \frac{1}{2} > w$ or $\frac{\varepsilon}{\tau} + \frac{1}{2} < w$ for all ε small, respectively, but we may also have any $u(t)$ with

$$1 - \frac{1}{2w} \leq u'(t) \leq 1 + \frac{1}{2w}$$

if we have precisely $\frac{\varepsilon}{\tau} + \frac{1}{2} = w$ for all ε small, since in this case, at every time step, we may choose any of the two minimizers giving the extremal velocities, and then obtain any such u' as a weak limit of piecewise-constant functions taking only those two values. Note therefore that in this case the limit is not determined only by w , and in particular it may depend on the subsequence even if the limit (2.21) exists.

Example 2.4.2 (a heterogeneous case). We now examine a variation of the previous example obtained by introducing a heterogeneity parameter $1 \leq \lambda \leq 2$ and defining

$$F^\lambda(x) = \begin{cases} -2 \left\lfloor \frac{x}{2} \right\rfloor & \text{if } 2 \left\lfloor \frac{x}{2} \right\rfloor \leq x < 2 \left\lfloor \frac{x}{2} \right\rfloor + \lambda \\ -2 \left\lfloor \frac{x}{2} \right\rfloor & \text{if } 2 \left\lfloor \frac{x}{2} \right\rfloor + \lambda \leq x < 2 \left\lfloor \frac{x}{2} \right\rfloor + 1. \end{cases} \quad (2.23)$$

Note that if $\lambda = 1$ we are in the previous situation.

We apply the minimizing-movement scheme to the functions

$$F_\varepsilon(x) = F_\varepsilon^\lambda(x) = \varepsilon F^\lambda\left(\frac{x}{\varepsilon}\right).$$

Arguing as above, we can reduce to the two cases

$$(a) \quad x_k \in 2\varepsilon\mathbb{Z}, \quad \text{or} \quad (b) \quad x_k \in 2\varepsilon\mathbb{Z} + \varepsilon\lambda. \quad (2.24)$$

Taking into account that x_{k+1} is determined as the point in $2\varepsilon\mathbb{Z} \cup (2\varepsilon\mathbb{Z} + \varepsilon\lambda)$ closer to τ (as above, we only consider the cases when we have a unique solution to the minimum problems in the iterated procedure), we can characterize it as follows.

In case (a) we have the two sub cases:

(a₁) if we have

$$2n < \frac{\tau}{\varepsilon} - \frac{\lambda}{2} < 2n + 1$$

for some $n \in \mathbb{N}$ then

$$x_{k+1} = x_k + (2n + \lambda)\varepsilon.$$

In particular, $x_{k+1} \in 2\varepsilon\mathbb{Z} + \varepsilon\lambda$;
 (a₂) if we have

$$2n - 1 < \frac{\tau}{\varepsilon} - \frac{\lambda}{2} < 2n$$

for some $n \in \mathbb{N}$ then

$$x_{k+1} = x_k + 2n\varepsilon.$$

In particular, $x_{k+1} \in 2\varepsilon\mathbb{Z}$. Note that $x_{k+1} = x_k$ (pinning) if $\frac{\tau}{\varepsilon} < \frac{\lambda}{2}$.

In case (b) we have the two sub cases:
 (b₁) if we have

$$2n < \frac{\tau}{\varepsilon} + \frac{\lambda}{2} < 2n + 1$$

for some $n \in \mathbb{N}$ then

$$x_{k+1} = x_k + 2n\varepsilon.$$

In particular, $x_{k+1} \in 2\varepsilon\mathbb{Z} + \varepsilon\lambda$. Note that $x_{k+1} = x_k$ (pinning) if $\frac{\tau}{\varepsilon} < 1 - \frac{\lambda}{2}$, which is implied by the pinning condition in (a₂);
 (b₂) if we have

$$2n - 1 < \frac{\tau}{\varepsilon} + \frac{\lambda}{2} < 2n$$

for some $n \in \mathbb{N}$ then

$$x_{k+1} = x_k + 2n\varepsilon - \varepsilon\lambda.$$

In particular, $x_{k+1} \in 2\varepsilon\mathbb{Z}$.

Eventually, we have the two cases:

(1) when

$$\left| \frac{\tau}{\varepsilon} - 2n \right| < \frac{\lambda}{2}$$

for some $n \in \mathbb{N}$ then, after possibly one iteration, we are either in the case (a₂) or (b₁). Hence, either $x_k \in 2\varepsilon\mathbb{Z}$ or $x_k \in 2\varepsilon\mathbb{Z} + \varepsilon\lambda$ for all k . The velocity in this case is then

$$\frac{x_{k+1} - x_k}{\tau} = 2n \frac{\varepsilon}{\tau};$$

(2)

$$\left| \frac{\tau}{\varepsilon} - (2n + 1) \right| < 1 - \frac{\lambda}{2}$$

for some $n \in \mathbb{N}$ then we are alternately in case (a₁) or (b₂). In this case we have an *averaged velocity*: the speed of the orbit $\{x_k\}$ oscillates between two values with an average speed given by

$$\frac{x_{k+2} - x_k}{2\tau} = \frac{2n\varepsilon + \lambda\varepsilon}{2\tau} + \frac{2(n+1)\varepsilon - \lambda\varepsilon}{2\tau} = 2(n+1) \frac{\varepsilon}{\tau}.$$

This is an additional feature with respect to the previous example.

Summarizing, if we define w as in (2.21) then (taking into account only the cases with a unique limit) the minimizing movement along the sequence F_ε with initial datum x_0 is given by $x(t) = x_0 + vt$ with $v = \frac{1}{w}f(w)$, and f is given by

$$f(w) = \begin{cases} 2n & \text{if } |w - 2n| \leq \frac{\lambda}{2}, n \in \mathbb{N} \\ 2n + 1 & \text{if } |w - (2n + 1)| < 1 - \frac{\lambda}{2}, n \in \mathbb{N}. \end{cases}$$

Note that the pinning threshold is now $\lambda/2$. We can compare this minimizing movement with the one given in (2.22): for $2n + 1/2 < w < 2n + \lambda/2$ the new minimizing movement is slower, while for $2n + 2 - \lambda/2 < w < 2n + 2 - 1/2$ it is faster.

2.5 A scaling of the energies is a time-scaling

In this and the next section, we give some preliminary remarks useful for the definition of a *backward* (i.e., reversed time) motion in Chapter 7.

We introduce a new parameter $\lambda > 0$ and follow the iterative minimizing scheme from an initial datum u_0 by considering $u_k, k \geq 1$ defined recursively as a minimizer of

$$\min \left\{ \frac{1}{\lambda} F_\varepsilon(v) + \frac{1}{2\tau} \|v - u_{k-1}\|^2 \right\}, \quad (2.25)$$

and setting $u^\tau(t) = u^{\tau, \lambda}(t) = u_{\lfloor t/\tau \rfloor}$. Equivalently, we may view this as applying the minimizing-movement scheme to

$$\min \left\{ F_\varepsilon(v) + \frac{\lambda}{2\tau} \|v - u_{k-1}\|^2 \right\}. \quad (2.26)$$

We may compare this scheme with the one for unscaled energies, where u_k are defined as minimizers of minimizing-movement scheme with time scale $\eta = \tau/\lambda$. This other scheme gives a function u^η which is a discrete function on a lattice of lattice step η . Then we have

$$u^\tau(t) = u_{\lfloor t/\tau \rfloor} = u_{\lfloor t/\lambda\eta \rfloor} = u^\eta\left(\frac{t}{\lambda}\right).$$

Hence, the scaling of the energies F_ε by λ corresponds to a scaling of time in the minimizing-movement scheme.

2.6 Negative scaling and discrete approximation: backward motions

In a finite-dimensional setting, a condition that ensures the possibility of defining a minimizing movement for a functional F is that

$$u \rightarrow F(u) + \frac{1}{2\tau} |u - \bar{u}|^2 \quad (2.27)$$

be lower semicontinuous and coercive for all \bar{u} and for τ sufficiently small. This is not in contrast with requiring that also

$$u \rightarrow -F(u) + \frac{1}{2\tau}|u - \bar{u}|^2 \quad (2.28)$$

satisfy the same conditions; for example if F is continuous and of quadratic growth. This can be seen as a further extension of the time-scaling argument in Section 2.5, with $\lambda = -1$. If the iterative scheme (2.27) gives a solution for the gradient flow,

$$\begin{cases} u'(t) = \nabla F(u(t)) & \text{for } t \geq 0 \\ u(0) = u_0. \end{cases}$$

a minimizing movement v for the second scheme produces a solution $v(t) = u(-t)$ to the backward problem

$$\begin{cases} v'(t) = -\nabla F(v(t)) & \text{for } t \leq 0 \\ v(0) = u_0. \end{cases}$$

In an infinite-dimensional setting the two requirements of being able to define both the minimizing movement (2.27) and (2.28) greatly limits the choice of F , and rules out all interesting cases. A possible approach to the definition of a backward minimizing movement is then to introduce a finite-dimensional or discrete approximation F_ε to F , for which we can define a minimizing movement along $-F_\varepsilon$.

Chapter 3

Geometric minimizing movements

In view of the results about the motion of discrete interfaces contained in the next chapters, we now examine some minimizing movements describing the motion of sets: the *geometric minimizing movements*. Such a motion can be framed in the setting of the previous chapter after identification of a set E with its characteristic function $u = \chi_E$. The energies we are going to consider are of perimeter type; i.e., with

$$F(E) = \mathcal{H}^1(\partial E) \quad (3.1)$$

as a prototype in the notation of the previous chapter. Here we follow Braides [11], Chapter 9.

3.1 Motion by mean curvature

The prototype of a geometric motion is *motion by mean curvature*; i.e., a family of sets $E(t)$ whose boundary moves in the normal direction with velocity proportional to its curvature (inwards in convex regions and outwards in concave regions). In the simplest case of initial datum a ball in \mathbb{R}^2 , $E(0) = E_0 = B_{R_0}(0)$, the motion is given by concentric balls with radii satisfying

$$\begin{cases} \dot{R}(t) = -\frac{c}{R(t)} \\ R(0) = R_0; \end{cases} \quad (3.2)$$

i.e., $R(t) = \sqrt{R_0^2 - 2ct}$, valid until the *extinction time* $T = R_0^2/2c$, when the radius vanishes.

A heuristic argument suggests that the variation of the perimeter be linked to the notion of curvature; hence, we expect to be able to obtain motion by mean curvature as a minimizing movement for the perimeter functional. We will see that, in order to obtain geometric motions as minimizing movements, we will have to modify the procedure described in the previous chapter.

Example 3.1.1 (pinning for the perimeter motion). We apply the minimizing-movement procedure to the perimeter functional (3.1) with initial datum $E_0 = B_{R_0}(0)$ in \mathbb{R}^2 . With fixed τ , since

$$\int_{\mathbb{R}^2} |\chi_A - \chi_B|^2 dx = |A \triangle B|,$$

the minimization to determine E_1 is

$$\min \left\{ \mathcal{H}^1(\partial E) + \frac{1}{2\tau} |E \triangle E_0| \right\}. \quad (3.3)$$

We note that we can restrict our analysis to sets E contained in E_0 , since otherwise taking $E \cap E_0$ as test sets in their place would decrease both terms in the minimization. Once this is observed, we also note that, given $E \subset E_0$, if $B_R(x) \subset E_0$ has the same measure as E then, by the isoperimetric inequality, it decreases the perimeter part of the energy (strictly, if E itself is not a ball) while keeping the second term fixed. Hence, we can limit our analysis to balls $B_R(x) \subset E_0$, for which the energy depends only on R . The incremental problem is then given by

$$\min \left\{ 2\pi R + \frac{\pi}{2\tau} (R_0^2 - R^2) : 0 \leq R \leq R_0 \right\}, \quad (3.4)$$

whose minimizer is either $R = 0$ (with value $\frac{\pi}{2\tau} R_0^2$) or $R = R_0$ (with value $2\pi R_0$), since in (3.4) we are minimizing a concave function of R . For τ small the minimizer is then R_0 . This means that the motion is trivial: $E_k = E_0$ for all k , and hence also the resulting minimizing movement is trivial.

3.2 A variational approach to curvature-driven motion

In order to obtain motion by curvature, Almgren, Taylor and Wang [3] have introduced a variation of the implicit-scheme described above, where the term $|E \triangle E_k|$ is substituted by an integral term which favours variations which are ‘uniformly distant’ to the boundary of E_k . The problem defining E_k is then

$$\min \left\{ \mathcal{H}^1(\partial E) + \frac{1}{\tau} \int_{E \triangle E_{k-1}} \text{dist}(x, \partial E_{k-1}) dx \right\}, \quad (3.5)$$

where $\text{dist}(\cdot, A)$ denotes the euclidean distance from the set A . Note that the integral term can be interpreted as an L^2 -distance between the boundaries of the sets.

We will check the convergence of this scheme to the mean-curvature motion for $E_0 = B_{R_0}$ in \mathbb{R}^2 .

In this case, we note that if E_{k-1} is a ball centered in 0 then we have

- E_k is contained in E_{k-1} . To check this, note that, given a test set E , considering $E \cap E_{k-1}$ as a test set in its place decreases the energy in (3.5), strictly if $E \setminus E_{k-1} \neq \emptyset$;
- E_k is convex with baricenter in 0. For this, note first that each connected component of E_k is convex. Otherwise, considering the convex envelopes

decreases the energy (strictly, if one of the connected components is not convex). Then note that if 0 is not the baricenter of a connected component of E_k , then a small translation towards 0 strictly decreases the energy (this follows by computing the derivative of the volume term along the translation). In particular, we only have one (convex) connected component.

From these properties we can conclude that E_k is indeed a ball centered in 0. Were it not so, there would be a line through 0 such that the boundary of E_k does not intersect perpendicularly this line. By a reflection argument we then obtain a non-convex set \tilde{E}_k with total energy not greater than the one of E_k (note that the line considered subdivides E_k into two subsets with equal total energy). Its convexification would then strictly decrease the energy. This shows that each E_k is of the form

$$E_k = B_{R_k} = B_{R_k}(0).$$

We can now compute the equation satisfied by R_k , by minimizing (after passing to polar coordinates)

$$\min \left\{ 2\pi R + \frac{2\pi}{\tau} \int_R^{R_{k-1}} (R_{k-1} - \rho) \rho \, d\rho \right\}, \quad (3.6)$$

which gives

$$\frac{R_k - R_{k-1}}{\tau} = -\frac{1}{R_k}. \quad (3.7)$$

Passing to the limit gives the desired mean curvature equation (3.2).

3.3 Motion by crystalline curvature

We now consider the functional

$$F(E) = \int_{\partial^* E} \|\nu\|_1 \, d\mathcal{H}^1, \quad (3.8)$$

defined on all sets of finite perimeter (ν denotes the normal to $\partial^* E$), which is called *crystalline perimeter*. A minimizing movement for F is called a *flat flow*.

The incremental problems for the minimizing-movement scheme for F in (3.8) are of the form

$$\min \left\{ F(E) + \frac{1}{\tau} \int_{E \triangle E_{k-1}} \text{dist}_\infty(x, \partial E_{k-1}) \, dx \right\}, \quad (3.9)$$

where, for technical reasons, we consider the ∞ -distance

$$\text{dist}_\infty(x, B) = \inf \{ \|x - y\|_\infty : y \in B \}.$$

We only consider the case when the initial datum E_0 is a rectangle, and we show that the flat flow is the motion by crystalline curvature (see Almgren and Taylor [2], Taylor [47]). We can prove that if E_{k-1} is a rectangle, then we can limit the computation in (3.9) to

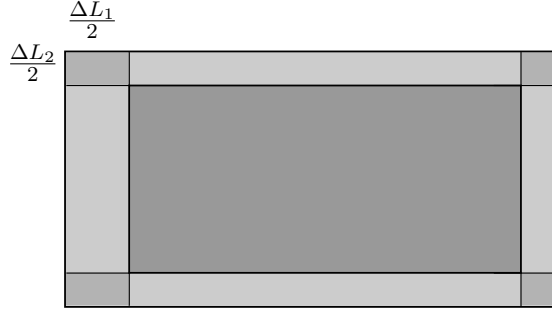


Figure 3.1. Incremental crystalline minimization.

- E contained in E_{k-1} , otherwise $E \cap E_{k-1}$ strictly decreases the energy;
- E with each connected component a rectangle, otherwise taking the least rectangle containing a given component would decrease the energy, strictly if E is not a rectangle;
- E connected and with the same center as E_0 , since translating the center towards 0 decreases the energy.

Hence, we may suppose that

$$E_k = \left[-\frac{L_{k,1}}{2}, \frac{L_{k,1}}{2} \right] \times \left[-\frac{L_{k,2}}{2}, \frac{L_{k,2}}{2} \right]$$

for all k . In order to iteratively determine $L_{k,j}$, we have to minimize the energy

$$\min \left\{ 2(L_{k,1} + \Delta L_1) + 2(L_{k,2} + \Delta L_2) + \frac{1}{\tau} \int_{E \triangle E_{k-1}} \text{dist}_\infty(x, \partial E_{k-1}) dx \right\}. \quad (3.10)$$

For τ small, the integral term in (3.10) can be substituted by

$$2 \left[\frac{L_{k,1}}{4} (\Delta L_2)^2 + \frac{L_{k,2}}{4} (\Delta L_1)^2 \right].$$

This argument amounts to noticing that the contribution of the small rectangles at the corners highlighted in Fig. 3.1 is negligible as $\tau \rightarrow 0$. The optimal decrements ΔL_j are then determined by the conditions

$$\begin{cases} 1 + \frac{L_{k,2}}{4\tau} \Delta L_1 = 0 \\ 1 + \frac{L_{k,1}}{4\tau} \Delta L_2 = 0. \end{cases} \quad (3.11)$$

Hence, we have the difference equations

$$\frac{\Delta L_1}{\tau} = -\frac{4}{L_{k,2}}, \quad \frac{\Delta L_2}{\tau} = -\frac{4}{L_{k,1}}, \quad (3.12)$$

which finally gives the system of differential equations for the limit rectangles, with edges of length $L_1(t)$ and $L_2(t)$, respectively, solving

$$\begin{cases} \dot{L}_1(t) = -\frac{4}{L_2(t)} \\ \dot{L}_2(t) = -\frac{4}{L_1(t)}. \end{cases} \quad (3.13)$$

From a geometrical point of view, this means that each edge of the rectangle moves inwards with velocity inversely proportional to its length; more precisely, equal to twice the inverse of its length (so that the other edge contracts with twice this velocity). Hence, the inverse of the length of an edge plays the role of the curvature in this context, the *crystalline curvature*.

Note that by (3.13) all rectangles are homothetic, since $\frac{d}{dt} \frac{L_1}{L_2} = 0$, and with area satisfying

$$\frac{d}{dt} L_1 L_2 = -8,$$

so that $L_1(t)L_2(t) = L_{0,1}L_{0,2} - 8t$, which gives the extinction time $t = L_{0,1}L_{0,2}/8$. In the case of an initial datum a square of side length L_0 , the sets are squares whose side length at time t is given by $L(t) = \sqrt{L_0^2 - 8t}$, in analogy with the evolution of balls by mean curvature flow (Section 3.1).

Chapter 4

Motion of discrete interfaces in homogeneous media

In this chapter we present the results contained in the paper by Braides, Gelli and Novaga [14], where the Almgren-Taylor-Wang approach of Section 3.2 has been used coupled to a homogenization procedure to study the variational motion of discrete interfaces driven by ferromagnetic interactions.

4.1 Lattice energies as interfacial energies

We consider the simplest *lattice energy*, that is, depending on a discrete variable $u = \{u_i\}$ indexed by the nodes i of the standard lattice \mathbb{Z}^2 , given by

$$P(u) = \frac{1}{4} \sum_{|i-j|=1} (u_i - u_j)^2, \quad (4.1)$$

where u_i takes only the two values $+1$ and -1 (*spin systems*). Note that its density only differs by constants from the usual ferromagnetic energy density $-u_i u_j$. After identifying a function u with the set E obtained as the union of all closed unit squares with centers i such that $u_i = 1$, the energy P can be rewritten as a perimeter functional

$$P(E) = \mathcal{H}^1(\partial E), \quad (4.2)$$

and hence can be interpreted as an interfacial energy.

We are interested in energy-driven motions deriving from this type of functional, but since no motion by gradient flow is directly possible in the discrete environment (as all u are isolated points), we perform an analysis in a discrete-to-continuous framework, where we scale the lattice and the energy P by introducing a small parameter ε .

As a result, we have the scaled energies

$$P_\varepsilon(u) = \frac{1}{4} \sum_{|i-j|=\varepsilon} \varepsilon (u_i - u_j)^2, \quad (4.3)$$

where $u : \varepsilon\mathbb{Z}^2 \rightarrow \{\pm 1\}$. This functional may again be identified with the perimeter

$$P_\varepsilon(E) = \mathcal{H}^1(\partial E), \quad (4.4)$$

with the constraint that E be the union of squares of side length ε .

In the associated Almgren, Taylor and Wang scheme, the perimeters and the distances depend on a small parameter ε , and consequently, after introducing a time scale τ , the time-discrete motions are the $E_k^{\tau,\varepsilon}$, $k \geq 1$ defined iteratively by

$$E_k^{\tau,\varepsilon} \text{ is a minimizer of } \min \left\{ P_\varepsilon(E) + \frac{1}{\tau} D_\varepsilon(E, E_{k-1}^{\tau,\varepsilon}) \right\}, \quad (4.5)$$

D_ε being a suitable distance between sets (see Section 4.3). The time-continuous limit $E(t)$ of $\{E_k^{\tau,\varepsilon}\}$ then may depend how mutually ε and τ tend to 0, and this problem can be cast in the general framework of *minimizing movements along a Γ -converging sequence* (see Chapter 2, Section 2.2). In particular, the limit motion will be pinned if $\tau \ll \varepsilon$ suitably fast (in a sense, we can pass to the limit in τ first and then apply the Almgren-Taylor-Wang approach). On the contrary, if $\varepsilon \ll \tau$ fast enough then the limit E will be the evolution related to the limit P , which is the crystalline perimeter (4.10) (again, in a sense, in this case we can pass to the limit in ε first). Hence, the critical regime $\tau \sim \varepsilon$ is more interesting and captures the main features of the motion. The relevant case for the description of the motion is that of initial data coordinate rectangles, since the motion of more general sets can be reduced to the study of this one.

Overview of the chapter. In Section 4.2 we define the discrete ‘ferromagnetic-type’ energies that we will consider. In Section 4.3 we define the discrete distance term in the energy and formulate the minimization scheme, showing that the limit motion depends on the ε - τ regime chosen. Section 4.4 contains the description of the convergence of the discrete scheme, at the critical regime, in the case of initial data coordinate rectangles. The evolve of a coordinate rectangle by minimization of the energy is a coordinate rectangle, and the velocity of each side is quantized and uniquely determined, up to a discrete set of side-lengths (Theorem 4.4.1). In case of uniqueness, the limit motion (Theorem 4.4.2) is described by a system of degenerate differential equations, whose right hand sides are discontinuous functions of the curvature. A comparison with the crystalline motion is contained in Remark 4.4.3, showing new features due to discreteness of the problem. In Section 4.5 we recall the extension of the previous results to the case of initial data coordinate polyrectangles, which is the first step to treat the case of more general initial sets.

4.2 Homogeneous ferromagnetic energies on discrete sets

We recall in details the definition of the energies (4.3), given in a more general framework with respect to Braides, Gelli and Novaga [14].

Let $\alpha > 0$ ($\alpha = 1$ in [14]). With fixed space mesh $\varepsilon > 0$, for a set of indices $\mathcal{I} \subset \varepsilon\mathbb{Z}^2$ we consider the energy

$$P_\varepsilon^\alpha(\mathcal{I}) = \alpha\varepsilon \# \{(i, j) \in \varepsilon\mathbb{Z}^2 \times \varepsilon\mathbb{Z}^2 : i \in \mathcal{I}, j \notin \mathcal{I}, |i - j| = \varepsilon\}. \quad (4.6)$$

In order to study the continuous limit as $\varepsilon \rightarrow 0$ of these energies, it will be convenient to identify each subset of $\varepsilon\mathbb{Z}^2$ with a measurable subset of \mathbb{R}^2 (namely, unions of ε -squares), in such a way that equi-boundedness of the energies implies pre-compactness

of such sets in the sense of sets of finite perimeter. This identification is as follows: we denote by $Q = [-1/2, 1/2]^2$ the closed coordinate unit square of center 0; if $\varepsilon > 0$ and $i \in \varepsilon\mathbb{Z}^2$, we denote by $Q_\varepsilon(i) = i + \varepsilon Q$ the closed coordinate square with side length ε and centered in i . To a set of indices $\mathcal{I} \subset \varepsilon\mathbb{Z}^2$, we associate the set

$$E_{\mathcal{I}} = \bigcup_{i \in \mathcal{I}} Q_\varepsilon(i). \quad (4.7)$$

The space of *admissible sets* related to indices in the two-dimensional square lattice is then defined by

$$\mathcal{D}_\varepsilon := \left\{ E \subseteq \mathbb{R}^2 : E = E_{\mathcal{I}} \text{ for some } \mathcal{I} \subseteq \varepsilon\mathbb{Z}^2 \right\}. \quad (4.8)$$

We note that the value of the energy $P_\varepsilon^\alpha(\mathcal{I})$ is the same as the perimeter (up to multiply it by α) of the corresponding set $E_{\mathcal{I}} \in \mathcal{D}_\varepsilon$, so that it can be thought as a *discrete perimeter* of \mathcal{I} .

We denote, with a slight abuse of notation,

$$P_\varepsilon^\alpha(E_{\mathcal{I}}) = P_\varepsilon^\alpha(\mathcal{I}) = \alpha \mathcal{H}^1(\partial E_{\mathcal{I}}). \quad (4.9)$$

The latter equality shows that sequences of sets E_ε with $\sup_\varepsilon P_\varepsilon^\alpha(E_\varepsilon) < +\infty$ are pre-compact with respect to the local L^1 -convergence in \mathbb{R}^2 of their characteristic functions, and their limits are sets of finite perimeter in \mathbb{R}^2 . The continuum limit of these energies is the crystalline perimeter (see Alicandro, Braides and Cicalese [1])

$$P^\alpha(E) = \alpha \int_{\partial E} \|\nu\|_1 d\mathcal{H}^1, \quad (4.10)$$

where ν is the normal to ∂E and $\|\nu\|_1 = \|(\nu_1, \nu_2)\|_1 = |\nu_1| + |\nu_2|$.

4.3 A discrete-in-time minimization scheme

Now we define explicitly the distance term D_ε in (4.5).

For $\mathcal{I} \subset \varepsilon\mathbb{Z}^2$, we define the *discrete ℓ^∞ -distance* from $\partial\mathcal{I}$ as

$$d_\infty^\varepsilon(i, \partial\mathcal{I}) = \begin{cases} \inf\{\|i - j\|_\infty : j \in \mathcal{I}\} & \text{if } i \notin \mathcal{I} \\ \inf\{\|i - j\|_\infty : j \in \varepsilon\mathbb{Z}^2 \setminus \mathcal{I}\} & \text{if } i \in \mathcal{I}, \end{cases}$$

where $\|z\|_\infty = \max\{|z_1|, |z_2|\}$. Note that we have

$$d_\infty^\varepsilon(i, \partial\mathcal{I}) = d_\infty(i, \partial E_{\mathcal{I}}) + \frac{\varepsilon}{2},$$

where d_∞ denotes the usual ℓ^∞ -distance. This distance can be extended to all $\mathbb{R}^2 \setminus \partial E_{\mathcal{I}}$ by setting

$$d_\infty^\varepsilon(x, \partial\mathcal{I}) = d_\infty^\varepsilon(i, \partial\mathcal{I}) \quad \text{if } x \in Q_\varepsilon(i).$$

In the following we will directly work with $E \in \mathcal{D}_\varepsilon$, so that the distance can be equivalently defined by

$$d_\infty^\varepsilon(x, \partial E) = d_\infty(i, \partial E) + \frac{\varepsilon}{2}, \quad \text{if } x \in Q_\varepsilon(i).$$

Note that this is well defined as a measurable function, since its definition is unique outside the union of the boundaries of the squares Q_ε (that are a negligible set).

We now fix a time step $\tau > 0$ and introduce a discrete motion with underlying time step τ obtained by successive minimization. At each time step we will minimize an energy $\mathcal{F}_{\varepsilon, \tau}^\alpha : \mathcal{D}_\varepsilon \times \mathcal{D}_\varepsilon \rightarrow \mathbb{R}$ defined as

$$\mathcal{F}_{\varepsilon, \tau}^\alpha(E, F) = P_\varepsilon^\alpha(E) + \frac{1}{\tau} \int_{E \Delta F} d_\infty^\varepsilon(x, \partial F) dx. \quad (4.11)$$

Note that the integral can be indeed rewritten as a sum on the set of indices $\varepsilon\mathbb{Z}^2 \cap (E \Delta F)$. More precisely, if $\mathcal{I} = E \cap \varepsilon\mathbb{Z}^2$, $\mathcal{J} = F \cap \varepsilon\mathbb{Z}^2$, then

$$\begin{aligned} \mathcal{F}_{\varepsilon, \tau}^\alpha(\mathcal{I}, \mathcal{J}) &= P_\varepsilon^\alpha(\mathcal{I}) + \frac{1}{\tau} \sum_{i \in \mathcal{I} \Delta \mathcal{J}} \varepsilon^2 d_\infty^\varepsilon(i, \partial \mathcal{J}) \\ &= P_\varepsilon^\alpha(\mathcal{I}) + \frac{1}{\tau} \left(\sum_{i \in \mathcal{I} \setminus \mathcal{J}} \varepsilon^2 d_\infty(i, \mathcal{J}) + \sum_{i \in \mathcal{J} \setminus \mathcal{I}} \varepsilon^2 d_\infty(i, \varepsilon\mathbb{Z}^2 \setminus \mathcal{J}) \right). \end{aligned}$$

Given an initial set E_ε^0 , we define recursively a sequence $E_{\varepsilon, \tau}^k$ in \mathcal{D}_ε by requiring the following:

- (i) $E_{\varepsilon, \tau}^0 = E_\varepsilon^0$,
- (ii) $E_{\varepsilon, \tau}^{k+1}$ is a minimizer of the functional $\mathcal{F}_{\varepsilon, \tau}^\alpha(\cdot, E_{\varepsilon, \tau}^k)$.

The *discrete flat flow* associated to functionals $\mathcal{F}_{\varepsilon, \tau}^\alpha$ is thus defined by

$$E_{\varepsilon, \tau}(t) = E_{\varepsilon, \tau}^{\lfloor t/\tau \rfloor}, \quad t \geq 0. \quad (4.12)$$

Assuming that the initial data E_ε^0 tend, in the Hausdorff sense (see Section 1.2), to a sufficiently regular set E_0 , we are interested in identifying the motion described by any converging subsequence of $E_{\varepsilon, \tau}(t)$ as $\varepsilon, \tau \rightarrow 0$.

As remarked in Section 4.1, the interaction between the two discretization parameters, in time and space, plays a relevant role in such a limiting process. More precisely, the limit motion depends strongly on their relative decrease rate to 0.

We have the following ‘extreme’ asymptotic behaviors:

- (a)(**crystalline motion**) if $\varepsilon \ll \tau$, then we may first let $\varepsilon \rightarrow 0$, so that $P_\varepsilon^\alpha(E)$ can be directly replaced by the limit anisotropic perimeter $P^\alpha(E)$ and $\frac{1}{\tau} \int_{E \Delta F} d_\infty^\varepsilon(x, \partial F) dx$ by $\frac{1}{\tau} \int_{E \Delta F} d_\infty(x, \partial F) dx$. As a consequence, the approximated flat motions tend to the solution of the continuous ones studied by Almgren and Taylor [2], that is, the crystalline motion;
- (b)(**pinning**) if $\varepsilon \gg \tau$, then there is no motion (i.e., ‘pinning’) and $E_{\varepsilon, \tau}^k \equiv E_\varepsilon^0$. Indeed, for any $F \neq E_\varepsilon^0$ and for τ small enough we have

$$\frac{1}{\tau} \int_{E_\varepsilon^0 \Delta F} d_\infty^\varepsilon(x, \partial F) dx \geq c \frac{\varepsilon}{\tau} > P_\varepsilon^\alpha(E_\varepsilon^0).$$

In this case, the limit motion is the constant state E_0 .

An heuristic computation suggests that the meaningful regime is the intermediate case $\tau \sim \varepsilon$. We will describe the study of this case, the behaviour in the other regimes being immediately deduced (by scaling) from this analysis.

4.4 Motion of a rectangle

We treat the case of initial data E_ε^0 that are *coordinate rectangles*; that is, rectangles with sides parallel to the coordinate directions, of lengths $L_{1,\varepsilon}^0, L_{2,\varepsilon}^0$, respectively.

We assume that

$$\tau = \gamma\varepsilon \quad \text{for some } \gamma \in (0, +\infty),$$

(note that γ here plays the role of α in [14]) and, correspondingly, we omit the dependence on τ in the notation of

$$E_\varepsilon^k = E_{\varepsilon,\tau}^k (= E_{\varepsilon,\gamma\varepsilon}^k).$$

We note that the results remain true also in the more general case

$$\lim_{\varepsilon \rightarrow 0^+} \frac{\tau}{\varepsilon} = \gamma.$$

The following characterization of any limit motion holds.

Theorem 4.4.1 (quantization of the limit velocity). *For all $\varepsilon > 0$, let $E_\varepsilon^0 \in \mathcal{D}_\varepsilon$ be a coordinate rectangle with sides $S_{1,\varepsilon}, \dots, S_{4,\varepsilon}$. Assume also that*

$$\lim_{\varepsilon \rightarrow 0} d_{\mathcal{H}}(E_\varepsilon^0, E_0) = 0$$

for some fixed coordinate rectangle E_0 . Then, up to a subsequence, the piecewise-constant motion $E_\varepsilon(t)$ defined by (4.12) converges as $\varepsilon \rightarrow 0$ locally in time to $E(t)$, where $E(t)$ is a coordinate rectangle with sides $S_i(t)$, and such that $E(0) = E_0$. Any S_i moves inward with velocity $v_i(t)$ solving the following differential inclusions

$$v_i(t) \begin{cases} = \frac{1}{\gamma} \left\lfloor \frac{2\alpha\gamma}{L_i(t)} \right\rfloor & \text{if } \frac{2\alpha\gamma}{L_i(t)} \notin \mathbb{N} \\ \in \left[\frac{1}{\gamma} \left(\frac{2\alpha\gamma}{L_i(t)} - 1 \right), \frac{1}{\gamma} \frac{2\alpha\gamma}{L_i(t)} \right] & \text{if } \frac{2\alpha\gamma}{L_i(t)} \in \mathbb{N} \end{cases} \quad (4.13)$$

where $L_i(t) := |S_i(t)|$ denotes the length of the side $S_i(t)$, until the extinction time when $L_i(t) = 0$.

Proof. For the complete proof, see Theorem 1 in [14]. Here we just give a sketch of it, highlighting the main steps; this will be useful in the sequel for a comparison with the inhomogeneous case (see Proposition 5.3.5). The first remark is that, for ε fixed, coordinate rectangles evolve into sets of the same type. This is checked recursively, by showing that if E_ε^k is a coordinate rectangle and F is a minimizer for the minimum problem for $\mathcal{F}_{\varepsilon,\tau}^\alpha(\cdot, E_\varepsilon^k)$, then F is a coordinate rectangle. In order to

prove the assertion, let $F = F_1 \cup F_2 \cup \dots \cup F_m$, $m \geq 1$ be the decomposition of F into its connected components. Then the main steps of this geometric part of the proof are the following:

Step 1: Rectangularization. Each F_i is a coordinate rectangle contained in E_ε^k ; in fact, if we replace each F_i with the *rectangularization* of $F_i \cap E_\varepsilon^k$, i.e., the minimum coordinate rectangle containing $F_i \cap E_\varepsilon^k$, its energy decreases since its perimeter is not greater than that of F_i and the symmetric difference with E_ε^k decreases as well.

Step 2: Connectedness of F . Actually, there is only one connected component; in fact, each connected component F_i can be translated in direction of the center of E_ε^k without increasing its energy.

Step 3: F contains the center of E_ε^k . We can argue by contradiction, and by assuming that F does not contain the center of E_ε^k , we can construct a competitor which contradicts the connectedness of F .

The second part of the proof deals with the explicit computation of the minimizer E_ε^1 (and then of E_ε^k , by iterating this procedure). We set $L_{i,\varepsilon} := |S_{i,\varepsilon}|$ and let εN_i be the distance of the side $S_{i,\varepsilon}$ from S_i . We can write the functional $\mathcal{F}_{\varepsilon,\tau}^\alpha(F, E_\varepsilon^k)$ in terms of the integer distances N_1, \dots, N_4 from the relative sides, and we get that $N_{1,\varepsilon}, \dots, N_{4,\varepsilon}$ are minimizers of the function

$$\begin{aligned} f(N_1, \dots, N_4) &= -2\alpha\varepsilon \sum_{i=1}^4 N_i + \frac{\varepsilon}{\gamma} \sum_{i=1}^4 \sum_{k=1}^{N_i} k L_{i,\varepsilon} - \frac{\varepsilon^2}{\gamma} e_\varepsilon \\ &= \varepsilon \sum_{i=1}^4 \left(-2\alpha N_i + \frac{1}{\gamma} \frac{N_i(N_i+1)}{2} L_{i,\varepsilon} \right) - \frac{\varepsilon^2}{\gamma} e_\varepsilon, \end{aligned} \quad (4.14)$$

where $0 \leq e_\varepsilon \leq C \max(N_1, \dots, N_4)^3$. In the computation above we have subdivided the rectangle between $S_{i,\varepsilon}$ and S_i in N_i stripes indexed by k , for each of which the discrete distance is $k\varepsilon$; the last term is due to the contribution of the bulk term close to the corners of the rectangle F , where two neighboring rectangles between $S_{i,\varepsilon}$ and S_i intersect, and is negligible as $\varepsilon \rightarrow 0$ (see Fig. 4.1). The minimizer $N_{1,\varepsilon}, \dots, N_{4,\varepsilon}$

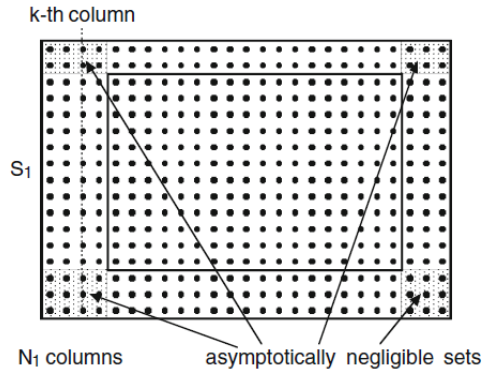


Figure 4.1. Computation of the time-step minimization (original picture from [14]).

are identified by the inequalities

$$f(\dots, N_{i,\varepsilon}, \dots) \leq f(\dots, N_{i,\varepsilon} \pm 1, \dots).$$

A direct computation shows that $N_{i,\varepsilon}$ is equal to $\lfloor 2\alpha\gamma/L_{i,\varepsilon} \rfloor$, except for the singular case in which $2\alpha\gamma/L_{i,\varepsilon}$ lies in a small neighborhood of the integers, infinitesimal as $\varepsilon \rightarrow 0$. In this case, there exists a threshold, varying with ε , for which both an integer N and the subsequent are minimizers.

Therefore, the side $S_{i,\varepsilon}$ moves inward of a distance $N_{i,\varepsilon}\varepsilon$, with the value $N_{i,\varepsilon}$ estimated in terms of the quantity $2\alpha\gamma/L_{i,\varepsilon}$ as above. \square

The following theorem characterizes the limit evolutions in case of uniqueness.

Theorem 4.4.2 (unique limit motions). *Let E_ε, E_0 be as in the statement of Theorem 4.4.1. Assume in addition that the lengths L_1^0, L_2^0 of the sides of the initial set E_0 satisfy one of the three following conditions (we assume that $L_1^0 \leq L_2^0$):*

- (a) $L_1^0, L_2^0 > 2\alpha\gamma$ (total pinning);
- (b) $L_1^0 < 2\alpha\gamma$ and $L_2^0 \leq 2\alpha\gamma$ (vanishing in finite time);
- (c) $L_1^0 < 2\alpha\gamma$ and $2\alpha\gamma/L_1^0 \notin \mathbb{N}$, and $L_2^0 > 2\alpha\gamma$ (partial pinning);

then $E_\varepsilon(t)$ converges locally in time to $E(t)$ as $\varepsilon \rightarrow 0$, where $E(t)$ is the unique rectangle with sides of lengths $L_1(t)$ and $L_2(t)$ which solve the following system of ordinary differential equations

$$\begin{cases} \dot{L}_1(t) = -\frac{2}{\gamma} \left\lfloor \frac{2\alpha\gamma}{L_2(t)} \right\rfloor \\ \dot{L}_2(t) = -\frac{2}{\gamma} \left\lfloor \frac{2\alpha\gamma}{L_1(t)} \right\rfloor \end{cases} \quad (4.15)$$

for almost every t , with initial conditions $L_1(0) = L_1^0$ and $L_2(0) = L_2^0$.

Proof. See Theorem 2 in [14]. Note that in (a) ‘total pinning’ means $E(t) \equiv E_0$, that is, $\dot{L}_1 = \dot{L}_2 \equiv 0$. Under the assumption (c), we have ‘partial pinning’, that is the side whose initial length is $L_2^0 > 2\alpha\gamma$ stays pinned until it reaches the critical length $L_2 = 2\alpha\gamma$, due to the motion of the other one. \square

Remark 4.4.3 (new features with respect to the crystalline motion). Here we highlight the main differences between the limit motion described by Theorem 4.4.2 and the crystalline motion, whose equations are given by (3.13) in Section 3.3.

(i) **‘Degenerate equations’.** The motion defined in Theorem 4.4.2 is described by a system of degenerate ordinary differential equations (4.15), whose right-hand sides are discontinuous. In fact, the discrete motion is obtained by overcoming some energy barriers in a ‘quantized’ manner. Moreover, we may read in the equations the effect of the Γ -limit energy (through the crystalline form of the evolution and the coefficient α) and of the interplay between the time and space scales (through the scaling γ).

(ii) **A pinning threshold.** In the hypothesis (a) of Theorem 4.4.2 we have pinning for large rectangles: if both the initial side-lengths are above the *pinning threshold* $\tilde{L} = 2\alpha\gamma$, then the right-hand sides of equations (4.15) are zero and the motion is

pinned. This threshold is obtained by computing the values for which a side of length L may not move inwards of ε by decreasing the energy $\mathcal{F}_{\varepsilon,\tau}^\alpha$. The corresponding variation of the energy is given by

$$-2\alpha\varepsilon + \frac{1}{\gamma}L\varepsilon, \quad (4.16)$$

which is positive if and only if

$$L \geq \tilde{L} = 2\alpha\gamma. \quad (4.17)$$

(iii) Inhomogeneity of the motion. The limit motion (4.15) cannot be obtained following the Almgren-Taylor-Wang approach for any perimeter functional. It can be regarded as a non-homogeneous crystalline motion, with a velocity depending on a function of the curvature: if the curvature κ of a side is identified with the inverse of its length, then the law for the velocity v of that side is

$$v = f(\kappa)\kappa,$$

where $f(\kappa) = \frac{1}{\gamma} \lfloor 2\alpha\gamma\kappa \rfloor \frac{1}{\kappa}$. Note that f is always less or equal than 2, the coefficient in the continuous case, which shows how an additional discreteness effect is to slow down the crystalline motion.

4.5 Motion of a polyrectangle

In this section we recall the extension of the results, obtained previously for coordinate rectangles, to the case in which the limit initial set is a *polyrectangle* ([14], Section 3.2).

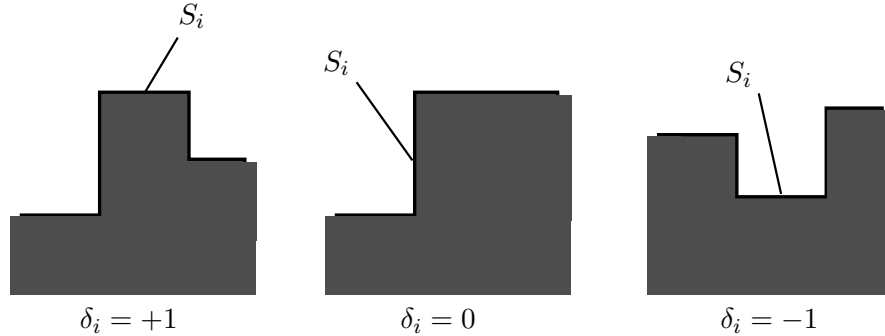


Figure 4.2. Sides of a polyrectangle with different curvature signs.

We first give the definition of polyrectangle and we assign a curvature sign on each side.

Definition 4.5.1. A set E is a coordinate polyrectangle if ∂E is locally a Lipschitz graph, and consists of a finite union of segments (sides), which are parallel to one of the coordinate axes. For any polyrectangle E we assign to each side S_i an integer number δ_i (the sign of the curvature of S_i) as follows (see Fig. 4.2): $\delta_i = 1$ (resp. $\delta_i = -1$) if there exists $r > 0$ such that $E \cap (S_i + B_r)$ (resp. $(\mathbb{R}^2 \setminus E) \cap (S_i + B_r)$) is a convex set, we set $\delta_i = 0$ if none of the two conditions holds.

Hence, locally convex sides move inwards, locally concave sides move outwards while the other ones stay pinned. The characterization of any limit motion is the following.

Theorem 4.5.2 (Motion of polyrectangles). *Let E_0 be a connected polyrectangle with sides S_1, S_2, \dots, S_N . For all $\varepsilon > 0$, let $E_\varepsilon^0 \in \mathcal{D}_\varepsilon$ be connected polyrectangles with sides $S_{1,\varepsilon}, S_{2,\varepsilon}, \dots, S_{N,\varepsilon}$, such that*

$$\lim_{\varepsilon \rightarrow 0} d_{\mathcal{H}}(E_\varepsilon^0, E_0) = 0.$$

Then there exists $T > 0$ such that, up to a subsequence, $E_\varepsilon(t)$ converges as $\varepsilon \rightarrow 0$, in the Hausdorff topology and locally uniformly on $[0, T)$, to a polyrectangle $E(t)$ with $E(0) = E_0$. Moreover, the sides S_i of $E(t)$, $1 \leq i \leq N$, move with velocity $v_i(t)$ solving the following differential inclusions

$$v_i(t) \begin{cases} = \frac{\delta_i}{\gamma} \left\lfloor \frac{2\alpha\gamma}{L_i(t)} \right\rfloor & \text{if } \frac{2\alpha\gamma}{L_i(t)} \notin \mathbb{N} \\ \in \left[\frac{\delta_i}{\gamma} \left(\frac{2\alpha\gamma}{L_i(t)} - 1 \right), \frac{\delta_i}{\gamma} \frac{2\alpha\gamma}{L_i(t)} \right] & \text{if } \frac{2\alpha\gamma}{L_i(t)} \in \mathbb{N} \end{cases} \quad (4.18)$$

where $L_i(t) := |S_i(t)|$. As a consequence, if we further assume that $2\alpha\gamma/L_i^0 \notin \mathbb{N}$ for all $1 \leq i \leq N$, the lengths $L_i(t)$ solve the following system of differential equations

$$\dot{L}_i(t) = - \left(\frac{\delta_{i-1}}{\gamma} \left\lfloor \frac{2\alpha\gamma}{L_{i-1}(t)} \right\rfloor + \frac{\delta_{i+1}}{\gamma} \left\lfloor \frac{2\alpha\gamma}{L_{i+1}(t)} \right\rfloor \right). \quad (4.19)$$

Proof. See Theorem 3 in [14]. □

The time $T > 0$ can be chosen as the first time for which $\lim_{t \rightarrow T} L_i(t) = 0$, for some $i \in \{1, \dots, N\}$.

As a final remark, we note that in [14] more effects due to discreteness are described (partial pinning, non-uniqueness, pinning after initial motion, etc.) which are related to the evolution of more general initial data (e.g., a rhombus, crystalline convex sets, etc.).

Chapter 5

Motion of discrete interfaces in ‘high-contrast’ periodic media

In this chapter we present the results contained in a joint work with A. Braides [19] about the motion of discrete interfaces in *high-contrast* periodic media; that is, media with periodic inclusions which are not energetically favourable, and hence are avoided by the interface.

5.1 Motivation and survey of the main results

In the spirit of the previous chapter (in particular, Remark 4.4.3), our aim is to show that a periodic microstructure can affect the limit evolution, without changing the Γ -limit. Hence, the Γ -limit is not sufficient to completely characterize the limit evolution at the critical regime. To this end, we will introduce a further inhomogeneity in the perimeters P_ε^α by considering, for any subset $E \subset \varepsilon\mathbb{Z}^2$,

$$P_\varepsilon^{\alpha,\beta}(E) = \frac{1}{2}\varepsilon \sum \{c_{ij} : (i,j) \in \mathbb{Z}^2 \times \mathbb{Z}^2, \varepsilon i \in E, \varepsilon j \notin E, |i-j|=1\},$$

(we use the notation $\sum\{x_a : a \in A\} = \sum_{a \in A} x_a$) where the coefficients c_{ij} equal $\alpha > 0$ except for some well-separated periodic square inclusions where $c_{ij} = \beta > \alpha$ (high-contrast medium). These inclusions are not energetically favorable and they can be neglected in the computation of the Γ -limit, which is still the perimeter P^α (4.10), with the same coefficient α (see Remark 5.2.1). They can be considered as “obstacles” that can be bypassed when computing minimizers of $P_\varepsilon^{\alpha,\beta}$; however their presence is felt in the minimizing-movement procedure (4.5) since they may influence the choice of $E_k^{\tau,\varepsilon}$ through the interplay between the distance and perimeter terms. As a result, the motion can be either decelerated or accelerated with respect to the homogeneous case (Chapter 4).

As already remarked in the previous chapter, the relevant case for the description of the motion is that of initial data coordinate rectangles, since all other cases can be reduced to the study of this one. We will then restrict our analysis to that case, in the critical regime $\tau = \gamma\varepsilon$. This (apparently) simple situation already contains all the relevant features of the evolution and highlights the differences with respect to the motion in a homogeneous medium. We will show that the limit motion can still

be described through a system of degenerate ordinary differential equations of the form

$$\begin{cases} \dot{L}_1(t) = -\frac{2}{\gamma} f\left(\frac{\gamma}{L_2(t)}\right) \\ \dot{L}_2(t) = -\frac{2}{\gamma} f\left(\frac{\gamma}{L_1(t)}\right) \end{cases}$$

with f a locally constant function on compact subsets of $(0, +\infty)$ which depends on α , the period and size N_β of the inclusions but not on γ (neither on the value β).

The *effective velocity* f is obtained by a homogenization formula which optimizes the motion of the sides of the rectangle; it results in an oscillation around a linear motion with velocity $\frac{1}{\gamma}f(\gamma/L)$ (which is locally constant, as noted above). Note that, in the case of no inclusions, the system is of the same form with $f(Y) = \lfloor 2\alpha Y \rfloor$ (equation (4.15)). The dependence on the inclusions gives a new pinning threshold

$$\bar{L} = \frac{4\gamma\alpha}{2 + N_\beta}$$

depending on the size of the inclusion N_β . The reason for this new pinning threshold is that, in order that a side may move, it need to be able to overcome a barrier of N_β inclusions. Note that, if the initial data have side lengths $\bar{L} < L < \tilde{L}$, \tilde{L} the pinning threshold (4.17), then we may have a microscopic motion which stops after a finite number of time steps, and is not eventually detected in the limit. It should be remarked that the presence of the inclusions may indeed accelerate the motion, so that $f(Y) > \lfloor 2\alpha Y \rfloor$ for some Y .

Overview of the chapter. In Section 5.2 we define all the energies we will consider. Section 5.3 contains the proof of the convergence of the discrete scheme in the case of a rectangular initial set. Contrary to the proof of Theorem 4.4.1, it is not trivial to show that the minimizers of this scheme are actually rectangles. This is a technical result contained in Proposition 5.3.5. Section 5.3.1 contains the computation of the new pinning threshold, showing that it depends on the percentage N_β of defects in the lattice. Section 5.3.2 deals with the new definition of the effective velocity of a side by means of a homogenization formula resulting from a one-dimensional ‘oscillation-optimization’ problem. This velocity can be expressed uniquely (up possibly to a discrete set of values) as a function the ratio of γ and the side length (Definition 5.3.8). The description of the homogenized limit motion is contained in Section 5.3.3. In the last two sections we compute explicitly the velocity function by means of algebraic formulas in some simple cases, showing a nontrivial comparison with the case with no inclusions.

5.2 Inhomogeneous ferromagnetic energies on discrete sets

The energies we consider are interfacial energies defined in an inhomogeneous environment as follows: let $0 < \alpha < \beta < +\infty$, $N_\alpha, N_\beta \geq 1$ and set $N_{\alpha\beta} = N_\alpha + N_\beta$.

We consider the $N_{\alpha\beta}$ -periodic coefficients c_{ij} indexed on *nearest-neighbours* of \mathbb{Z}^2 (i.e., $i, j \in \mathbb{Z}^2$ with $|i - j| = 1$) defined for i, j such that

$$0 \leq \frac{i_1 + j_1}{2}, \frac{i_2 + j_2}{2} < N_{\alpha\beta}$$

by

$$c_{ij} = \begin{cases} \beta & \text{if } 0 \leq \frac{i_1 + j_1}{2}, \frac{i_2 + j_2}{2} \leq N_\beta \\ \alpha & \text{otherwise.} \end{cases} \quad (5.1)$$

These coefficients label the bonds between points in \mathbb{Z}^2 , so that they describe a matrix of α -bonds with $N_{\alpha\beta}$ -periodic inclusions of β -bonds grouped in squares of side-length N_β . The periodicity cell is pictured in Fig. 5.1.

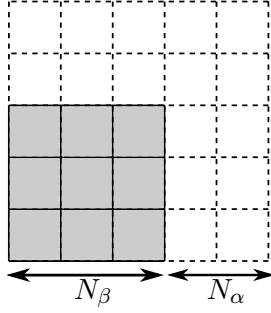


Figure 5.1. Periodicity cell. Continuous lines represent β -bonds, dashed lines α -bonds.

Correspondingly, to these coefficients we associate the energy defined on subsets \mathcal{I} of \mathbb{Z}^2 by

$$P^{\alpha,\beta}(\mathcal{I}) = \sum \left\{ c_{ij} : |i - j| = 1, i \in \mathcal{I}, j \in \mathbb{Z}^2 \setminus \mathcal{I} \right\}. \quad (5.2)$$

Here we use the notation $\sum \{x_a : a \in A\} = \sum_{a \in A} x_a$. In order to examine the overall properties of $P^{\alpha,\beta}$, we introduce the family of scaled energies defined on subsets \mathcal{I} of $\varepsilon\mathbb{Z}^2$ by

$$P_\varepsilon^{\alpha,\beta}(\mathcal{I}) = \sum \left\{ \varepsilon c_{i/\varepsilon, j/\varepsilon} : |i - j| = \varepsilon, i \in \mathcal{I}, j \in \varepsilon\mathbb{Z}^2 \setminus \mathcal{I} \right\}; \quad (5.3)$$

i.e., $P_\varepsilon^{\alpha,\beta}(\mathcal{I}) = \varepsilon P^{\alpha,\beta}(\frac{1}{\varepsilon}\mathcal{I})$. To study the continuous limit as $\varepsilon \rightarrow 0$ of these energies, it will be convenient to identify each subset \mathcal{I} of $\varepsilon\mathbb{Z}^2$ with a measurable subset $E_\mathcal{I}$ of \mathbb{R}^2 as in Section 4.2, that is, $E_\mathcal{I} = \bigcup_{i \in \mathcal{I}} \varepsilon(i + Q)$. The class of finite unions of ε -squares still will be denoted by \mathcal{D}_ε .

As an easy remark, we note that

$$P_\varepsilon^{\alpha,\beta}(E_\mathcal{I}) \geq \varepsilon \alpha \# \left\{ (i, j) : |i - j| = \varepsilon, i \in \mathcal{I}, j \in \varepsilon\mathbb{Z}^2 \setminus \mathcal{I} \right\} = \alpha \mathcal{H}^1(\partial E_\mathcal{I}), \quad (5.4)$$

which shows that sequences of sets E_ε with $\sup_\varepsilon P_\varepsilon^{\alpha,\beta}(E_\varepsilon) < +\infty$ are pre-compact with respect to the local L^1 -convergence in \mathbb{R}^2 of their characteristic function and their limits are sets of finite perimeter in \mathbb{R}^2 . Hence, this defines a meaningful convergence with respect to which compute the Γ -limit of $P_\varepsilon^{\alpha,\beta}$ as $\varepsilon \rightarrow 0$.

In our case the presence of the β -inclusions does not influence the form of the Γ -limit, which is still the crystalline perimeter P^α (4.10), as in the following remark.

Remark 5.2.1 (Γ -convergence of inhomogeneous perimeter energies). The energies $P_\varepsilon^{\alpha,\beta}$ defined by (5.3) Γ -converge, as $\varepsilon \rightarrow 0$, to the anisotropic crystalline perimeter functional

$$P^\alpha(E) = \alpha \int_{\partial^* E} \|\nu\|_1 d\mathcal{H}^1.$$

This limit is independent of N_α, N_β , and equals the one obtained when $\beta = \alpha$.

The lower bound for the Γ -limit is immediately obtained from the case $\alpha = \beta$ in [1] after remarking that $P_\varepsilon^{\alpha,\beta} \geq P_\varepsilon^{\alpha,\alpha} = P_\varepsilon^\alpha$. In order to verify the upper bound, it suffices to note that recovery sequences for the Γ -limit of $P_\varepsilon^{\alpha,\beta}$ can be constructed at a scale $N_{\alpha\beta}\varepsilon$, thus ‘avoiding’ the β -connections. To this end, define

$$Q_\varepsilon^{N_{\alpha\beta}} = \bigcup \left\{ Q_\varepsilon(i) : i \in \varepsilon\mathbb{Z}^2, 0 \leq \|i\|_\infty < \varepsilon N_{\alpha\beta} \right\}.$$

This is a square of side length $N_{\alpha\beta}\varepsilon$ whose boundary intersects only α -bonds. We consider $P_\varepsilon^{N_{\alpha\beta}}$ the restriction of $P_\varepsilon^{\alpha,\beta}$ to the class

$$\mathcal{D}_\varepsilon^{N_{\alpha\beta}} = \left\{ E \subseteq \mathbb{R}^2 : E \text{ is a finite union of } \varepsilon\mathbb{Z}^2\text{-translations of } Q_\varepsilon^{N_{\alpha\beta}} \right\}.$$

Note that we have $P_\varepsilon^{\alpha,\beta}(E) = P_\varepsilon^{\alpha,\alpha}(E)$ for $E \in \mathcal{D}_\varepsilon^{N_{\alpha\beta}}$, and that sets in $\mathcal{D}_\varepsilon^{N_{\alpha\beta}}$ differ from sets in $\mathcal{D}_{\varepsilon N_{\alpha\beta}}$ by a fixed translation of order ε . Hence, we have (see Chapter 1 for details on the properties of Γ -upper limits)

$$\Gamma\text{-}\limsup_{\varepsilon \rightarrow 0} P_\varepsilon^{\alpha,\beta}(E) \leq \Gamma\text{-}\limsup_{\varepsilon \rightarrow 0} P_\varepsilon^{N_{\alpha\beta}}(E) = \Gamma\text{-}\lim_{\varepsilon \rightarrow 0} P_{N_{\alpha\beta}\varepsilon}^{\alpha,\beta}(E),$$

and the latter is again equal to $P^\alpha(E)$. This inequality just states that we can take sets in $\mathcal{D}_\varepsilon^{N_{\alpha\beta}}$, which are small translations of a recovery sequence for $P_{N_{\alpha\beta}\varepsilon}^{\alpha,\beta}(E)$, as a recovery sequence for $P_\varepsilon^{\alpha,\beta}(E)$.

5.3 Motion of a rectangle

We consider the same discrete-in-time scheme as in Section 4.3, and at each time step we will minimize an energy $\mathcal{F}_{\varepsilon,\tau}^{\alpha,\beta} : \mathcal{D}_\varepsilon \times \mathcal{D}_\varepsilon \rightarrow \mathbb{R}$ defined as

$$\mathcal{F}_{\varepsilon,\tau}^{\alpha,\beta}(E, F) = P_\varepsilon^{\alpha,\beta}(E) + \frac{1}{\tau} \int_{E \Delta F} d_\infty^\varepsilon(x, \partial F) dx. \quad (5.5)$$

As before, the relevant case is when ε and τ are of the same order and the initial data are coordinate rectangles E_ε^0 , which will be the content of this section. We assume that $\tau = \gamma\varepsilon$ and use the same notation for E_ε^k as before.

Due to the lack of uniqueness of minimizers in the discrete minimization scheme described in Section 4.3, a standard comparison principle cannot hold. We recall a *weak comparison principle* for our motion in the discrete case (see Proposition 1 in Braides, Gelli and Novaga [14] for the proof).

Proposition 5.3.1 (Discrete weak comparison principle). *Let $\varepsilon > 0$ and let $R_\varepsilon, K_\varepsilon \in \mathcal{D}_\varepsilon$ be such that $R_\varepsilon \subseteq K_\varepsilon$ and R_ε is a coordinate rectangle. Let K_ε^k be a motion from K_ε constructed by successive minimizations. Then $R_\varepsilon^k \subseteq K_\varepsilon^k$ for all $k \geq 1$, where R_ε^k is a motion from R_ε constructed by successively choosing a minimizer of $\mathcal{F}_{\varepsilon,\tau}^\alpha(\cdot, R_\varepsilon^{k-1})$ having smallest measure.*

Remark 5.3.2. The set $\mathbb{R}^2 \setminus K_\varepsilon^k$ is the k -step evolution of the complementary $\mathbb{R}^2 \setminus K_\varepsilon^k$ of K_ε . As a consequence, if we have $R_\varepsilon \subseteq \mathbb{R}^2 \setminus K_\varepsilon^k$, from Proposition 5.3.1 it follows that

$$R_\varepsilon^k \subseteq \mathbb{R}^2 \setminus K_\varepsilon^k, \quad \text{for all } k \geq 1.$$

Definition 5.3.3 (α -type rectangle). A coordinate rectangle whose sides intersect only α -bonds will be called an α -type rectangle.

Remark 5.3.4. As a trivial remark, we note that the minimizers of $\mathcal{F}_{\varepsilon,\tau}^{\alpha,\alpha}$, characterized in the proof of Theorem 4.4.1, are coordinate α -type rectangles.

The first result is that coordinate rectangles evolve into α -type rectangles, hence avoiding β -bonds. Note that we cannot perform the same proof as in Theorem 4.4.1, because rectangularization and translation towards the origin of a connected component may increase the perimeter term of the energy in an inhomogeneous environment. However, the proof of the connectedness is the same as in the case of a polyrectangle (see Theorem 3 in [14]), this argument being independent of the microstructure.

Proposition 5.3.5. *If $E_\varepsilon^0 \in \mathcal{D}_\varepsilon$ is a coordinate rectangle and F is a minimizer for the minimum problem for $\mathcal{F}_{\varepsilon,\tau}^{\alpha,\beta}(\cdot, E_\varepsilon^k)$, $k \geq 0$, then for all $\delta > 0$ F is a coordinate α -type rectangle as long as the sides of E_ε^k are larger than δ and ε is small enough.*

Proof. Step 1: connectedness of F . We want to prove that each E_ε^k is connected. It will suffice to show this for $F = E_\varepsilon^1$. We first need an estimate on the area of the “small components” of E_ε^1 ; this estimate will be obtained by using the comparison principle in Proposition 5.3.1.

Let $\ell > 0$ be the maximum number such that for each point $x \in E_\varepsilon^0$ there exists $y \in \mathbb{R}^2$ such that $x \in (y + Q_\ell) \subseteq E_\varepsilon^0$, where $Q_\ell = [-\ell/2, \ell/2] \times [-\ell/2, \ell/2]$, and the same property holds for $x \notin E_\varepsilon^0$. If $E_\varepsilon^0 = [-L_1/2, L_1/2] \times [-L_2/2, L_2/2]$, we can choose $\ell = \min\{L_1, L_2\}$. By applying Proposition 5.3.1 and Remark 5.3.2 to the union of squares contained in E_ε^0 , and to those outside E_ε^0 , respectively, and taking into account that a side of length ℓ shrinks by $\left\lfloor \frac{2\alpha\gamma}{\ell} \right\rfloor \varepsilon$ in absence of defects (see (4.13)), it follows that

$$d_{\mathcal{H}}(\partial E_\varepsilon^1, \partial E_\varepsilon^0) \leq \left(\frac{2\alpha\gamma}{\ell} + 1 \right) \varepsilon.$$

In this way, it is not possible to have a configuration as in Fig. 5.2, with two large components for E_ε^1 .

Assume by contradiction that E_ε^1 is not connected. In this case we should have only one large component as in Fig. 5.3. We consider the decomposition

$$E_\varepsilon^1 = E_{0,\varepsilon}^1 \cup \bigcup_{i=1}^N E_{i,\varepsilon}^1,$$

with $E_{0,\varepsilon}^1$ the component containing all the points of E_ε^1 having distance more than $C'\varepsilon$ from ∂E_ε^0 for a suitable constant $C' < 2\alpha\gamma/\ell + 1$.

Therefore for a suitable constant C'' we have

$$d_\infty^\varepsilon(x, \partial E_\varepsilon^0) \leq C''\varepsilon \quad \text{for all } x \in E_{i,\varepsilon}^1 \text{ and } i \geq 1.$$

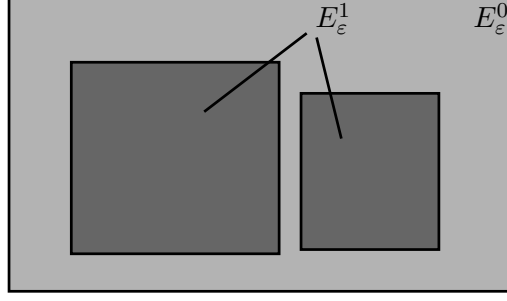


Figure 5.2. Test set with E_ε^1 with two large components.

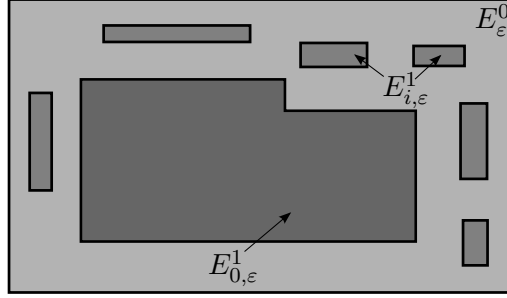


Figure 5.3. Small components of E_ε^1 .

By using the isoperimetric inequality, for ε small enough we infer

$$\frac{1}{\tau} \int_{E_{i,\varepsilon}^1} d_\infty^\varepsilon(x, \partial E_\varepsilon^0) dx \leq (C''/\gamma) |E_{i,\varepsilon}^1| < C_{\text{iso}} \sqrt{|E_{i,\varepsilon}^1|} \leq P_\varepsilon^{\alpha,\alpha}(E_{i,\varepsilon}^1) \leq P_\varepsilon^{\alpha,\beta}(E_{i,\varepsilon}^1),$$

with C_{iso} being the constant of the isoperimetric inequality. Thus, we get a contradiction since we can decrease strictly the energy by eliminating the small components of E_ε^1 and considering the set $E' = E_{0,\varepsilon}^1$ as a competitor.

Step 2: α -rectangularization. Consider the maximal α -type rectangle R^α with each side intersecting F . We call the set $F' = F \cup R^\alpha$ the α -rectangularization of F . This set is either an α -type rectangle (and in this case we conclude) or it has some protrusions intersecting β -bonds (Fig. 5.4). In both cases $P_\varepsilon^{\alpha,\beta}(F') \leq P_\varepsilon^{\alpha,\beta}(F)$,

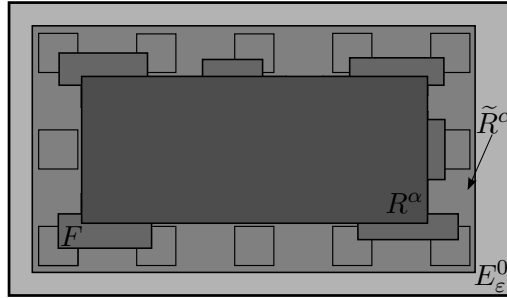


Figure 5.4. α -rectangularization.

and the symmetric difference with E_ε^0 decreases. To justify this, note that the α -rectangularization reduces (or leaves unchanged) $P_\varepsilon^{\alpha,\alpha}$ and it reduces the symmetric difference.

As a consequence of this observation, we also deduce an *a priori* estimate on the maximal distance between ∂E_ε^0 and ∂E_ε^1 . By the argument above, F contains an α -type rectangle R^α and is strictly contained in an α -type rectangle \tilde{R}^α whose sides have a distance from the corresponding sides of R^α of not more than $(N_\beta + 1)\varepsilon$. We only check the *a priori* estimate in the simplifying hypothesis that E_ε^0 is of α -type and that E_ε^0 and R^α are both concentric squares, so that we can express this estimate in terms of the length L of the sides of E_ε^0 and the distance between ∂E_ε^0 and ∂R^α , which can be expressed as εN . Note that we have

$$\alpha \mathcal{H}^1(\partial E_\varepsilon^0) \geq \mathcal{F}_{\varepsilon, \tau}^{\alpha, \beta}(E_\varepsilon^1, E_\varepsilon^0) \geq \alpha \mathcal{H}^1(\partial R^\alpha) + \frac{1}{\tau} \int_{E_\varepsilon^0 \setminus \tilde{R}^\alpha} d_\infty^\varepsilon(x, \partial E_\varepsilon^0) dx,$$

which translates into

$$4\alpha L \geq 4\alpha(L - 2\varepsilon N) + \frac{2L}{\gamma} \varepsilon(N - N_\beta)^2 + O(\varepsilon^2),$$

and gives (for ε sufficiently small)

$$N \leq \frac{c_1}{L} + c_2 N_\beta =: c(L). \quad (5.6)$$

The same type of estimate holds in the general case taking L the minimal length of sides of E_ε^0 .

Step 3: profile of protrusions on β -squares. Now we want to describe the form of the optimal profiles of the boundary of F intersecting β -squares.

As noted above, F contains an α -type rectangle $R^\alpha = [\varepsilon m_1, \varepsilon M_1] \times [\varepsilon m_2, \varepsilon M_2]$ and is contained in the α -type rectangle

$$\tilde{R}^\alpha = [\varepsilon(m_1 - N_\beta), \varepsilon(M_1 + N_\beta)] \times [\varepsilon(m_2 - N_\beta), \varepsilon(M_2 + N_\beta)]$$

whose side exceed the ones of R^α by at most $2\varepsilon N_\beta$. We will describe separately the possible profile of F close to each side of R^α ; e.g., in the rectangle $[\varepsilon(m_1 - N_\beta), \varepsilon(M_1 + N_\beta)] \times [\varepsilon M_2, \varepsilon(M_2 + N_\beta)]$ (i.e., close to the upper horizontal side of R^α). We first consider the possible behavior of the boundary of F at a single β -square Q .

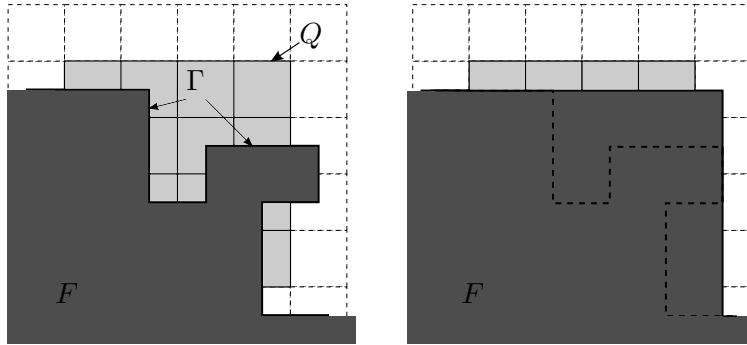


Figure 5.5. Envelope of ∂F when intersecting opposite sides.

We suppose that such Q is not one of the two extremal squares, for which a slightly different analysis holds. First, if a portion Γ of ∂F intersects Q in exactly two points

on opposite vertical sides, then we may consider in place of F the union of F and all the ε -squares with centers (x, y) in $Q \cap \varepsilon\mathbb{Z}^2$ and

$$y \leq \max\{z_2 : z \in \Gamma\}.$$

The new set, pictured in Fig. 5.5, has both lower perimeter and less symmetric difference with E_ε^0 . If a portion Γ intersects Q in exactly two points on the same

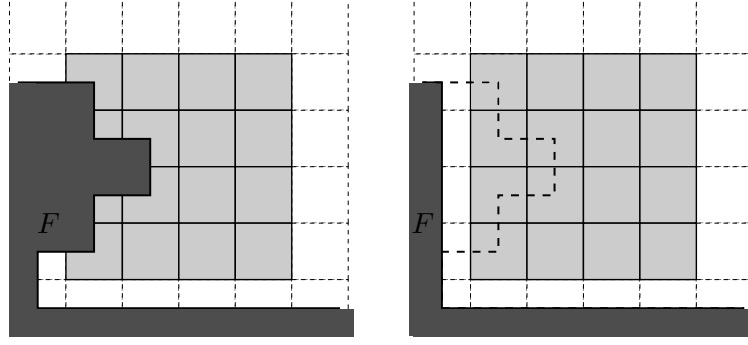


Figure 5.6. Removal of ∂F when intersecting one side.

side (horizontal or vertical) or adjacent sides, then we may remove all the ε -squares with centers in the portion of $Q \cap F$ with boundary Γ . The two cases are pictured in Fig. 5.6 and Fig. 5.7, respectively. This operation decreases the perimeter of at

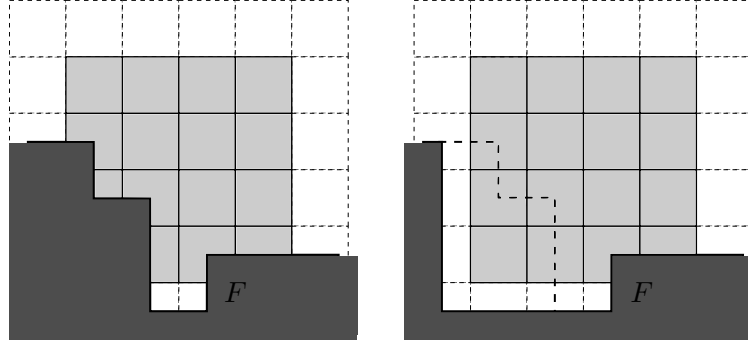


Figure 5.7. Removal of ∂F when intersecting two adjacent sides.

least $\varepsilon(\beta - \alpha)$ while at most increases the bulk term by $\frac{1}{\tau}\varepsilon^3 N_\beta^2 c(L)$ ($c(L)$ given by (5.6)). The total change in the energy is thus

$$-\varepsilon(\beta - \alpha) + \frac{1}{\gamma}\varepsilon^2 N_\beta^2 c(L), \quad (5.7)$$

which is negative if ε is small enough. As a consequence, then either $F \cap Q = \emptyset$ or $\partial F \cap Q$ is a horizontal segment.

The same type of analysis applies to the extremal squares, for which we deduce instead that $F \cap Q$ is a rectangle with one vertex coinciding with a vertex of \tilde{R}^α .

We now consider the interaction of consecutive β -squares. Let Q_1, \dots, Q_K be a maximal array of consecutive β -squares with $F \cap Q_k \neq \emptyset$ for $k = 1, \dots, K$ and

such that Q_1 is not a corner square. If we substitute F with $F \cup R$, where R is the maximal rectangle of ε -squares containing all $F \cap Q_k$ and not intersecting other β -squares, then the corresponding energy has a not larger perimeter part, and a bulk part which is strictly lower if $F \cup R \neq F$. This substitution is pictured in Fig. 5.8. If the subsequent β -squares $Q_{K+1} \dots, Q_{K+K'}$ are a maximal array which do not

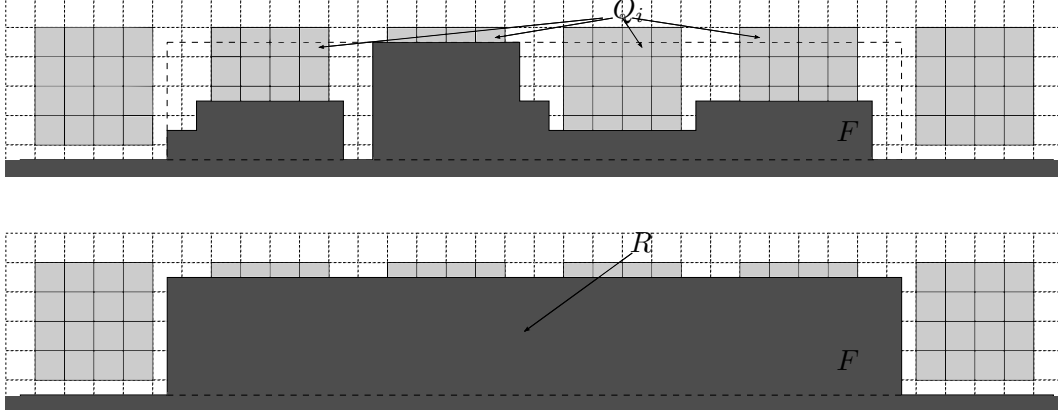


Figure 5.8. Envelope of ∂F in consecutive squares.

intersect F then we may further substitute $F \cup R$ with $(F \setminus R) \cup (R + \varepsilon N_{\alpha\beta} K'(1, 0))$, where we translate R until it meets another portion of F (if any). This translation is pictured in Fig. 5.9. Note that if it does meet another portion of F , then the

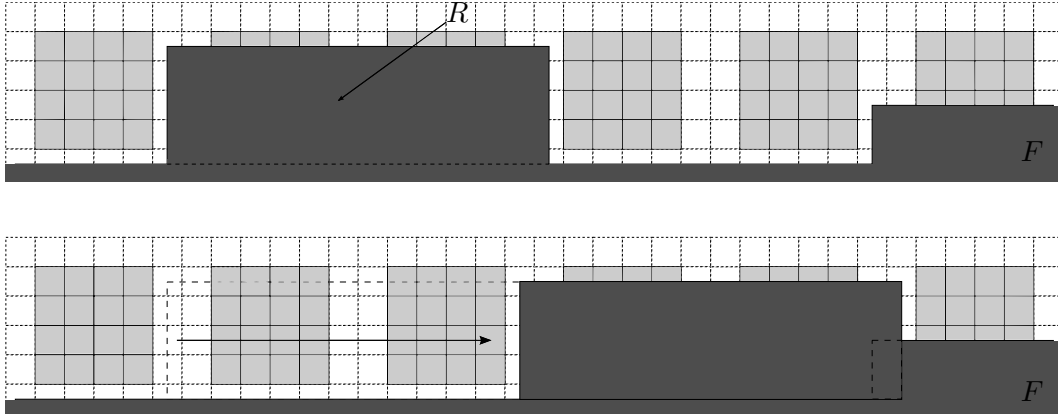


Figure 5.9. Translation argument to join protrusions.

change in energy is at most

$$-2\varepsilon\alpha + \frac{1}{\gamma}\varepsilon^2 N_\beta N_\alpha c(L), \quad (5.8)$$

which is negative if ε is small enough. In this case, at this point we may iterate this analysis since we now have a larger array of consecutive β -squares intersecting F . Note, moreover, that the same argument can be repeated shifting the rectangle R to the left instead than to the right, if energetically convenient. As a conclusion, we obtain that F may only either intersect one array of consecutive β -squares, or two

such arrays if they contain the two corner β -squares; i.e., we have one of the two situations pictured in Fig. 5.10.

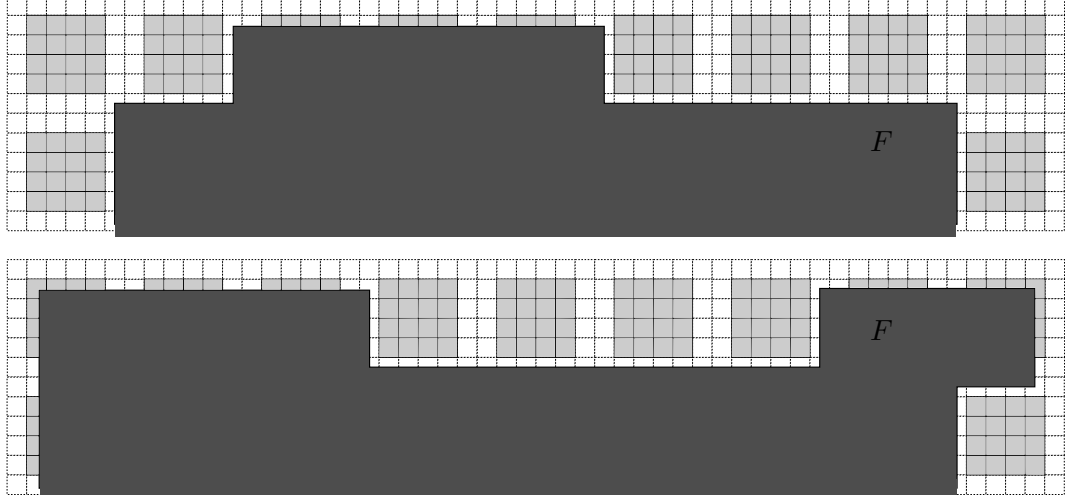


Figure 5.10. Profiles of candidate minimal F .

Step 4: all β -connections can be removed except those at the four corners. At this point, we are in the situations pictured in Fig. 5.10. If we are as in the upper figure, then by removing all ε -squares external to R^α the variation of the energy is less or equal than

$$-(\beta - \alpha)(N_\beta + 1)N\varepsilon + c(L)\frac{(N + 1)N_\alpha N_\beta}{\gamma}\varepsilon^2,$$

where N is the number of modified β -squares. For ε small this variation is negative, showing that F does not contain any protrusion.

If we are as in the lower figure, then we may remove all β -connections inside the border β -squares, except those in the two periodicity squares at the corners as in Fig. 5.11; in this case, the variation of the energy functional is less or equal than

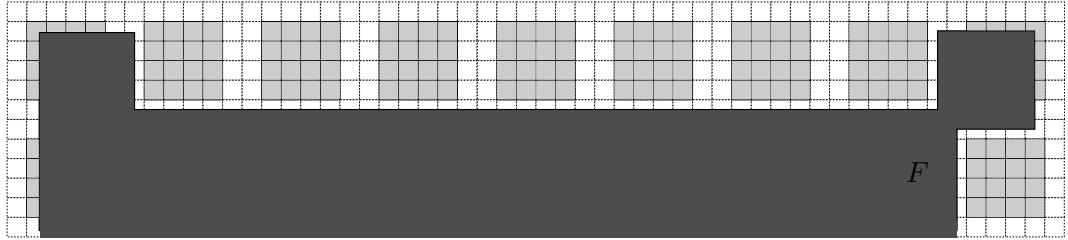


Figure 5.11. Removing β -connections except in the two β -squares at the corners.

$$-(\beta - \alpha)(N_\beta + 1)N\varepsilon + c(L)\frac{NN_\alpha N_\beta}{\gamma}\varepsilon^2,$$

where N is the number of modified cells. For ε small this variation is negative, showing that the profile in Fig. 5.11 is energetically convenient. We can repeat this

procedure for each side, and finally we obtain that F is the union of a coordinate α -type rectangle R and possibly one to four rectangles $\tilde{R}_i, i = 1, \dots, 4$ of side lengths at most $N_{\alpha\beta}\varepsilon$ such that the intersection of \tilde{R}_i with each corner β -square is a rectangle (see Fig. 5.12)

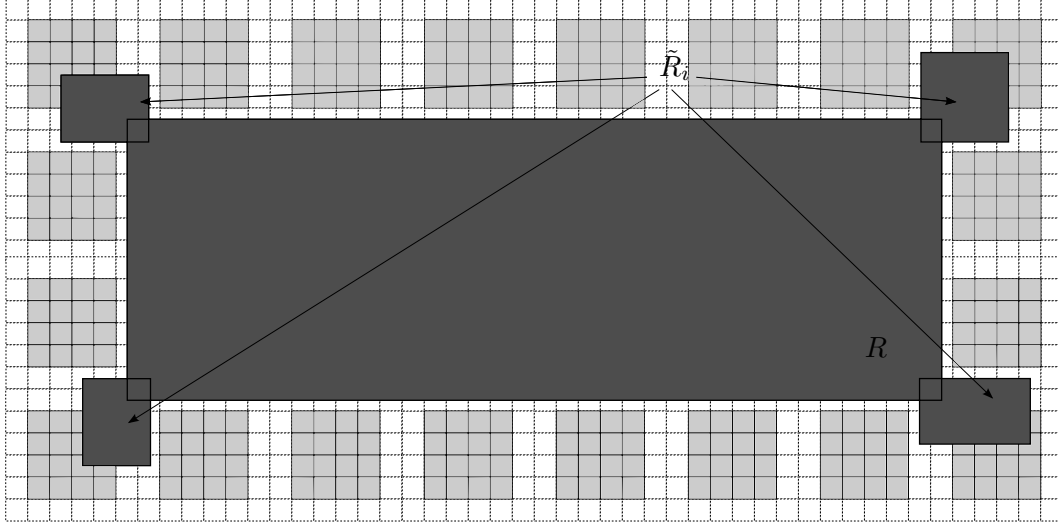


Figure 5.12. The set obtained in Step 4.

Step 5: conclusion. It remains to prove that the rectangles \tilde{R}_i in the previous step are actually not there. This is immediately checked by comparing such an F with R^α : if $\tilde{R}_i \neq \emptyset$ then by removing it the energy changes at most by

$$-2\beta\varepsilon + \frac{1}{\gamma}c(L)\varepsilon^2 N_{\alpha\beta}^2,$$

which is negative for small ε .

We finally note that all the estimates above can be iterated and hold uniformly as long as the sides of E_ε^k are larger than δ , since they depend only on $c(\delta)$. \square

The proposition above shows that we may restrict our analysis to α -type rectangles; indeed, for fixed ε this assumption is not restrictive until the sides of the rectangles are larger than a constant, which vanishes as $\varepsilon \rightarrow 0$. As a consequence, once we suppose the convergence of the initial data, up to subsequences, the discrete motions $E_{\varepsilon,\tau}(t)$ converge, as $\varepsilon \rightarrow 0$, to a limit $E(t)$ such that E is a rectangle for all t , up to its extinction time. Note, moreover, that it is not restrictive to suppose that also the initial data are α -type rectangles, up to substituting E_ε^0 with E_ε^1 .

As shown in Section 4.4, the motion of each side of E_ε^k can be studied separately, since the constraint of being an α -type rectangle does not influence the argument therein, which consists in remarking that the bulk term due to the small corner rectangles in Fig. 5.13 is negligible. As a consequence, we can describe the motion in terms of the length of the sides of E_ε^k . This will be done in the following sections.

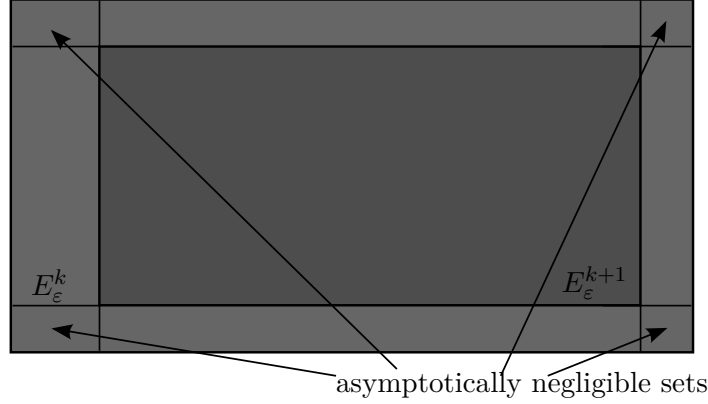


Figure 5.13. Picture of E_ε^{k+1} inside E_ε^k .

5.3.1 A new pinning threshold

We first examine the case when the limit motion is trivial; i.e., all $E_k = E_\varepsilon^k$ are the same after a finite number of steps. This will be done by computing the *pinning threshold*; i.e., the critical value of the side length L above which it is energetically not favorable for a side to move. We recall that, in the case $\alpha = \beta$, this threshold is (see (4.16))

$$\tilde{L} = 2\alpha\gamma.$$

In our case, by the condition that E_k be an α -type rectangle, we have to impose that it is not energetically favorable for a side to move inwards by $(N_\beta + 1)\varepsilon$ (see Fig. 5.14). We then write the variation of the energy functional $\mathcal{F}_{\varepsilon,\tau}^{\alpha,\beta}$ from

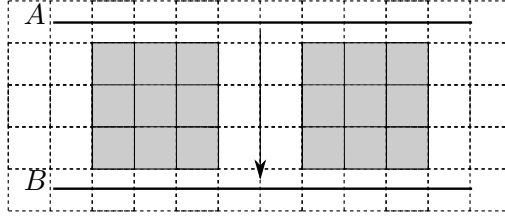


Figure 5.14. Motion is possible if the side can move at least by $(N_\beta + 1)\varepsilon$.

configuration A to configuration B in Fig. 5.14, regarding a side of length L . If we impose it to be positive, we have

$$-2(N_\beta + 1)\alpha\varepsilon + \frac{1}{\tau} \sum_{k=1}^{N_\beta+1} (k\varepsilon)L\varepsilon = (N_\beta + 1)\varepsilon \left[-2\alpha + \frac{L}{2\gamma}(N_\beta + 2) \right] \geq 0$$

and we obtain the pinning threshold

$$\bar{L} := \frac{4\gamma\alpha}{N_\beta + 2}. \quad (5.9)$$

Note that this threshold depends on N_β and not on the value $\beta > \alpha$. Moreover, $\bar{L} \leq \tilde{L}$ and if $N_\beta = 0$ (or, otherwise, $\alpha = \beta$), we recover the previous threshold \tilde{L} .

5.3.2 Definition of the effective velocity

As remarked above, up to an error vanishing as $\varepsilon \rightarrow 0$, the motion of each side is independent of the other ones. As a consequence, its description can be reduced to a one-dimensional problem, where the unknown represents, e.g., the location of the left-hand vertical side of E_k . Let x_k represents the projection of this side of E_k on

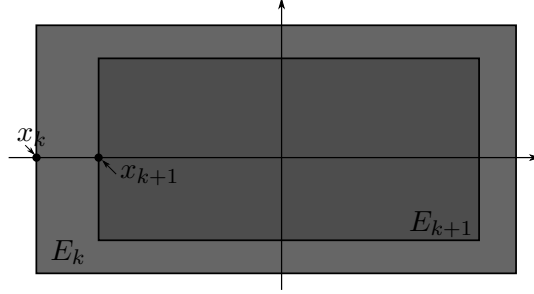


Figure 5.15. Reduction to a one-dimensional problem.

the horizontal axis, as in Fig. 5.15. The location of x_{k+1} depends on a minimization argument involving x_k and the length L_k of the corresponding side of E_k . However, we will see that this latter dependence is locally constant, except for a discrete set of values of L_k . Indeed, for all $Y > 0$ (which in our case will be of the form $Y = \gamma/L_k$) consider the minimum problems

$$\min \left\{ -2\alpha N + \frac{N(N+1)}{2Y} : N \in \mathbb{N}, \quad [x + N]_{N_{\alpha\beta}} \in \mathbb{Z}_{N_{\alpha}} \right\}, \quad (5.10)$$

for $x \in \{0, \dots, N_{\alpha\beta}\}$, where $[z]_{N_{\alpha\beta}}$ denotes the congruence class of z modulo $N_{\alpha\beta}$ and

$$\mathbb{Z}_{N_{\alpha}} = \{[0]_{N_{\alpha\beta}}, \dots, [N_{\alpha} - 1]_{N_{\alpha\beta}}\}.$$

Then the set of $Y > 0$ for which (5.10) does not have a unique solution is discrete. To check this it suffices to remark that the function to minimize

$$-4\alpha XY + X(X+1)$$

is a parabola with vertex in

$$X = 2\alpha Y - \frac{1}{2}.$$

The minimizers N are points with $[x + N]_{N_{\alpha\beta}} \in \mathbb{Z}_{N_{\alpha}}$ of minimal distance from the vertex X . These are not unique in some cases: first if the vertex X is equidistant from two consecutive points in $\mathbb{Z}_{N_{\alpha}}$; i.e., if

$$2\alpha Y - \frac{1}{2} \in \frac{1}{2} + \mathbb{Z},$$

or, equivalently,

$$Y \in \frac{1}{2\alpha} \mathbb{Z}. \quad (5.11)$$

The second case is when we have two points in \mathbb{Z}_{N_α} of minimal distance from X which are not consecutive. In this case the distance between these points is $N_\beta + 1$, so that we have

$$2\alpha Y - \frac{1}{2} \in N_\beta + \frac{1}{2} + \mathbb{Z},$$

or, equivalently,

$$Y \in \frac{1}{2\alpha} \left(\frac{N_\beta}{2} + \mathbb{Z} \right).$$

If N_β is even then this condition is equivalent to (5.11), while if N_β is odd then we have

$$Y \in \frac{1}{4\alpha} + \frac{1}{2\alpha} \mathbb{Z}. \quad (5.12)$$

Definition 5.3.6 (singular set). We define the (possibly) singular set S_{N_β} for problems (5.10) as

$$S_{N_\beta} = \frac{1}{2\alpha} \left(\mathbb{Z} \cup \left(\frac{1}{2} + \mathbb{Z} \right) \right).$$

We will examine the iterated minimizing scheme for $\gamma/L_k = \gamma/L \in (0, +\infty) \setminus S_{N_\beta}$ fixed, which reads

$$\begin{cases} x_{k+1}^L = x_k^L + \bar{N}_k, & k \geq 0 \\ x_0^L = x^0 \end{cases} \quad (5.13)$$

with $x^0 \in \{0, 1, \dots, N_{\alpha\beta} - 1\}$ and $\bar{N}_k \in \mathbb{N}$ the minimizer of

$$\min \left\{ -2\alpha N + \frac{1}{\gamma} \frac{N(N+1)}{2} L : N \in \mathbb{N}, \quad [x_k^L + N]_{N_{\alpha\beta}} \in \mathbb{Z}_{N_\alpha} \right\}, \quad (5.14)$$

which is unique by the requirement that $\gamma/L \notin S_{N_\beta}$.

After at most N_α steps, $\{x_k^L\}_{k \geq 0}$ is *periodic modulo* $N_{\alpha\beta}$, as expressed by the following proposition.

Proposition 5.3.7. *There exist integers $\bar{k} \leq N_\alpha, M \leq N_\alpha$ and $n \geq 1$ such that*

$$x_{k+M}^L = x_k^L + n N_{\alpha\beta} \quad \text{for all } k \geq \bar{k}. \quad (5.15)$$

Moreover, the quotient n/M depends only on γ/L .

Proof. First remark that, if x_k^L is defined recursively by (5.13), we have

$$[x_k^L]_{N_{\alpha\beta}} \in \mathbb{Z}_{N_\alpha} \quad \text{for all } k \geq 1.$$

Since $\#\mathbb{Z}_{N_\alpha} = N_\alpha$, there exist integers $0 \leq j \leq N_\alpha$ and $l > j$, with $l - j \leq N_\alpha$, such that

$$[x_j^L]_{N_{\alpha\beta}} = [x_l^L]_{N_{\alpha\beta}}. \quad (5.16)$$

Let l be the minimal such l . Define $\bar{k} = j$, $M = l - j$ and $n = \frac{x_l^L - x_j^L}{N_{\alpha\beta}}$ to obtain (5.15).

It remains to show the last statement of the theorem. It suffices to show that the quotient n/M is independent of x_0 . We start by proving a monotonicity property of the orbits defined in (5.13) with respect to the initial datum: if $\{x_k\}$ and $\{x'_k\}$ are orbits obtained as above, we have

$$\text{if } x_0 \leq x'_0, \text{ then } x_k \leq x'_k, \quad \text{for all } k \geq 1. \quad (5.17)$$

This can be seen iteratively from (5.10), since the problems with $x = x_{k-1}$ and $x = x'_{k-1}$ consist in a constrained minimization of a parabola and its translation by $x'_{k-1} - x_{k-1}$, and, as previously remarked, the minimizer in (5.10) is the closest point to the vertex of the parabola with $[x + N]_{N_{\alpha\beta}} \in \mathbb{Z}_{N_{\alpha}}$.

Consider the orbits with initial data x_0 , x'_0 and $x_0 + N_{\alpha\beta}$, and let $n(x)$ and $M(x)$ denote the indices above with initial datum $x \in \{x_0, x'_0, x_0 + N_{\alpha\beta}\}$. Since the orbit with initial datum $x_0 + N_{\alpha\beta}$ is the translation by $N_{\alpha\beta}$ of the one with initial datum x_0 , we have $n(x_0 + N_{\alpha\beta}) = n(x_0)$ and $M(x_0 + N_{\alpha\beta}) = M(x_0)$. Taking into account the ordering of the initial conditions

$$x_0 \leq x'_0 \leq x_0 + N_{\alpha\beta},$$

by (5.15) for k_0 sufficiently large and taking $k = k_0 + TM(x_0)M(x'_0)$ with $T \in \mathbb{N}$, from $x_k \leq x'_k \leq x_k + N_{\alpha\beta}$ we get

$$\begin{aligned} x_{k_0} + Tn(x_0)M(x'_0)N_{\alpha\beta}N_{\alpha\beta} &\leq x'_{k_0} + Tn(x'_0)M(x_0)N_{\alpha\beta} \\ &\leq x_{k_0} + Tn(x_0)M(x'_0)N_{\alpha\beta} + N_{\alpha\beta}. \end{aligned}$$

In order that this inequality hold for all $T \geq 1$ we must have

$$n(x_0)M(x'_0) = n(x'_0)M(x_0),$$

which is the desired equality. \square

Definition 5.3.8 (effective velocity function). We define the *effective velocity function* $f : (0, +\infty) \setminus S_{N_{\beta}} \rightarrow [0, +\infty)$ by setting

$$f(Y) = \frac{nN_{\alpha\beta}}{M}, \quad (5.18)$$

with M and n in (5.15) defined by L and γ such that $Y = \gamma/L$. By Proposition 5.3.7, this is a good definition.

Remark 5.3.9. The terminology for formula (5.18) is motivated by the fact that we can define the velocity of a side as a *mean velocity* averaging on a period; that is,

$$v = \frac{nN_{\alpha\beta}\varepsilon}{M\tau}. \quad (5.19)$$

In (5.19) the velocity is the ratio between the minimal (periodic) displacement of the side and the product of the time-scale τ and the number of steps necessary to describe the minimal period, each of which considered as a 1-time step.

Remark 5.3.10 (properties of the velocity function f). The velocity function f has the following properties:

(a) f is constant on each interval contained in its domain;

(b) $f(Y) = 0$ if

$$Y < \bar{Y} := \frac{N_\beta + 2}{4\alpha};$$

in particular

$$\lim_{\gamma \rightarrow 0^+} \frac{1}{\gamma} f\left(\frac{\gamma}{L}\right) = 0.$$

Note that $(0, \bar{Y}) \cap S_{N_\beta} \neq \emptyset$;

(c) $f(Y)$ is a rational value;

(d) f is non decreasing;

(e) we have

$$\lim_{\gamma \rightarrow +\infty} \frac{1}{\gamma} f\left(\frac{\gamma}{L}\right) = \frac{2\alpha}{L}.$$

(f) $f(Y)$ is independent of β but depends on N_β .

(a) holds since on each component of $(0, +\infty) \setminus S_{N_\beta}$ the minimum problems (5.10) have a unique solution independent of Y , so that the values n and M in Proposition 5.3.7 are independent of Y . Note, however, that $f(Y)$ may be equal on neighboring components since the corresponding n and M may be equal even without uniqueness in (5.15);

(b) holds since we have $\bar{Y} = \gamma/\bar{L}$, where \bar{L} is the pinning threshold (5.9), and the computation of the pinning threshold is equivalent to the requirement that the orbit be constant after a finite number of steps;

(c) is immediate from the formula for $f(Y)$;

(d) is again a consequence of the fact that (5.10) are minimum problems related to a parabola with vertex in $2\alpha Y - \frac{1}{2}$ and the latter is an increasing function of Y ;

(e) using the same argument as in (d) above, we deduce in particular that

$$\left| \bar{N}_k - 2\alpha Y + \frac{1}{2} \right| \leq N_\beta,$$

which for $Y = \gamma/L$ implies that

$$\frac{2\alpha}{L} - 2N_\beta + \frac{1}{2\gamma} \leq \frac{1}{\gamma} f\left(\frac{\gamma}{L}\right) \leq \frac{2\alpha}{L} + 2N_\beta + \frac{1}{2\gamma},$$

and the desired equality letting $\gamma \rightarrow +\infty$;

(f) is an immediate consequence of the definition of $f(Y)$.

Remark 5.3.11 (singular cases). Let $\gamma/L \in S_{N_\beta}$, and let $\{x_k^L\}$ be defined by (5.13) with \bar{N}_k chosen to be a minimizer of (5.14), which may be not unique. Then arguing by monotonicity as in (d) above, we have $x_k^{L^+} \leq x_k^L \leq x_k^{L^-}$, where L^\pm are any two values with $L^- < L < L^+$ and γ/L^\pm belonging to the two intervals of $(0, +\infty) \setminus S_{N_\beta}$ with one endpoint equal to L , and $\{x_k^{L^\pm}\}$ have the same initial data.

5.3.3 Description of the homogenized limit motion.

The following characterization of any limit motion holds.

Theorem 5.3.12. *For all $\varepsilon > 0$, let $E_\varepsilon^0 \in \mathcal{D}_\varepsilon$ be a coordinate rectangle with sides $S_{1,\varepsilon}^0, \dots, S_{4,\varepsilon}^0$. Assume also that*

$$\lim_{\varepsilon \rightarrow 0^+} d_{\mathcal{H}}(E_\varepsilon^0, E_0) = 0$$

for some fixed coordinate rectangle E_0 . Let $\gamma > 0$ be fixed and let $E_\varepsilon(t) = E_{\varepsilon, \gamma\varepsilon}(t)$ be the piecewise-constant motion with initial datum E_ε^0 defined as in (4.12). Then, up to a subsequence, $E_\varepsilon(t)$ converges as $\varepsilon \rightarrow 0$ to $E(t)$, where $E(t)$ is a coordinate rectangle with sides $S_i(t), i = 1, \dots, 4$ and such that $E(0) = E_0$. Each S_i moves inward with velocity $v_i(t)$ satisfying

$$v_i(t) \in \left[\frac{1}{\gamma} f\left(\frac{\gamma}{L_i(t)}\right)^-, \frac{1}{\gamma} f\left(\frac{\gamma}{L_i(t)}\right)^+ \right], \quad (5.20)$$

where f is given by Definition 5.18, $L_i(t) := \mathcal{H}^1(S_i(t))$ denotes the length of the side $S_i(t)$, until the extinction time when $L_i(t) = 0$, and $f(Y)^-, f(Y)^+$ are the lower and upper limits of the effective-velocity function at $Y \in (0, +\infty)$.

Proof. We will apply the results of the previous sections with $\tau = \gamma\varepsilon$. Let $S_{\varepsilon,i}(t)$ be the sides of $E_\varepsilon(t)$, and let $L_{i,\varepsilon}^k = \mathcal{H}^1(S_{\varepsilon,i}(k\tau))$; i.e., $L_{i,\varepsilon}^k$ is the length of the i -th side of E_ε^k in the notation of the previous sections. If $\Delta S_{\varepsilon,i}^k = d_{\mathcal{H}}(S_{\varepsilon,i}(\gamma\varepsilon k), S_{\varepsilon,i}(\gamma\varepsilon(k+1)))$ denotes the distance from corresponding sides of E_ε^k , then note that

$$L_{i,\varepsilon}^{k+1} - L_{i,\varepsilon}^k = -(\Delta S_{\varepsilon,i-1}^k + \Delta S_{\varepsilon,i+1}^k)$$

(where the indices i rotate cyclically). By (5.6) we have

$$\frac{\Delta S_{\varepsilon,i}^k}{\tau} \leq \frac{c_1}{L_{i,\varepsilon}^k} + c_2.$$

This implies that if we define $L_{i,\varepsilon}(t)$ as the affine interpolation in $[k\tau, (k+1)\tau]$ of the values $L_{i,\varepsilon}^k$, then $L_{i,\varepsilon}(t)$ is a decreasing continuous function of t and the sequence is uniformly Lipschitz continuous on all intervals $[0, T]$ such that $L_{i,\varepsilon}(T) \geq c > 0$. Hence, it converges (up to a subsequence), as $\varepsilon \rightarrow 0$, to a function $L_i(t)$, which is also decreasing. It follows that $E_\varepsilon(t)$ converges as $\varepsilon \rightarrow 0$, up to a subsequence and in the Hausdorff sense, to a limit rectangle $E(t)$, for all $t \geq 0$.

It remains to justify formula (5.20) for the velocity v_i of the side $S_i(t)$. Let $[t^-, t^+]$ and L_i^\pm be such that $\gamma/L_i^\pm \in (0, +\infty) \setminus S_{N_\beta}$ and

$$L_i^- < L_i(t) < L_i^+ \quad \text{for } t^- \leq t \leq t^+.$$

Then the corresponding $L_{i,\varepsilon}(t)$ satisfy the same inequalities for ε small enough. By Remarks 5.3.11 and 5.3.9 we then have

$$\frac{1}{\gamma} f\left(\frac{\gamma}{L_i^+}\right) \leq v_i(t) \leq \frac{1}{\gamma} f\left(\frac{\gamma}{L_i^-}\right) \text{ for } t^- \leq t \leq t^+$$

By optimizing in L_i^\pm , and recalling that f is not decreasing, we obtain (5.20). \square

Theorem 5.3.13 (unique limit motions). *Let E_ε, E be as in the statement of Theorem 5.3.12. Assume in addition that the lengths L_1^0, L_2^0 of the sides of the initial set E_0 satisfy one of the following conditions (we assume that $L_1^0 \leq L_2^0$):*

- (a) $L_1^0, L_2^0 > \frac{4\alpha\gamma}{N_\beta + 2}$ (total pinning);
- (b) $L_1^0 < \frac{4\alpha\gamma}{N_\beta + 2}$ and $L_2^0 \leq \frac{4\alpha\gamma}{N_\beta + 2}$ (vanishing in finite time);

then $E_\varepsilon(t)$ converges locally in time to $E(t)$ as $\varepsilon \rightarrow 0$, where $E(t)$ is the unique rectangle with sides of lengths $L_1(t)$ and $L_2(t)$ which solve the following system of ordinary differential equations

$$\begin{cases} \dot{L}_1(t) = -\frac{2}{\gamma} f\left(\frac{\gamma}{L_2(t)}\right) \\ \dot{L}_2(t) = -\frac{2}{\gamma} f\left(\frac{\gamma}{L_1(t)}\right) \end{cases} \quad (5.21)$$

for almost every t , with initial conditions $L_1(0) = L_1^0$ and $L_2(0) = L_2^0$, where f is given by Definition 5.18.

Proof. In case (a) the statement follows by Theorem 5.3.12 noticing that we have $v_1(t) = v_2(t) = 0$ for all $t \geq 0$, which is equivalent to $\dot{L}_1 = \dot{L}_2 = 0$.

In case (b) the lengths of L_i are strictly decreasing until the extinction time. This implies that the set of t such that $f(\gamma/L_i(t))^- \neq f(\gamma/L_i(t))^+$ is negligible, and (5.21) follows since $\dot{L}_i = -2v_{i+1}$. \square

Remark 5.3.14 (general evolutions). More general initial data can be considered. Since their treatment follow from Theorem 5.3.12 as in Braides, Gelli and Novaga [14], we do not include the details. We only recall that:

- all velocities v_i satisfying (5.20) can be obtained, with a proper choice of the initial data E_ε^0 ;
- if we take initial data E_0 coordinate polyrectangles (see Section 4.5) then the motion can be characterized with the same velocities, with the convention that convex sides move inwards, concave sides move outwards, other sides remain pinned (according to Definition 4.5.1 and subsequent remark);
- more general initial data E_0 can be dealt with once we remark that, at level ε , the assumption that E_ε^0 is a polyrectangle is always satisfied.

5.4 Computation of the velocity function

The velocity function in Definition 5.18 may be not easily described for generic N_α and N_β . In this section we compute it, by means of algebraic formulas, in the simpler cases $N_\beta = 1$ and $N_\beta = 2$, with varying N_α . These are prototypes for the cases N_β

odd and N_β even, respectively. We also give two easy examples for N_α fixed and equal to 1, and we compare the new velocity function with the homogeneous case showing that the inhomogeneities in the lattice may accelerate or decelerate the motion. We can assume, without loss of generality, that $\gamma = 1$.

5.4.1 The case $N_\beta = 1$.

Let $Y > \bar{Y} = \frac{3}{4\alpha}$. We assume also that Y is not in the singular set; i.e.,

$$Y \notin \left\{ \frac{k + j(N_\alpha + 1)}{2\alpha}, k = 1, \dots, N_\alpha - 1, j \geq 0 \right\} \cup \left\{ \frac{N_\alpha + (2j + 1)(N_\alpha + 1)}{4\alpha}, j \geq 0 \right\}.$$

As shown by Proposition 5.3.7, the minimal period is independent of the starting point of the orbits, so there is no restriction to assume that $x^0 = 0$ in (5.13)-(5.14). We divide the analysis in three cases (a), (b) and (c) below.

(a) If $Y \in \left(\frac{k + j(N_\alpha + 1)}{2\alpha}, \frac{k + 1 + j(N_\alpha + 1)}{2\alpha} \right)$, $k = 1, 2, \dots, N_\alpha - 1, j \geq 0$, then we denote the minimizer of problem (5.14) in the homogeneous case $N_\beta = 0$ by $N = k + j(N_\alpha + 1)$. The velocity function $f(Y)$ will be characterized by algebraic relations between N and N_α . We have two sub-cases:

(a₁) N and $N_\alpha + 1$ are coprime. In this case, by iterating the scheme (5.13), after at most N_α steps the side encounters a defect, that is

$$[nN]_{N_\alpha+1} = [N_\alpha]_{N_\alpha+1}$$

for some $1 \leq n \leq N_\alpha$. In this case, we denote by $\bar{n} \geq 0$ the minimal solution of the congruence equation

$$nN \equiv N_\alpha \pmod{N_\alpha + 1}, \quad n \geq 1, \quad (5.22)$$

and $\bar{k} \geq 0$ is given by

$$\bar{k} = \frac{\bar{n}N - N_\alpha}{N_\alpha + 1}.$$

If $Y \in \left(\frac{k + j(N_\alpha + 1)}{2\alpha}, \frac{2k + 2j(N_\alpha + 1) + 1}{4\alpha} \right)$, then the location of the side at step n is at $N_\alpha - 1 + \bar{k}(N_\alpha + 1)$ (which is equal to -2 modulo $N_\alpha + 1$).

This computation shows that we can limit our analysis to periodic orbits modulo $N_\alpha + 1$ with initial datum equal to -2 (or, equivalently, $N_\alpha - 1$). The period of such orbits is obtained as follows. We solve the congruence equation

$$nN \equiv 1 \pmod{N_\alpha + 1}, \quad (5.23)$$

for $n \geq 1$ and denote by n_{\min} the minimal positive solution of equation (5.23); that is, the minimal positive integer in the class

$$\left[N^{\varphi(N_\alpha+1)-1} \right]_{\text{mod } N_\alpha + 1}.$$

The function $\varphi(n)$ is the *Euler’s totient function* and it counts the integers m such that $1 \leq m < n$ and m has no common divisors with n . If we define

$$k_{\min} = \frac{n_{\min}N - 1}{N_{\alpha} + 1},$$

then we have that

$$\begin{aligned} f(Y) &= \frac{k_{\min}(N_{\alpha} + 1)}{k_{\min}(N_{\alpha} + 1) + 1} = \left(\frac{k_{\min}(N_{\alpha} + 1)}{k_{\min}(N_{\alpha} + 1) + 1} \right) \lfloor 2\alpha Y \rfloor \\ &= \left(\frac{1}{1 + \frac{1}{k_{\min}(N_{\alpha} + 1)}} \right) \lfloor 2\alpha Y \rfloor. \end{aligned} \quad (5.24)$$

Note that $f(Y) < \lfloor 2\alpha Y \rfloor$, so that the velocity of the side reduces (deceleration) with respect to the homogeneous case.

Suppose now that $Y \in \left(\frac{2k + 2j(N_{\alpha} + 1) + 1}{4\alpha}, \frac{k + 1 + j(N_{\alpha} + 1)}{2\alpha} \right)$, then the location of the side at step n is $N_{\alpha} + 1 + \bar{k}(N_{\alpha} + 1)$, which is equal to 0 modulo $N_{\alpha} + 1$. We have that

$$f(Y) = \left(\frac{(\bar{k} + 1)(N_{\alpha} + 1)}{(\bar{k} + 1)(N_{\alpha} + 1) - 1} \right) \lfloor 2\alpha Y \rfloor = \left(\frac{1}{1 - \frac{1}{(\bar{k} + 1)(N_{\alpha} + 1)}} \right) \lfloor 2\alpha Y \rfloor. \quad (5.25)$$

Note that $f(Y) > \lfloor 2\alpha Y \rfloor$, so the velocity of the side increases (acceleration) with respect to the homogeneous case.

(a₂) N and $N_{\alpha} + 1$ are not coprime. In this case the side does not meet any β -bond and the velocity function has the same value as in the homogeneous case, i.e.

$$f(Y) = \lfloor 2\alpha Y \rfloor.$$

(b) If $Y \in \left(\frac{N_{\alpha} + j(N_{\alpha} + 1)}{2\alpha}, \frac{N_{\alpha} + (2j + 1)(N_{\alpha} + 1)}{4\alpha} \right)$, then we argue as in (a₁).

(c) If $Y \in \left(\frac{N_{\alpha} + (2j + 1)(N_{\alpha} + 1)}{4\alpha}, \frac{1 + (j + 1)(N_{\alpha} + 1)}{2\alpha} \right)$, then

$$f(Y) = N_{\alpha} + 1 + j(N_{\alpha} + 1).$$

Note that $f(Y) > \lfloor 2\alpha Y \rfloor$ if $Y \in \left(\frac{N_{\alpha} + (2j + 1)(N_{\alpha} + 1)}{4\alpha}, \frac{(j + 1)(N_{\alpha} + 1)}{2\alpha} \right)$, while $f(Y) = \lfloor 2\alpha Y \rfloor$ if $Y \in \left(\frac{(j + 1)(N_{\alpha} + 1)}{2\alpha}, \frac{1 + (j + 1)(N_{\alpha} + 1)}{2\alpha} \right)$.

Example 5.4.1 (the case $N_{\alpha} = N_{\beta} = 1$). In this case the velocity function is given by

$$\bar{f}(Y) = \begin{cases} 0 & \text{if } Y < \frac{3}{4\alpha}, \\ 2k & \text{if } Y \in \left(\frac{4k - 1}{4\alpha}, \frac{4k + 3}{4\alpha} \right), \quad k \geq 1; \end{cases}$$

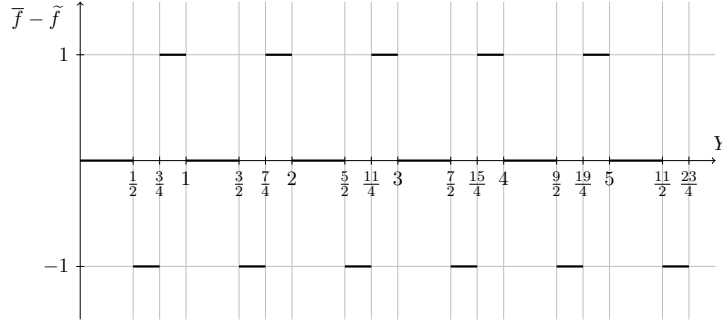


Figure 5.16. Difference between inhomogeneous-homogeneous velocity function ($\alpha = 1$).

i.e.,

$$\bar{f}(Y) = 2 \left\lfloor \alpha Y + \frac{1}{4} \right\rfloor.$$

We compare it with the homogeneous case in Fig. 5.16; here it is pictured the difference between $\bar{f}(Y)$ and $\tilde{f}(Y) = \lfloor 2\alpha Y \rfloor$, with $\alpha = 1$.

5.4.2 The case $N_\beta = 2$

We now study the case $N_\beta = 2$. Let $Y > \bar{Y} = \frac{1}{\alpha}$ and we assume also that Y is not in the singular set, i.e.,

$$Y \notin \left\{ \frac{k + j(N_\alpha + 2)}{2\alpha}, k = 1, \dots, N_\alpha - 1, j \geq 0 \right\} \cup \left\{ \frac{N_\alpha + 1 + j(N_\alpha + 2)}{2\alpha}, j \geq 0 \right\}.$$

(a) If $Y \in \left(\frac{k + j(N_\alpha + 2)}{2\alpha}, \frac{k + 1 + j(N_\alpha + 2)}{2\alpha} \right)$, $k = 1, 2, \dots, N_\alpha - 2, j \geq 0$, then $N = k + j(N_\alpha + 2)$ and we have two sub-cases:

(a₁) N and $N_\alpha + 2$ are coprime. We compute $\bar{k} = \min(k_1, k_2) \geq 0$, where k_1 is the minimal positive solution of the congruence equation

$$kN \equiv N_\alpha \pmod{N_\alpha + 2},$$

and k_2 is the minimal positive solution of the congruence equation

$$kN \equiv N_\alpha + 1 \pmod{N_\alpha + 2};$$

that is k_1 is the minimal positive integer in the class $\left[N_\alpha N^{\varphi(N_\alpha + 2) - 1} \right]_{\text{mod } N_\alpha + 2}$ and k_2 is the minimal positive integer in the class $\left[(N_\alpha + 1) N^{\varphi(N_\alpha + 2) - 1} \right]_{\text{mod } N_\alpha + 2}$.

If $\bar{k} = k_1$, then

$$f(Y) = \left(\frac{k_1(N_\alpha + 2)}{k_1(N_\alpha + 2) + 1} \right) \lfloor 2\alpha Y \rfloor = \left(\frac{1}{1 + \frac{1}{k_1(N_\alpha + 2)}} \right) \lfloor 2\alpha Y \rfloor, \quad (5.26)$$

and $f(Y) < \lfloor 2\alpha Y \rfloor$.

If $\bar{k} = k_2$, then

$$f(Y) = \left(\frac{k_2(N_\alpha + 2)}{k_2(N_\alpha + 2) - 1} \right) \lfloor 2\alpha Y \rfloor = \left(\frac{1}{1 - \frac{1}{k_2(N_\alpha + 2)}} \right) \lfloor 2\alpha Y \rfloor, \quad (5.27)$$

and $f(Y) > \lfloor 2\alpha Y \rfloor$.

(a₂) N and $N_\alpha + 2$ are not coprime. In this case

$$f(Y) = \lfloor 2\alpha Y \rfloor$$

as in the homogeneous case.

(b) If $Y \in \left(\frac{N_\alpha + 1 + j(N_\alpha + 2)}{2\alpha}, \frac{(j+1)(N_\alpha + 2) + 1}{2\alpha} \right)$, $j \geq 0$, then

$$f(Y) = (j+1)(N_\alpha + 2).$$

Note that, in this case, if $Y \in \left(\frac{N_\alpha + 1 + j(N_\alpha + 2)}{2\alpha}, \frac{(j+1)(N_\alpha + 2)}{2\alpha} \right)$ then $f(Y) > \lfloor 2\alpha Y \rfloor$, while if $Y \in \left(\frac{(j+1)(N_\alpha + 2)}{2\alpha}, \frac{(j+1)(N_\alpha + 2) + 1}{2\alpha} \right)$ then $f(Y) = \lfloor 2\alpha Y \rfloor$.

(c) If $Y \in \left(\frac{N_\alpha - 1 + j(N_\alpha + 2)}{2\alpha}, \frac{N_\alpha + 1 + j(N_\alpha + 2)}{2\alpha} \right)$, $j \geq 0$, then we could reason as in the case (a).

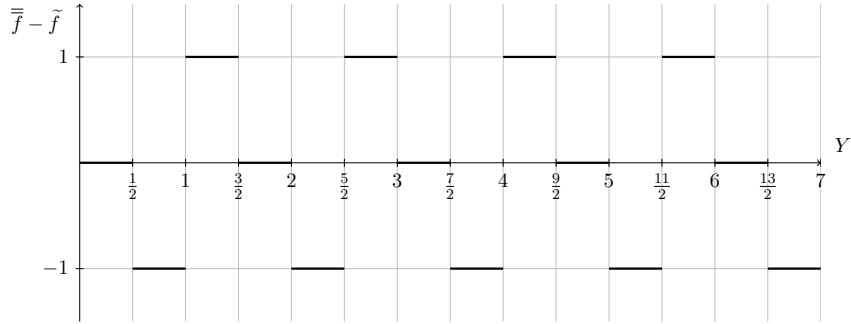


Figure 5.17. Difference between inhomogeneous-homogeneous velocity function ($\alpha = 1$).

Example 5.4.2 (the case $N_\alpha = 1, N_\beta = 2$). The velocity function is given by

$$\bar{\bar{f}}(Y) = \begin{cases} 0 & \text{if } Y < \frac{1}{\alpha}, \\ 3k & \text{if } Y \in \left(\frac{3k-1}{2\alpha}, \frac{3k+2}{2\alpha} \right), \quad k \geq 1; \end{cases}$$

i.e.,

$$\bar{\bar{f}}(Y) = 3 \left\lfloor \frac{2}{3}\alpha Y + \frac{1}{3} \right\rfloor.$$

The comparison with the homogeneous case is pictured in Fig. 5.17.

Chapter 6

Motion of discrete interfaces in ‘low-contrast’ periodic media

In this chapter, we present the results contained in the paper by myself [44] about motion in “low-contrast” periodic media, that is described by α connections with periodic inclusions β such that $\beta - \alpha \rightarrow 0$ as $\varepsilon \rightarrow 0$.

6.1 Motivation and results

Here we give another example of the fact that the microstructure can affect the limit evolution without changing the Γ -limit, along the lines of Chapter 5. To this end, we perform a multi-scale analysis by introducing a *contrast parameter* δ_ε and considering a *low-contrast* medium, that is a periodic mixture of two homogeneous materials whose propagating properties are close to each other. One of them can be considered as a fixed background medium (described by α -connections) and the other as a small (vanishing) perturbation from that one, that is with $\beta = \beta_\varepsilon = \beta(\varepsilon)$ and $\beta_\varepsilon - \alpha = \delta_\varepsilon \rightarrow 0$ as $\varepsilon \rightarrow 0$. With the same notation as in Chapter 5, we restrict ourselves to the case $N_\alpha = N_\beta = 1$; despite of its simplicity, the choice of this particular geometry will suffice to show new features of the motion. The main result is the existence of a threshold value of the contrast parameter below which we have a new homogenized effective velocity, which takes into account the propagation velocities in both the connections α and β ; above this threshold, instead, it is independent of the value of β and the motion is obtained by considering only the α -connections.

First of all, we determine the correct scaling for δ_ε to have that a straight interface may stay on β -connections. To this end, we consider a coordinate α -type rectangle (Definition 5.3.3), we write the variation of the energy $\mathcal{F}_{\varepsilon,\tau}^{\alpha,\beta_\varepsilon}$ (given by (5.5) with $\beta = \beta_\varepsilon$) associated to the displacement by ε of the upper horizontal side of length L (see Fig. 6.1) and we impose it to be zero. We have that

$$-2\alpha\varepsilon + (\beta_\varepsilon - \alpha)L + \frac{cL}{\gamma}\varepsilon = -2\alpha\varepsilon + \delta_\varepsilon L + \frac{cL}{\gamma}\varepsilon = 0,$$

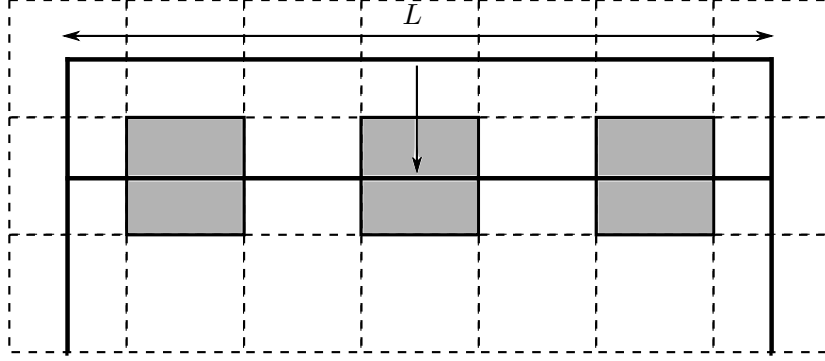


Figure 6.1. Displacement of a side from α -connections to β -connections.

where $c = c(L)$ is a constant depending on L (see (5.6)), from which we deduce that

$$\delta_\varepsilon = \left(\frac{2\alpha}{L} - \frac{c}{\gamma} \right) \varepsilon = O(\varepsilon) \quad \text{as } \varepsilon \rightarrow 0.$$

This heuristic computation suggests that the correct scaling is

$$\beta_\varepsilon - \alpha = \delta_\varepsilon = \delta \varepsilon$$

for some constant $\delta > 0$.

As in Section 5.3, we will assume that $\tau = \gamma \varepsilon$ and we will restrict the description of the motion to the case of initial data coordinate rectangles. The evolute of a coordinate rectangle by minimization of the energy is again a coordinate rectangle. We will show that there exists a threshold $\tilde{\delta} = \frac{1}{2\gamma}$ such that if $\delta < \tilde{\delta}$ (subcritical regime) then the evolute rectangles may have some β -type side (that is, a side intersecting only β -connections), while if $\delta \geq \tilde{\delta}$ (supercritical regime) the β -connections are avoided as in the case $\beta > \alpha$. Note that this result gives information also for more general choices of the vanishing rate of δ_ε : if $\delta_\varepsilon \ll \varepsilon$, we reduce to the subcritical case, while if $\delta_\varepsilon \gg \varepsilon$, we are in the supercritical case. The limit motion can still be described through a system of degenerate ordinary differential equations as in (5.21) with a new effective velocity function f depending on δ . We also have a new effective pinning threshold given by

$$\bar{L}_\delta = \max \left\{ \frac{2\alpha\gamma}{\delta\gamma + 1}, \frac{4}{3}\alpha\gamma \right\}.$$

Overview of the chapter. In Section 6.2 we define the new energies that we will consider. Section 6.3 contains the description of the convergence of the discrete scheme in the case of a rectangular initial set. We show that the minimizers of this scheme are rectangles also in the low-contrast framework. Section 6.3.1 deals with the definition of the effective velocity of a side by means of a homogenization formula, as in Section 5.3.2. This velocity can be expressed uniquely (up possibly to a discrete set of values) as a function of the ratio of γ and the side length, and of δ (Definition 6.3.6). Section 6.3.2 contains the computation of the effective pinning threshold, showing that it is affected by microstructure because it also depends on the parameter δ (for δ ‘small’). In Section 6.3.3 we compute explicitly the velocity

function, showing a comparison with the homogeneous case $\alpha = \beta$ (Chapter 4) and the high-contrast case $\beta > \alpha$ (Chapter 5). The description of the homogenized limit motion is contained in Section 6.3.4. Section 6.4 deals with the case of non-uniform inclusions distributed into periodic uniform layers.

6.2 Inhomogeneous ‘low-contrast’ ferromagnetic energies

The energies we consider are interfacial energies defined in an inhomogeneous low-contrast environment as follows. Let $\alpha, \delta > 0$ and we fix $\varepsilon > 0$. We consider 2ε -periodic coefficients c_{ij}^ε indexed on nearest-neighbors of $\varepsilon\mathbb{Z}^2$ (i.e., $i, j \in \varepsilon\mathbb{Z}^2$ with $|i - j| = \varepsilon$) defined for i, j such that

$$0 \leq \frac{i_1 + j_1}{2}, \frac{i_2 + j_2}{2} < 2\varepsilon$$

by

$$c_{ij}^\varepsilon = \begin{cases} \beta_\varepsilon = \alpha + \delta\varepsilon, & \text{if } 0 \leq \frac{i_1 + j_1}{2}, \frac{i_2 + j_2}{2} \leq \varepsilon \\ \alpha & \text{otherwise.} \end{cases} \quad (6.1)$$

These coefficients label the bonds between points in $\varepsilon\mathbb{Z}^2$, so that they describe a matrix of α -bonds with 2ε -periodic inclusions of β -bonds grouped in squares of side length ε . The periodicity cell is pictured in Fig. 6.2. As before, the continuous lines represent β -bonds while the dashed lines the α ones.

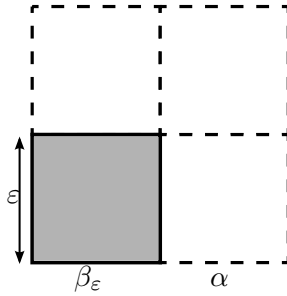


Figure 6.2. The periodicity cell.

Correspondingly, to coefficients (6.1) we associate the energy defined on subsets \mathcal{I} of $\varepsilon\mathbb{Z}^2$ by

$$P_\varepsilon^{\alpha, \beta_\varepsilon}(\mathcal{I}) = \sum \left\{ \varepsilon c_{ij}^\varepsilon : |i - j| = \varepsilon, i \in \mathcal{I}, j \in \varepsilon\mathbb{Z}^2 \setminus \mathcal{I} \right\}, \quad (6.2)$$

with the same notation as in Section 5.2. We perform the same identification on unions of ε -squares (i.e., the class \mathcal{D}_ε defined in Section 4.2) and we remark that energies $P_\varepsilon^{\alpha, \beta_\varepsilon}$ Γ -converge, as $\varepsilon \rightarrow 0$, to the anisotropic crystalline perimeter functional P^α (4.10). For this, we note that, for any $E \in \mathcal{D}_\varepsilon$, $P_\varepsilon^{\alpha, \beta_\varepsilon}(E) = P_\varepsilon^{\alpha, \alpha}(E) + C\varepsilon^2$ for some $C > 0$ and that $P_\varepsilon^{\alpha, \alpha}$ Γ -converges, as $\varepsilon \rightarrow 0$, to P^α (see Proposition 1.1.3).

6.3 Motion of a rectangle

We apply the same discrete-in-time minimization scheme as in Section 4.3 to energies $\mathcal{F}_{\varepsilon,\tau}^{\alpha,\beta\varepsilon}$, defined as in (5.5) with $P_{\varepsilon}^{\alpha,\beta\varepsilon}$ in place of $P_{\varepsilon}^{\alpha,\beta}$, with $\tau = \gamma\varepsilon$ and $E_{\varepsilon}^0 \in \mathcal{D}_{\varepsilon}$ a coordinate rectangle.

The result is that coordinate rectangles evolve into coordinate rectangles. This will be more precise in the following. In fact, we will show that if $\delta < \frac{1}{2\gamma}$ then the evolute rectangles may have some β -type side, while if $\delta \geq \frac{1}{2\gamma}$ they have only α -type sides.

Proposition 6.3.1. *If $E_{\varepsilon}^0 \in \mathcal{D}_{\varepsilon}$ is a coordinate rectangle and F is a minimizer for the minimum problem for $\mathcal{F}_{\varepsilon,\tau}^{\alpha,\beta\varepsilon}(\cdot, E_{\varepsilon}^k)$, $k \geq 0$, then for all $\eta > 0$ F is a coordinate rectangle as long as the sides of E_{ε}^k are larger than η and ε is small enough.*

Proof. It will suffice to show it for $F = E_{\varepsilon}^1$. We subdivide the proof into steps.

Step 1: connectedness of F and α -rectangularization. Some steps of the proof easily follow from Proposition 5.3.5. In particular, the fact that F is a connected set and that it is energetically convenient to replace F by its α -rectangularization, i.e. $F' = F \cup R^{\alpha}$, R^{α} being the maximal α -type rectangle with each side intersecting F . This set is either an α -type rectangle (and in this case we conclude) or it has some protrusions intersecting β -bonds. Moreover, we have that $d_{\mathcal{H}}(\partial E_{\varepsilon}^1, \partial E_{\varepsilon}^0) \leq c(L)\varepsilon$, where $c(L)$ is a constant depending on the length L of the smaller side of E_{ε}^0 (as remarked in (5.6)).

Step 2: optimal profiles of protrusions on β -squares. Now we describe the form of the optimal profiles of the boundary of F intersecting β -squares. As noted in the proof of Proposition 5.3.5, F contains an α -type rectangle $R^{\alpha} = [\varepsilon m_1, \varepsilon M_1] \times [\varepsilon m_2, \varepsilon M_2]$ and is contained in the α -type rectangle

$$\tilde{R}^{\alpha} = [\varepsilon(m_1 - 1), \varepsilon(M_1 + 1)] \times [\varepsilon(m_2 - 1), \varepsilon(M_2 + 1)],$$

whose sides exceed the ones of R^{α} by at most 2ε . We will analyze separately the possible profiles of F close to each side of R^{α} ; e.g., in the rectangle $[\varepsilon(m_1 - 1), \varepsilon(M_1 + 1)] \times [\varepsilon M_2, \varepsilon(M_2 + 1)]$ (i.e., close to the upper horizontal side of R^{α}). Our aim is to show that the optimal profile is straight. We first consider the possible behavior of

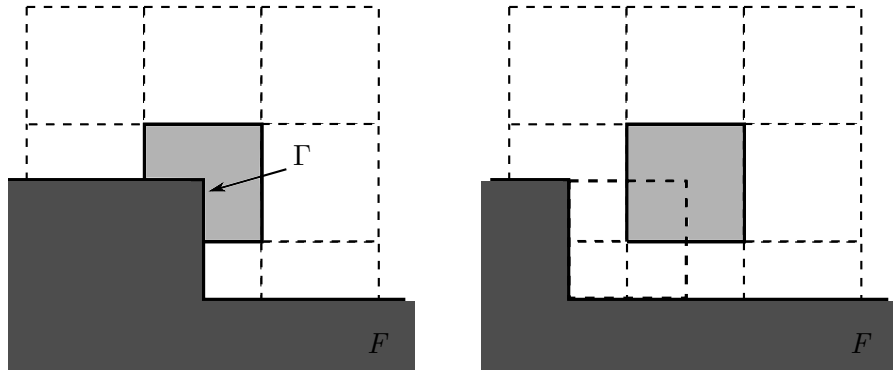


Figure 6.3. Removal of an ε -square for δ ‘large’.

the boundary of F at a single β -square Q , assuming that Q is not one of the two

extremal squares. We claim that either $F \cap Q = \emptyset$ or $\partial F \cap Q$ is a horizontal segment. In fact, if a portion Γ of ∂F intersects two adjacent sides of Q as in Fig. 6.3, then we may remove the ε -square whose center is in $Q \cap F$.

In this case, the variation of energy is

$$-2(\beta_\varepsilon - \alpha)\varepsilon + \frac{1}{\gamma}c(L)\varepsilon^2 = \left(-2\delta + \frac{1}{\gamma}c(L)\right)\varepsilon^2, \quad (6.3)$$

which is negative, for ε small, if and only if $\delta > c(L)/2\gamma$.

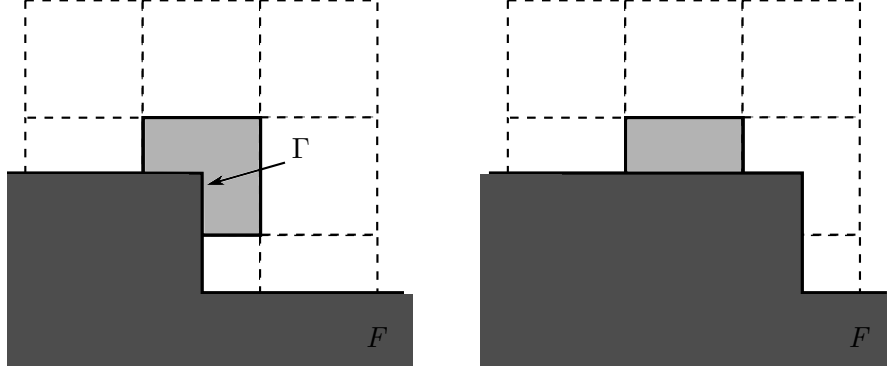


Figure 6.4. Addition of an ε -square for δ ‘small’.

If we add an ε -square as in Fig. 6.4, instead, the variation of the energy is simply

$$-\frac{1}{\gamma}c(L)\varepsilon^2, \quad (6.4)$$

which is negative for ε small. We note that the variation in (6.3) is less than the one in (6.4) if and only if $\delta > c(L)/\gamma$.

The same analysis applies to the extremal squares, for which we deduce that $F \cap Q$, if non-empty, is a rectangle with one vertex coinciding with a vertex of R^α .

We now consider the interaction of consecutive β -squares. Let Q_1, \dots, Q_K a

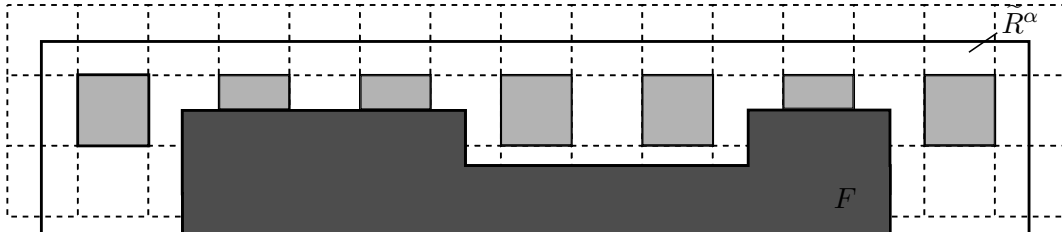


Figure 6.5. Interaction of consecutive β -squares.

maximal array of consecutive β -squares with $F \cap Q_k \neq \emptyset$ for $k = 1, \dots, K$ and such that Q_1 is not a corner square. If the subsequent β -squares $Q_{K+1}, \dots, Q_{K+K'}$ are a maximal array which do not intersect F , and $Q_{K+K'+1}, \dots, Q_{K+K'+K''}$ are another maximal array with $F \cap Q_k \neq \emptyset$ for $k = K+K'+1, \dots, K+K'+K''$ and such that $Q_{K+K'+K''}$ is not a corner square (see Fig. 6.5), then we may replace F by $F \cup R$ (see Fig. 6.6), where R is the rectangle given by the union of the ε -squares centered at the vertices of the β -squares $Q_{K+1}, \dots, Q_{K+K'}$.

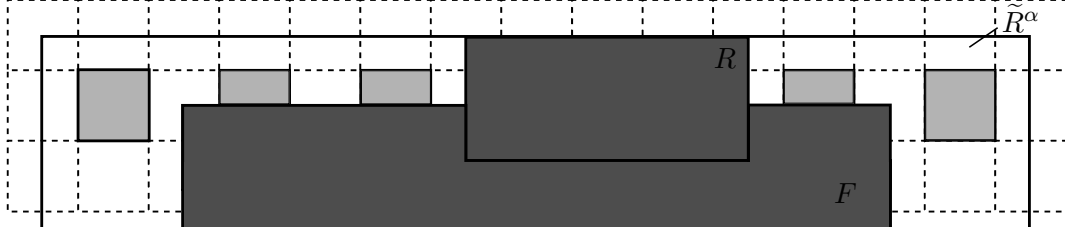


Figure 6.6. The new profile after replacing F by $F \cup R$.

This operation leaves unchanged the $P_\varepsilon^{\alpha, \beta_\varepsilon}$ and reduces the symmetric difference. We can repeat this procedure for any term of such arrays. At this point, if we replace F by $F \cup [\varepsilon m_1, \varepsilon M_1] \times [\varepsilon M_2, \varepsilon(M_2 + 1)]$, this strictly reduces $P_\varepsilon^{\alpha, \beta_\varepsilon}$ and the symmetric difference (see Fig. 6.7).



Figure 6.7. The new profile after replacing F by $F \cup [\varepsilon m_1, \varepsilon M_1] \times [\varepsilon M_2, \varepsilon(M_2 + 1)]$.

Note that, if the intersection of F and the left (resp., right) corner square is not empty, then we can consider as a competitor $F \cup [\varepsilon(m_1 - 1), \varepsilon M_1] \times [\varepsilon M_2, \varepsilon(M_2 + 1)]$ (resp., $F \cup [\varepsilon m_1, \varepsilon(M_1 + 1)] \times [\varepsilon M_2, \varepsilon(M_2 + 1)]$); if F has non empty intersection with both the corner squares, then we consider $F \cup [\varepsilon(m_1 - 1), \varepsilon(M_1 + 1)] \times [\varepsilon M_2, \varepsilon(M_2 + 1)]$. If there exists only one maximal array Q_1, \dots, Q_K and the intersection of F and

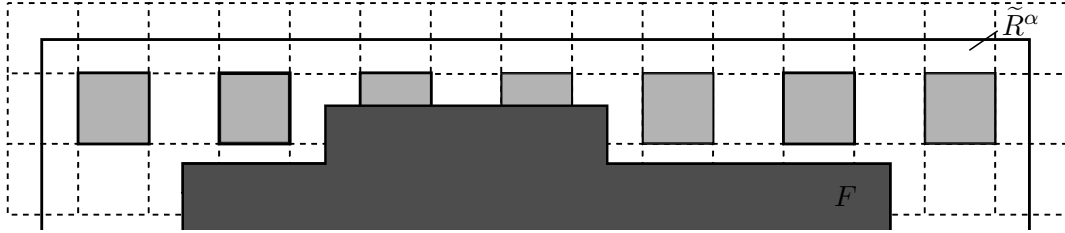


Figure 6.8. The case of a single maximal array of intersecting β -squares.

both the corner squares is empty (see Fig. 6.8), then we may remove all the ε -squares centered at vertices of Q_1, \dots, Q_K and the variation of energy is

$$-2\alpha\varepsilon + 2K(\beta_\varepsilon - \alpha)\varepsilon + \frac{1}{\gamma}2c(L)K\varepsilon^2 = -2\alpha\varepsilon - 2K\delta\varepsilon^2 + \frac{1}{\gamma}2c(L)K\varepsilon^2, \quad (6.5)$$

which is negative for ε small.

Another possibility is that F has a β -type side, that is the intersection of ∂F with the β -squares is a horizontal segment, as in Fig. 6.10.

Step 3: conclusion. We can repeat this procedure for each side, and finally, by α -rectangularization, we obtain that either F is an α -type rectangle or it has some

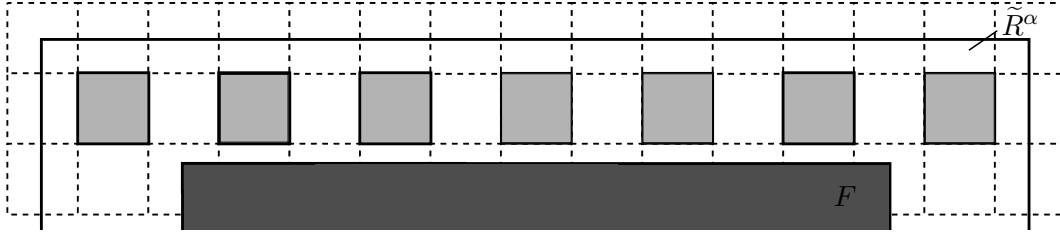


Figure 6.9. The profile after removing all the ε -squares.

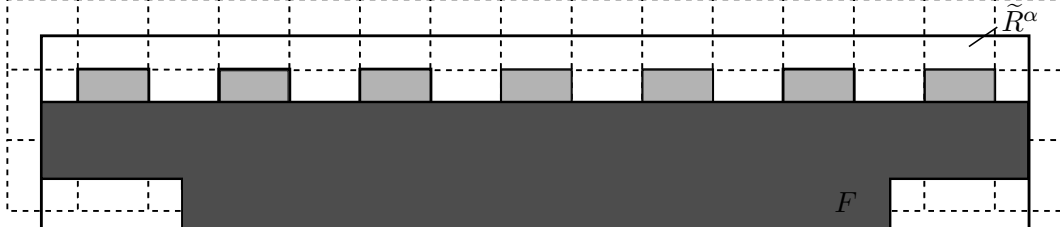


Figure 6.10. F has a β -side.

β -type side. However, F is a coordinate rectangle. We note that all the estimates above can be iterated and hold uniformly as long as the sides of E_ε^k are larger than η , since they depend only on $c(\eta)$. \square

6.3.1 Definition of the effective velocity

As remarked in Section 5.3.2, up to an error vanishing as $\varepsilon \rightarrow 0$, the motion of each side is independent of the other ones. As a consequence, its description can be reduced to a one-dimensional problem.

Let x_k represents the projection on the horizontal axis of the left-hand vertical side of $E_k = E_\varepsilon^k$, whose length is L_k . For all $Y = \gamma/L_k > 0$ consider the minimum problems

$$\min \{g(N) : N \in \mathbb{N}\} \quad (6.6)$$

where

$$g(N) = \begin{cases} -2\alpha N + \frac{N(N+1)}{2Y}, & [N]_2 = [0]_2, \\ -2\alpha N + \frac{\delta\gamma}{Y} + \frac{N(N+1)}{2Y}, & [N]_2 = [1]_2, \end{cases} \quad (6.7)$$

and $[z]_2$ denotes the congruence class of z modulo 2. Then, also in this case, the set of $Y > 0$ for which (6.6) does not have a unique solution is discrete. To check this it suffices to remark that the function to minimize is represented (up to multiplying by $2Y$) by two parabolas

$$-4\alpha Y X + X(X+1) \quad \text{and} \quad -4\alpha Y X + X(X+1) + 2\delta\gamma$$

with vertex in

$$X = 2\alpha Y - \frac{1}{2}.$$

The minimizers in (6.6) are not unique in the case that

$$g(N-1) = g(N) \quad \text{and} \quad g(N) = g(N+1), \quad (6.8)$$

that is for $Y = \frac{N + \delta\gamma}{2\alpha}$ and $Y = \frac{N + 1 - \delta\gamma}{2\alpha}$ if $[N]_2 = [1]_2$, while for $Y = \frac{N - \delta\gamma}{2\alpha}$ and $Y = \frac{N + 1 + \delta\gamma}{2\alpha}$ if $[N]_2 = [0]_2$.

Definition 6.3.2 (singular set). We define the singular set S_δ for problems (6.6) as

$$S_\delta = \frac{1}{2\alpha} [(2\mathbb{Z} + 1 + \delta\gamma) \cup (2\mathbb{Z} - \delta\gamma)]. \quad (6.9)$$

Remark 6.3.3. Note that, contrary to the high-contrast case $\beta > \alpha$, the singular set now depends on the particular value of β through δ .

The main result is the following.

Proposition 6.3.4. Let $Y \in (0, +\infty) \setminus S_\delta$. Then the minimum problem (6.6) may admit a solution \tilde{N} such that $[\tilde{N}]_2 = [1]_2$ if and only if $\delta < \tilde{\delta} := 1/2\gamma$. Otherwise, it is $[N]_2 = [0]_2$ for any solution N .

Proof. Let N be such that $[N]_2 = [1]_2$. Then N is the minimum in (6.6) if and only if

$$\begin{cases} N - \frac{1}{2} < 2\alpha Y - \frac{1}{2} < N + \frac{1}{2}, \\ g(N) < g(N-1) \\ g(N) < g(N+1) \end{cases} \quad (6.10)$$

that is,

$$\begin{cases} \frac{N}{2\alpha} < Y < \frac{N+1}{2\alpha} \\ Y > \frac{N + \delta\gamma}{2\alpha} \\ Y < \frac{N + 1 - \delta\gamma}{2\alpha}. \end{cases}$$

We note that it is

$$\frac{N + \delta\gamma}{2\alpha} < \frac{N + 1 - \delta\gamma}{2\alpha},$$

so that the system (6.10) has solutions, if and only if

$$\delta < \tilde{\delta} := \frac{1}{2\gamma}. \quad (6.11)$$

In this case, the minimum is $N - 1$ if and only if

$$N - \frac{3}{2} - \delta\gamma < 2\alpha Y - \frac{1}{2} < N - \frac{1}{2} + \delta\gamma,$$

that is,

$$\frac{N - 1 - \delta\gamma}{2\alpha} < Y < \frac{N + \delta\gamma}{2\alpha}.$$

If $\delta \geq 1/2\gamma$, then by (6.11) it follows that the discrete minimum is always even. \square

We will examine the iterated minimizing scheme for $\gamma/L_k = \gamma/L \in (0, +\infty) \setminus S_\delta$ fixed, which reads

$$\begin{cases} x_{k+1}^L = x_k^L + \bar{N}_k, & k \geq 0 \\ x_0^L = x^0 \end{cases} \quad (6.12)$$

with $x^0 \in \{0, 1\}$ and $\bar{N}_k \in \mathbb{N}$ the minimizer of

$$\min \begin{cases} -2\alpha N + \frac{1}{\gamma} \frac{N(N+1)}{2} L, & \text{if } [N]_2 = [0]_2, \\ -2\alpha N + \delta L + \frac{1}{\gamma} \frac{N(N+1)}{2} L, & \text{if } [N]_2 = [1]_2, \end{cases} \quad (6.13)$$

which is unique up to the requirement that $\gamma/L \notin S_\delta$.

Now we prove that, after at most two steps, $\{x_k^L\}_{k \geq 0}$ is periodic modulo 2, as expressed by the following proposition.

Proposition 6.3.5. *There exist integers $\bar{k}, M \leq 2$ and $n \geq 1$ such that*

$$x_{k+M}^L = x_k^L + 2n \quad \text{for all } k \geq \bar{k}. \quad (6.14)$$

Moreover the quotient n/M depends only on γ/L . In particular, if $\delta \geq 1/2\gamma$ then $\bar{k} = M = 1$.

Proof. By Proposition 6.3.4, the latter part of the statement is a straightforward consequence of Proposition 5.3.7 with $N_\alpha = N_\beta = 1$, so we restrict ourselves to the

case $\delta < 1/2\gamma$.

First remark that, if x_k^L is defined recursively by (6.12), we have

$$[x_k^L]_2 \in \mathbb{Z}_2 \quad \text{for all } k \geq 1.$$

Since $\#\mathbb{Z}_2 = 2$, there exist integers $0 \leq j \leq 2$ and $l > j$, with $l - j \leq 2$, such that

$$[x_j^L]_2 = [x_l^L]_2. \quad (6.15)$$

Let l be the minimal such l . Define $\bar{k} = j$, $M = l - j$ and $n = \frac{x_l^L - x_j^L}{2}$ to obtain (6.14).

Now we show that the quotient n/M is independent of x_0 . For this, we use a monotonicity property of the orbits defined in (6.12) with respect to the initial datum: if $\{x_k\}$ and $\{x'_k\}$ are orbits obtained as above, we have

$$\text{if } x_0 \leq x'_0, \text{ then } x_k \leq x'_k, \quad \text{for all } k \geq 1. \quad (6.16)$$

Consider the orbits with initial data x_0 , x'_0 and $x_0 + 2$, and let $n(x)$ and $M(x)$ denote the indices above with initial datum $x \in \{x_0, x'_0, x_0 + 2\}$. Since the orbit with initial datum $x_0 + 2$ is the translation by 2 of the one with initial datum x_0 , we have $n(x_0 + 2) = n(x_0)$ and $M(x_0 + 2) = M(x_0)$. Taking into account the ordering of the initial conditions

$$x_0 \leq x'_0 \leq x_0 + 2,$$

by (6.14) for k_0 sufficiently large and taking $k = k_0 + TM(x_0)M(x'_0)$ with $T \in \mathbb{N}$, from $x_k \leq x'_k \leq x_k + 2$ we get

$$\begin{aligned} x_{k_0} + 4Tn(x_0)M(x'_0) &\leq x'_{k_0} + 2Tn(x'_0)M(x_0) \\ &\leq x_{k_0} + 2Tn(x_0)M(x'_0) + 2. \end{aligned}$$

In order that this inequality hold for all $T \geq 1$ we must have

$$n(x_0)M(x'_0) = n(x'_0)M(x_0),$$

which is the desired equality. □

Definition 6.3.6 (effective velocity function). We define the *effective velocity function* $f_\delta : (0, +\infty) \setminus S_\delta \rightarrow [0, +\infty)$ by setting

$$f_\delta(Y) = \frac{2n}{M}, \quad (6.17)$$

with M and n in (6.14) defined by L and γ such that $Y = \gamma/L$. By Proposition 6.3.5, this is a good definition.

We recall some properties of the velocity function (for the proof we refer to Remark 5.3.10).

Remark 6.3.7 (properties of the velocity function f_δ). The velocity function f_δ has the following properties:

(a) f_δ is constant on each interval contained in its domain;

(b) $f_\delta(Y) = 0$ if

$$Y < \bar{Y} := \min \left\{ \frac{3}{4\alpha}, \frac{\delta\gamma + 1}{2\alpha} \right\};$$

in particular

$$\lim_{\gamma \rightarrow 0^+} \frac{1}{\gamma} f_\delta \left(\frac{\gamma}{L} \right) = 0$$

(see Section 6.3.2);

(c) $f_\delta(Y)$ is an integer value;

(d) f_δ is non decreasing;

(e) we have

$$\lim_{\gamma \rightarrow +\infty} \frac{1}{\gamma} f_\delta \left(\frac{\gamma}{L} \right) = \frac{2\alpha}{L}.$$

(f) $f_\delta(Y)$ depends on β_ε through δ .

6.3.2 The effective pinning threshold

If $0 \leq \delta < \tilde{\delta}$, to compute the pinning threshold we have to impose that it is not energetically favorable to move inward a side by ε . We then write the variation of the energy functional $\mathcal{F}_{\varepsilon, \tau}^{\alpha, \beta_\varepsilon}$ from configuration A to configuration B in Fig. 6.11, regarding a side of length L .

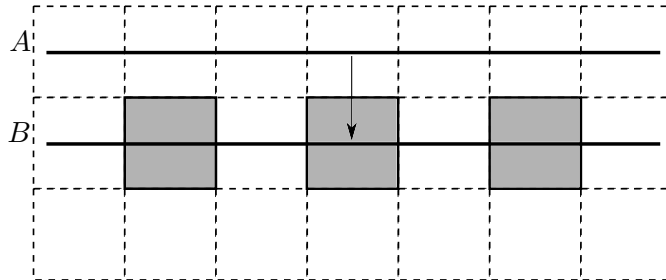


Figure 6.11. If $\delta < \tilde{\delta}$, the motion is possible if the side can move at least by ε .

If we impose it to be positive, we have

$$-2\alpha\varepsilon + L(\beta_\varepsilon - \alpha) + \frac{1}{\tau}L\varepsilon^2 = \varepsilon \left[-2\alpha + L \left(\delta + \frac{1}{\gamma} \right) \right] \geq 0$$

and we obtain the pinning threshold

$$\bar{L}_\delta := \frac{2\alpha\gamma}{\delta\gamma + 1}. \quad (6.18)$$

Note that if $\delta = 0$ (i.e., $\beta_\varepsilon = \alpha$), then we recover the threshold

$$\tilde{L} = 2\alpha\gamma.$$

If $\delta \geq \tilde{\delta}$, instead, by the condition that E_k be an α -type rectangle, we have to impose that it is not energetically favorable to move inward a side by 2ε (see Fig. 6.12). As shown in Section 5.3.1, in this way we obtain the pinning threshold

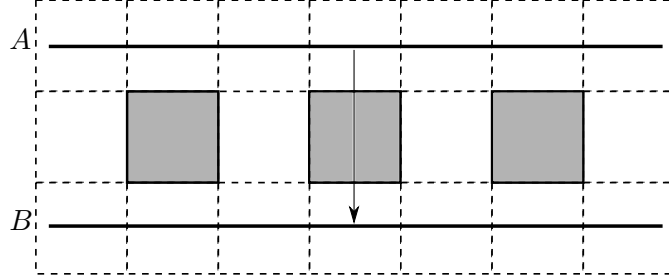


Figure 6.12. If $\delta \geq \tilde{\delta}$ the motion is possible if the side can move at least by 2ε .

$$\bar{L}_\delta = \frac{4}{3}\alpha\gamma.$$

Hence, the *effective pinning threshold* (see Fig. 6.13) is given by

$$\bar{L}_\delta = \max \left\{ \frac{2\alpha\gamma}{\delta\gamma + 1}, \frac{4}{3}\alpha\gamma \right\}. \quad (6.19)$$

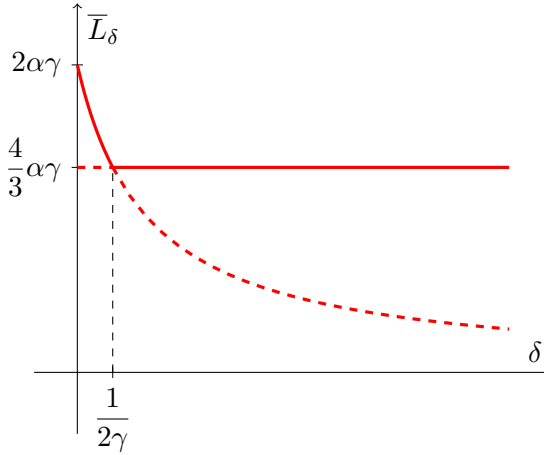


Figure 6.13. Effective pinning threshold (represented by the continuous line).

6.3.3 Computation of the velocity function

In this section we compute explicitly the velocity function assuming, without loss of generality, that $\gamma = 1$. We restrict ourselves to the case $\delta < 1/2$, because if $\delta \geq 1/2$ the velocity function is given by (see Section 5.4.1)

$$\bar{f}(Y) = 2 \left\lfloor \alpha Y + \frac{1}{4} \right\rfloor. \quad (6.20)$$

We denote by N the minimum of the problem (6.13) and subdivide the computation into different cases:

(a) x_n is even and $Y \in \left(\frac{2k+1+\delta}{2\alpha}, \frac{2k+2-\delta}{2\alpha} \right)$ for some $k \geq 0$; in this case $N = 2k+1$ and $x_{n+1} = x_n + N$ is odd. The next point is $x_{n+2} = x_{n+1} + N = x_n + 2N$, which is even, so that the sequence $\{x_n\}$ oscillates between α and β_ε . In this case,

$$f_\delta(Y) = \frac{x_{n+2} - x_n}{2} = \frac{2N}{2} = 2k + 1 = \lfloor 2\alpha Y \rfloor;$$

(b) x_n is odd and $Y \in \left(\frac{2k+1+\delta}{2\alpha}, \frac{2k+2-\delta}{2\alpha} \right)$ for some $k \geq 0$; in this case $x_{n+1} = x_n + N$ is even and $x_{n+2} = x_n + 2N$, is odd, so that as before

$$f_\delta(Y) = 2k + 1 = \lfloor 2\alpha Y \rfloor;$$

(c) x_n is even and $Y \in \left(\frac{2k-\delta}{2\alpha}, \frac{2k+1+\delta}{2\alpha} \right)$ for some $k \geq 0$; in this case $N = 2k$ and $x_{n+1} = x_n + N$ is even. Therefore the sequence $\{x_n\}$ consists of only α -bonds and in this case the velocity function is given by

$$f_\delta(Y) = x_{n+1} - x_n = N = 2k;$$

(d) x_n is odd and $Y \in \left(\frac{2k-\delta}{2\alpha}, \frac{2k+1+\delta}{2\alpha} \right)$ for some $k \geq 0$; in this case $x_{n+1} = x_n + N$ is also odd. Therefore the sequence $\{x_n\}$ consists of only β -bonds and in this case the velocity function is given again by

$$f_\delta(Y) = x_{n+1} - x_n = N = 2k.$$

Note that, collecting all the cases, we can write the velocity function as

$$f_\delta(Y) = \begin{cases} 0 & \text{if } Y < \frac{\delta+1}{2\alpha}, \\ 2k & \text{if } Y \in \left(\frac{2k-\delta}{2\alpha}, \frac{2k+1+\delta}{2\alpha} \right), \\ 2k+1 & \text{if } Y \in \left(\frac{2k+1+\delta}{2\alpha}, \frac{2k+2-\delta}{2\alpha} \right). \end{cases} \quad k \geq 0 \quad (6.21)$$

It can be rewritten equivalently as

$$f_\delta(Y) = \begin{cases} \lfloor 2\alpha Y \rfloor + 1 & \text{if } Y \in \left(\frac{2k - \delta}{2\alpha}, \frac{2k}{2\alpha} \right), \\ \lfloor 2\alpha Y \rfloor & \text{if } Y \in \left(\frac{2k}{2\alpha}, \frac{2k+1}{2\alpha} \right), \\ \lfloor 2\alpha Y \rfloor - 1 & \text{if } Y \in \left(\frac{2k+1}{2\alpha}, \frac{2k+1+\delta}{2\alpha} \right), \\ \lfloor 2\alpha Y \rfloor & \text{if } Y \in \left(\frac{2k+1+\delta}{2\alpha}, \frac{2k+2-\delta}{2\alpha} \right). \end{cases}$$

Therefore we notice accelerating and decelerating effects (due to the microstructure through δ) with respect to the velocity function \bar{f} obtained in the homogeneous case, that is

$$\tilde{f}(Y) = \begin{cases} 0 & \text{if } Y < \frac{1}{2\alpha}, \\ \lfloor 2\alpha Y \rfloor & \text{if } Y \in \left(\frac{k}{2\alpha}, \frac{k+1}{2\alpha} \right), k \geq 1. \end{cases}$$

Moreover, we recover \tilde{f} computing f_δ for $\delta = 0$. If we choose $\delta = 1/2$, we recover the velocity function \bar{f} (6.20) which corresponds to the high-contrast case.

We conclude this section by writing the general formula of the velocity function f_δ , valid for any δ and γ :

$$f_\delta(Y) = \begin{cases} 0 & \text{if } Y < \frac{C_{\delta,\gamma} + 1}{2\alpha}, \\ 2k & \text{if } Y \in \left(\frac{2k - C_{\delta,\gamma}}{2\alpha}, \frac{2k+1 + C_{\delta,\gamma}}{2\alpha} \right), \\ 2k+1 & \text{if } Y \in \left(\frac{2k+1 + C_{\delta,\gamma}}{2\alpha}, \frac{2k+2 - C_{\delta,\gamma}}{2\alpha} \right), \end{cases} \quad k \geq 0.$$

where $C_{\delta,\gamma} = \min\{\delta\gamma, 1/2\}$.

6.3.4 Description of the homogenized limit motion

The following characterization of any limit motion holds (see Theorem 5.3.12).

Theorem 6.3.8. *For all $\varepsilon > 0$, let $E_\varepsilon^0 \in \mathcal{D}_\varepsilon$ be a coordinate rectangle with sides $S_{1,\varepsilon}^0, \dots, S_{4,\varepsilon}^0$. Assume also that*

$$\lim_{\varepsilon \rightarrow 0^+} d_{\mathcal{H}}(E_\varepsilon^0, E_0) = 0$$

for some fixed coordinate rectangle E_0 . Let $\gamma > 0$ be fixed and let $E_\varepsilon(t) = E_{\varepsilon, \gamma \varepsilon}(t)$ be the piecewise-constant motion with initial datum E_ε^0 defined as in (4.12). Then, up to a subsequence, $E_\varepsilon(t)$ converges as $\varepsilon \rightarrow 0$ to $E(t)$, where $E(t)$ is a coordinate rectangle with sides $S_i(t)$ and such that $E(0) = E_0$. Each S_i moves inward with velocity $v_i(t)$ satisfying

$$v_i(t) \in \left[\frac{1}{\gamma} f_\delta \left(\frac{\gamma}{L_i(t)} \right)^-, \frac{1}{\gamma} f_\delta \left(\frac{\gamma}{L_i(t)} \right)^+ \right], \quad (6.22)$$

where f_δ is given by Definition 6.3.6, $L_i(t) := \mathcal{H}^1(S_i(t))$ denotes the length of the side $S_i(t)$, until the extinction time when $L_i(t) = 0$, and $f_\delta(Y)^-, f_\delta(Y)^+$ are the lower and upper limits of the effective-velocity function at $Y \in (0, +\infty)$.

In case of a unique evolution, the limit motion is described as follows (see Theorem 5.3.13).

Theorem 6.3.9 (unique limit motions). *Let E_ε, E be as in the statement of Theorem 6.3.8. Assume in addition that the lengths L_1^0, L_2^0 of the sides of the initial set E_0 satisfy one of the following conditions (we assume that $L_1^0 \leq L_2^0$):*

- (a) $L_1^0, L_2^0 > \bar{L}_\delta = \max \left\{ \frac{2\alpha\gamma}{\delta\gamma + 1}, \frac{4}{3}\alpha\gamma \right\}$ (total pinning);
- (b) $L_1^0 < \bar{L}_\delta$ and $L_2^0 \leq \bar{L}_\delta$ (vanishing in finite time);

then $E_\varepsilon(t)$ converges locally in time to $E(t)$ as $\varepsilon \rightarrow 0$, where $E(t)$ is the unique rectangle with sides of lengths $L_1(t)$ and $L_2(t)$ which solve the following system of ordinary differential equations

$$\begin{cases} \dot{L}_1(t) = -\frac{2}{\gamma} f_\delta \left(\frac{\gamma}{L_2(t)} \right) \\ \dot{L}_2(t) = -\frac{2}{\gamma} f_\delta \left(\frac{\gamma}{L_1(t)} \right) \end{cases} \quad (6.23)$$

for almost every t , with initial conditions $L_1(0) = L_1^0$ and $L_2(0) = L_2^0$.

6.4 The periodic case with K contrast parameters

In this section we study the same problem as before in a more general situation. We consider a medium with inclusions distributed into periodic uniform layers as follows.

Let $\varepsilon > 0$ be fixed and $\delta_1, \delta_2, \dots, \delta_K, K \in \mathbb{N}$ be positive. We consider $2K\varepsilon$ -periodic coefficients c_{ij}^ε indexed on nearest-neighbors of $\varepsilon\mathbb{Z}^2$ defined for i, j such that

$$0 \leq \frac{i_1 + j_1}{2}, \frac{i_2 + j_2}{2} < 2K\varepsilon$$

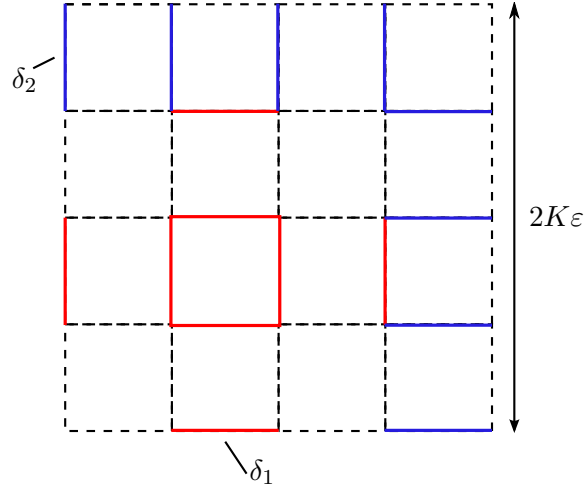


Figure 6.14. The periodicity cell for $K = 2$.

by

$$c_{ij}^\varepsilon = \begin{cases} \alpha + \delta_r \varepsilon, & \text{if } \frac{i_1 + j_1}{2}, \frac{i_2 + j_2}{2} = \left(2r - \frac{1}{2}\right) \varepsilon, r = 1, \dots, K \\ \alpha, & \text{otherwise.} \end{cases} \quad (6.24)$$

In Fig. 6.14 the periodicity cell is pictured in the case $K = 2$. Here the red lines represent the bonds with parameter δ_1 , the blue ones the bonds with parameter δ_2 and the dashed lines the α -bonds.

Correspondingly, to these coefficients we associate the energy $P_\varepsilon^{\alpha, \beta_\varepsilon}(\mathcal{I})$ defined on subsets \mathcal{I} of $\varepsilon\mathbb{Z}^2$ as in (6.2). We consider the same discrete-in-time minimization scheme for the energy $\mathcal{F}_{\varepsilon, \tau}^{\alpha, \beta_\varepsilon}$ with $\tau = \gamma\varepsilon$ as in Section 4.3 and we restrict our analysis to rectangular evolutions as in Section 6.3. We will see that the minimization problem and the velocity function depend on the choice of $\delta_r, r = 1, \dots, K$, in particular on their relative position with respect to $\tilde{\delta}$ defined by equation (6.11).

We will treat only the cases

$$\tilde{\delta} \leq \delta_r \quad \text{for some } r \in \{1, \dots, K\} \quad (6.25)$$

and

$$0 \leq \delta_r < \tilde{\delta}, \quad \forall r = 1, \dots, K, \quad (6.26)$$

because if $\tilde{\delta} \leq \delta_r$ for all r then we are in the high-contrast case already described in Chapter 5.

6.4.1 The pinning threshold

For the computation of the pinning threshold we refer to Section 6.3.2.

If assumption (6.25) holds, then after a finite number of steps the side is pinned if it cannot move inward by 2ε . In this case, the pinning threshold is given by

$$\bar{L}_{\delta} = \frac{4}{3}\alpha\gamma.$$

If (6.26) holds, instead, after a finite number of steps the side is pinned if it cannot move inward by ε . In particular, the pinning threshold now depends on $\delta_{\bar{r}} = \max_{1 \leq r \leq K} \{\delta_r\}$ and it is given by

$$\bar{L}_{\delta_{\bar{r}}} = \frac{2\alpha\gamma}{\delta_{\bar{r}}\gamma + 1}.$$

Hence, in the general case, the pinning threshold is given by

$$\min\{\bar{L}_{\delta_{\bar{r}}}, \bar{L}_{\delta}\}. \quad (6.27)$$

6.4.2 The effective velocity function

We use the same notation as in Section 6.3.1. For all $Y = \gamma/L_k > 0$ we consider the minimum problems

$$\min \{g(N) : N \in \mathbb{N}\} \quad (6.28)$$

where

$$g(N) = \begin{cases} -2\alpha N + \frac{N(N+1)}{2Y}, & \text{if } [N]_{2K} \in \{[0]_{2K}, [2]_{2K}, \dots, [2K-2]_{2K}\}, \\ -2\alpha N + \frac{\delta_r\gamma}{Y} + \frac{N(N+1)}{2Y}, & \text{if } [N]_{2K} = [2r-1]_{2K}, r = 1, \dots, K. \end{cases} \quad (6.29)$$

Then the set of $Y > 0$ for which (6.28) does not have a unique solution is discrete. For this we remark that the function to minimize is represented by $K+1$ parabolas

$$-4\alpha Y X + X(X+1) \quad \text{and} \quad -4\alpha Y X + X(X+1) + 2\delta_r\gamma \quad r = 1, \dots, K$$

with vertex in

$$X = 2\alpha Y - \frac{1}{2}.$$

As a consequence of (6.9) we have that the minimizers in (6.28) are not unique in the case that

$$Y \in S_{\delta_r} := \frac{1}{2\alpha} \left[(z + \min\{\delta_r\gamma, 1/2\}) \cup (z + 1 - \min\{\delta_r\gamma, 1/2\}) \right] \quad (6.30)$$

with $z \in \mathbb{Z}$ such that $[z]_{2K} = [2r-1]_{2K}$, $r = 1, \dots, K$.

Definition 6.4.1. We define the singular set $S_{\delta_1, \dots, \delta_K}$ for problems (6.28) as

$$S_{\delta_1, \dots, \delta_K} = \bigcup_{r=1}^K S_{\delta_r} \quad (6.31)$$

where S_{δ_r} is defined by (6.30).

We now examine the iterated minimizing scheme for $\gamma/L \in (0, +\infty) \setminus S_{\delta_1, \dots, \delta_K}$ fixed, which reads

$$\begin{cases} x_{k+1}^L = x_k^L + \bar{N}_k, & k \geq 0 \\ x_0^L = x^0 \end{cases} \quad (6.32)$$

with $x^0 \in \{0, 1, 2, \dots, 2K-1\}$ and $\bar{N}_k \in \mathbb{N}$ the minimizer of

$$\min \begin{cases} -2\alpha N + \frac{1}{\gamma} \frac{N(N+1)}{2} L, & \text{if } [N]_{2K} \in \{[0]_{2K}, [2]_{2K}, \dots, [2K-2]_{2K}\}, \\ -2\alpha N + \delta_r L + \frac{1}{\gamma} \frac{N(N+1)}{2} L, & \text{if } [N]_{2K} = [2r-1]_{2K}, r = 1, \dots, K, \end{cases} \quad (6.33)$$

which is unique up to the requirement that $\gamma/L \notin S_{\delta_1, \dots, \delta_K}$. With an analogous argument as in the proof of Proposition 6.3.5 we can prove that, after at most $2K$ steps, $\{x_k^L\}_{k \geq 0}$ is periodic modulo $2K$. Hence, we can define the effective velocity function f as in Definition 6.3.6.

6.4.3 Computation of the velocity function

In this section we give the expression of the velocity function without proof, because it follows by analogous computations as in Section 6.3.3. For simplicity of notation, we put

$$\bar{\delta}_{r,\gamma} = \min\{\delta_r \gamma, 1/2\}, \quad r = 1, \dots, K.$$

For any $\gamma, \delta_1, \dots, \delta_K$, the velocity function $f = f_{\delta_1, \dots, \delta_K}$ is given by

$$f_{\delta_1, \dots, \delta_K}(Y) = \begin{cases} 0, & \text{if } Y < \min \left\{ \frac{3}{4\alpha\gamma}, \frac{\delta_r \gamma + 1}{2\alpha\gamma} \right\}, \\ 2Kk, & \text{if } Y \in \left(\frac{2Kk - \bar{\delta}_{K,\gamma}}{2\alpha}, \frac{2Kk + 1 + \bar{\delta}_{1,\gamma}}{2\alpha} \right), \\ 2Kk + 1, & \text{if } Y \in \left(\frac{2Kk + 1 + \bar{\delta}_{1,\gamma}}{2\alpha}, \frac{2Kk + 2 - \bar{\delta}_{1,\gamma}}{2\alpha} \right), \\ 2Kk + 2, & \text{if } Y \in \left(\frac{2Kk + 2 - \bar{\delta}_{1,\gamma}}{2\alpha}, \frac{2Kk + 3 + \bar{\delta}_{2,\gamma}}{2\alpha} \right), \\ \vdots & \vdots \\ 2Kk + 2K - 1, & \text{if } Y \in \left(\frac{2K(k+1) - 1 + \bar{\delta}_{K,\gamma}}{2\alpha}, \frac{2K(k+1) - \bar{\delta}_{K,\gamma}}{2\alpha} \right), \end{cases}$$

with $k \geq 0$.

Chapter 7

Nucleation and backward motion of discrete interfaces

In this chapter we present the results contained in joint works with A. Braides [20, 21]. We consider a variation on the minimizing-movement scheme (4.5) motivated by some time-scaling argument. We use a discrete approximation of the motion by crystalline curvature to define an evolution of sets from a single point (nucleation) following a criterion of “maximization” of the perimeter, formally giving a *backward* version of the motion by crystalline curvature. This evolution depends on the approximation chosen.

7.1 The crystalline case: motivation

We consider the problem of defining a motion for sets which “expand” by *maximizing* the perimeter subject to a penalization of their distance from the previous set. Formally, this involves considering problems of the form

$$\min \left\{ -P(E) + \frac{1}{\tau} \int_{E \Delta E_{k-1}^\tau} \text{dist}(x, \partial E_{k-1}^\tau) dx \right\}, \quad (7.1)$$

which can be seen as a “backward” version of the previous ones (as remarked in Section 2.6) if the index k is considered as parameterizing negative time. Unfortunately, this problem is ill-posed, giving the trivial infimum $-\infty$ at the first step (see Remark 7.1.1). Following a suggestion by J.W. Cahn, we then consider a discrete approximation of P in the crystalline case, and use it to define a backward crystalline-curvature motion with prescribed extinction point (or, equivalently, *nucleation* of the motion defined for positive times).

We consider $\lambda > 0$ and initial data $E_0^{\tau, \varepsilon, \lambda} = Q_\varepsilon = \varepsilon Q = \varepsilon \left[-\frac{1}{2}, \frac{1}{2} \right]^d$ (which, in the discrete setting, all correspond to the singleton $\{0\}$), and define iteratively $E_k^{\tau, \varepsilon, \lambda} \in \mathcal{D}_\varepsilon$ (\mathcal{D}_ε as in (4.8)) as a minimizer of

$$\min \left\{ -\frac{1}{\lambda} P_\varepsilon(E) + \frac{1}{\tau} \int_{E \Delta E_{k-1}^{\tau, \varepsilon, \lambda}} d_\varepsilon(x, \partial E_{k-1}^{\tau, \varepsilon, \lambda}) dx \right\}, \quad (7.2)$$

where $P_\varepsilon(E) = \mathcal{H}^{d-1}(\partial E)$ and d_ε is a discrete distance (see Section 7.3).

Remark 7.1.1. Note that taking in (7.2) the crystalline perimeter (4.10) in place of P_ε and $d_\varepsilon = d_\infty^\varepsilon$ in dimension two would immediately give the value $-\infty$ in the minimum problem; e.g., by considering sets of the form

$$E_j = \{(\rho, \theta) : \rho \leq 3\varepsilon + \sin(j\theta)\},$$

which contain $E_0^{\tau, \varepsilon, \lambda}$, are contained in $B_{4\varepsilon}(0)$ and have a perimeter larger than $4j\varepsilon$ (see Fig. 7.1).

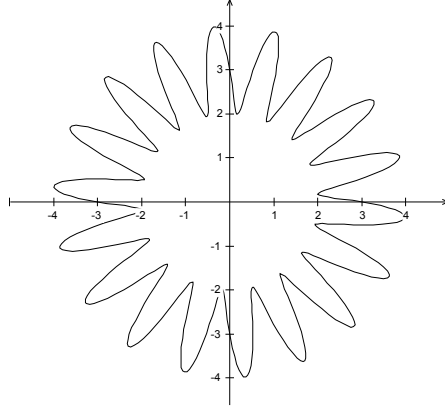


Figure 7.1. The set E_j for $\varepsilon = 1$ and $j = 500$.

Note also the new parameter λ in (7.2), which does not change the nature of the problems and whose introduction can be interpreted as a time-scaling of the trajectories with $\lambda = 1$ (see Section 2.5). We will study this problem for different choices of d_ε and in dimension $d = 2$ (the case $d \geq 2$ is in progress).

Overview of the chapter. In Section 7.2 we give a first simple example, treating the problem in the case of the ℓ^∞ -distance d_∞^ε . We show that each evolve by minimization of the energy is a even checkerboard structure containing the initial set εQ . The proof relies heavily on the structure of the ℓ^∞ -distance, for which all sublevel sets are cubes. The limit motion is a family of expanding cubes with constant velocity (see Theorem 7.2.1). In Section 7.3 we describe the necessary mathematical setting to treat the problem for a general distance d_φ , induced by a norm φ . This will be done in Section 7.4 and we will assume, as a technical hypothesis, that the minimal sets are checkerboard (this is not trivial as before, and it is a conjecture for the moment). In this case, we might not have that the minimal sets correspond to the same checkerboard structure (even or odd); in particular, we might have that they oscillate between even or odd checkerboard. However, this may happen only for a finite number of steps; eventually, they stabilize and correspond to the same parity (Proposition 7.4.4). Section 7.5 contains some examples of nucleation; in particular, in Section 7.5.2, we show an example where, for a sufficiently asymmetric distance, the limit set is a linearly growing segment.

7.2 A simple example: the ℓ^∞ -distance

The results of this section form the content of the joint work with A. Braides [21].

We consider the case that d_ε be the ∞ -distance d_∞^ε already defined in Section 4.3, adapted in any dimension $d \geq 2$, so that the integral term $\int_{E \Delta F} d_\infty^\varepsilon(x, \partial F) dx$ in the energy (7.2) for any $E, F \in \mathcal{D}_\varepsilon$ is given by

$$\sum_{i \in \mathbb{Z}^d \cap \frac{1}{\varepsilon} E} \varepsilon^{d+1} d_\infty\left(i, \mathbb{Z}^d \cap \frac{1}{\varepsilon} F\right) + \sum_{i \in \mathbb{Z}^d \cap \frac{1}{\varepsilon} (F \setminus E)} \varepsilon^{d+1} d_\infty\left(i, \mathbb{Z}^d \setminus \frac{1}{\varepsilon} F\right),$$

$$d_\infty(i, \mathcal{I}) = \min\{\|i - i'\|_\infty : i' \in \mathcal{I}\}, \mathcal{I} \subset \mathbb{Z}^d.$$

We first determine the correct scaling for λ and τ in terms of ε in order to have a non-trivial limit. To this end, we note that the minimal variation of the energy in (7.2) from the set $E_{k-1}^{\tau, \varepsilon, \lambda}$ corresponds to the addition of an ε -square with no side in common with $E_{k-1}^{\tau, \varepsilon, \lambda}$ (see Fig. 7.2). The variation is

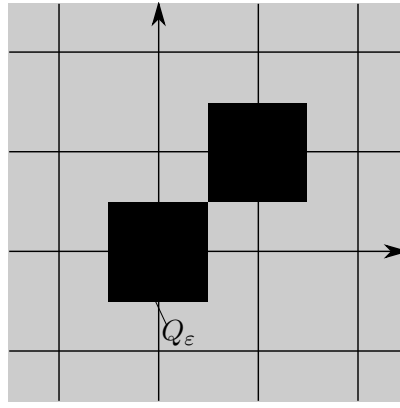


Figure 7.2. Example of configuration giving the minimal variation of the energy ($d = 2$).

$$-\frac{2d}{\lambda} \varepsilon^{d-1} + \frac{1}{\tau} K \varepsilon^{d+1} \quad (7.3)$$

with $0 \neq K \in \mathbb{N}$. This quantity may be negative if and only if

$$1 \leq \frac{2d\tau}{\lambda \varepsilon^2}. \quad (7.4)$$

The relative scaling of ε, τ and λ must be such that this condition be satisfied. We treat the case

$$\tau/\varepsilon = \gamma \in (0, +\infty), \quad \lambda \varepsilon = \alpha \in (0, +\infty), \quad (7.5)$$

so that (7.4) corresponds to

$$\frac{1}{2d} \leq \frac{\gamma}{\alpha}. \quad (7.6)$$

We can now describe the behaviour of the minimizing-movement scheme in (7.2).

Theorem 7.2.1 (nucleation). *Let τ, ε and λ satisfy condition (7.5); correspondingly, let $E^\tau(t) = E_{\lfloor t/\tau \rfloor}^{\tau, \varepsilon, \lambda}$, with $E_k^{\tau, \varepsilon, \lambda}$ given by (7.2) with initial data $E_0^{\tau, \varepsilon, \lambda} = \varepsilon Q$, and let*

$$\frac{2d\gamma}{\alpha} \notin \mathbb{N} \quad (7.7)$$

be satisfied. Then, for all fixed t , the Kuratowsky limit of the family $E^\tau(t)$ as $\tau \rightarrow 0$ is a cube of centre 0 and side length $2 \lfloor \frac{2d\gamma}{\alpha} \rfloor t$. In particular:

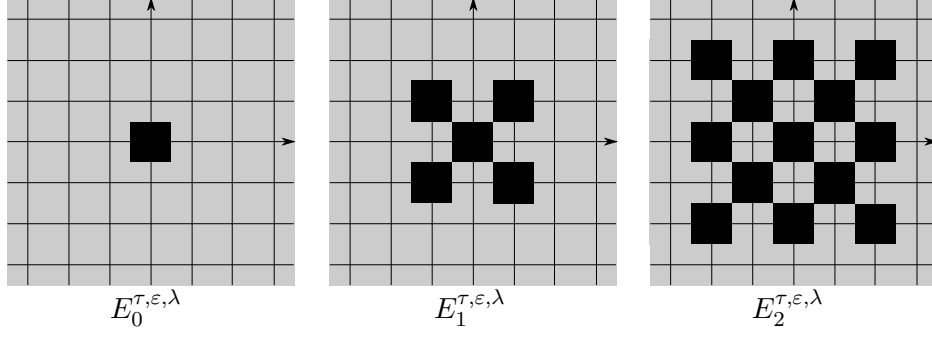


Figure 7.3. Some steps of the discrete evolution in dimension two.

- (a) (**pinning threshold**) if (7.6) is not satisfied, then the motion is trivial: $E(t) = \{0\}$;
- (b) (**linear expansion**) if (7.6) and (7.7) are satisfied, then the motion is given by a family of expanding cubes whose sides move with constant velocity $\lfloor \frac{2d\gamma}{\alpha} \rfloor$.

Remark 7.2.2 (singular cases). If $\frac{2d\gamma}{\alpha} \in \mathbb{N}$, then we obtain that the sets E are contained in the cubes moving with velocity $\frac{2d\gamma}{\alpha}$, and contain the cubes moving with velocity $\frac{2d\gamma}{\alpha} - 1$, but need not be cubes themselves. This is due to the non-uniqueness of the minimal sets in (7.2).

Proof. First note that if (7.6) is not satisfied, then every competing set E in the definition of $E_1^{\tau, \varepsilon, \lambda}$ gives a strictly larger value than the set $E_0^{\tau, \varepsilon, \lambda}$; hence, each discrete trajectory is trivial, and so is their limit.

Suppose now that (7.6) is satisfied. We then prove that $E_k^{\tau, \varepsilon, \lambda}$ is a (even) checkerboard structure containing εQ ; i.e., it is the union of cubes $\varepsilon(i + Q)$ with $i \in \mathbb{Z}^d$ and $\|i\|_1 = |i_1| + \dots + |i_d|$ even (for short, we say that i is even). Moreover,

$$\{i \in \mathbb{Z}^d : \varepsilon i \in E_k^{\tau, \varepsilon, \lambda}\} = \left\{ i \in \mathbb{Z}^d \text{ even}, \|i\|_\infty \leq \left\lfloor \frac{2d\gamma}{\alpha} \right\rfloor k \right\}. \quad (7.8)$$

The statement above can be proved inductively by showing that

$$\{i \in \mathbb{Z}^d : \varepsilon i \in E_k^{\tau, \varepsilon, \lambda}\} = \left\{ i \in \mathbb{Z}^d \text{ even}, d_\infty\left(i, \frac{1}{\varepsilon} E_{k-1}^{\tau, \varepsilon, \lambda}\right) \leq \left\lfloor \frac{2d\gamma}{\alpha} \right\rfloor \right\}. \quad (7.9)$$

To this end, it suffices to note that the contribution of the energy of a competitor E corresponding to points i with $d_\infty(i, E_{k-1}^{\tau, \varepsilon, \lambda}) = j$ for $1 \leq j \leq 2d\gamma/\alpha$ is minimal when no two such points have a nearest-neighbour in E , while if $j > 2d\gamma/\alpha$ it is minimal if E contains no such point. This shows that $E_k^{\tau, \varepsilon, \lambda} \setminus E_{k-1}^{\tau, \varepsilon, \lambda}$ corresponds to a checkerboard structure. Since the contribution of even and odd checkerboard structure outside $E_{k-1}^{\tau, \varepsilon, \lambda}$ is equal, and the even checkerboard structure allows to leave $E_{k-1}^{\tau, \varepsilon, \lambda}$ unchanged, we get the thesis. \square

7.3 Setting of the problem

Here we give the necessary preliminaries to formulate the problem for a generic distance d_φ , induced by a norm φ , in dimension $d = 2$ (see e.g. Rockafellar [42] and Schneider [43]).

We consider the partition of the standard lattice \mathbb{Z}^2 into sub-lattices given by

$$\mathbb{Z}^2 = \mathbb{Z}_e^2 \cup \mathbb{Z}_o^2, \quad (7.10)$$

where $\mathbb{Z}_e^2 = \{i \in \mathbb{Z}^2 : |i_1| + |i_2| \text{ is even}\}$ and $\mathbb{Z}_o^2 = \{i \in \mathbb{Z}^2 : |i_1| + |i_2| \text{ is odd}\}$.

We give some definitions for *lattice sets*, i.e., finite subsets of \mathbb{Z}^2 , which will be useful in the sequel.

Definition 7.3.1 (convex hull). *Given a lattice set $\mathcal{I} \subseteq \mathbb{Z}^2$, the convex hull of \mathcal{I} is the smallest convex polygon \mathcal{P} containing \mathcal{I} . We write*

$$\mathcal{P} = \text{conv}(\mathcal{I}).$$

Definition 7.3.2. *Let $\mathcal{I} \subseteq \mathbb{Z}^2$. We say that*

- (a) \mathcal{I} is checkerboard convex if either (a₁) $\mathcal{I} = \text{conv}(\mathcal{I}) \cap \mathbb{Z}_e^2$ or (a₂) $\mathcal{I} = \text{conv}(\mathcal{I}) \cap \mathbb{Z}_o^2$;
- (b) \mathcal{I} is origin symmetric if for any $i \in \mathcal{I}$, also $-i \in \mathcal{I}$.

\mathcal{I} is admissible if it is nonempty, checkerboard convex and origin symmetric.

Definition 7.3.3 (discrete Minkowski sum). *Let $\mathcal{I}, \mathcal{J} \subseteq \mathbb{Z}^2$. The Minkowski sum of \mathcal{I} and \mathcal{J} is defined as*

$$\mathcal{I} + \mathcal{J} = \{i + j : i \in \mathcal{I}, j \in \mathcal{J}\}, \quad (7.11)$$

where $(i + j)_1 = i_1 + j_1, (i + j)_2 = i_2 + j_2$.

Note that, by Def. 7.3.3, it follows that $\mathcal{I} + \{0\} = \mathcal{I}$ and $\mathcal{I} + \emptyset = \emptyset$.

Definition 7.3.4 (m-dilation). *Let $\mathcal{I} \subseteq \mathbb{Z}^2$ and $m > 0$. The set*

$$m\mathcal{I} = \{mi = (mi_1, mi_2) : i \in \mathcal{I}\} \quad (7.12)$$

is called the m-dilation (or m-dilate) of \mathcal{I} .

Definition 7.3.5. *If \mathcal{I} is a non-empty lattice set and $m \geq 1$, we define by induction from Def. 7.3.3 the set*

$$\mathcal{I}[m] := \underbrace{\mathcal{I} + \mathcal{I} + \cdots + \mathcal{I}}_{m\text{-times}}. \quad (7.13)$$

We now recall a property of commutability of Minkowski sum and the operation of taking the convex hull.

Proposition 7.3.6. *If $\mathcal{I}, \mathcal{J} \subseteq \mathbb{Z}^2$, then*

$$\text{conv}(\mathcal{I} + \mathcal{J}) = \text{conv}(\mathcal{I}) + \text{conv}(\mathcal{J}). \quad (7.14)$$

Lemma 7.3.7. *Let \mathcal{I}, \mathcal{J} be admissible subsets of \mathbb{Z}^2 . Then also $\mathcal{I} + \mathcal{J}$, defined by (7.11), is admissible.*

Proof. Trivially, $\mathcal{I} + \mathcal{J}$ is origin symmetric. We have three cases.

(i) $\mathcal{I}, \mathcal{J} \subseteq \mathbb{Z}_e^2$. In this case, $\mathcal{I} + \mathcal{J} \subseteq \mathbb{Z}_e^2$ and

$$\begin{aligned} \mathcal{I} + \mathcal{J} &= (\text{conv}(\mathcal{I}) \cap \mathbb{Z}_e^2) + (\text{conv}(\mathcal{J}) \cap \mathbb{Z}_e^2) = (\text{conv}(\mathcal{I}) + \text{conv}(\mathcal{J})) \cap \mathbb{Z}_e^2 \\ &= (\text{conv}(\mathcal{I} + \mathcal{J})) \cap \mathbb{Z}_e^2. \end{aligned} \quad (7.15)$$

(ii) $\mathcal{I}, \mathcal{J} \subseteq \mathbb{Z}_o^2$. Also in this case $\mathcal{I} + \mathcal{J} \subseteq \mathbb{Z}_e^2$ and

$$\mathcal{I} + \mathcal{J} = (\text{conv}(\mathcal{I} + \mathcal{J})) \cap \mathbb{Z}_e^2. \quad (7.16)$$

(iii) $\mathcal{I} \subseteq \mathbb{Z}_e^2, \mathcal{J} \subseteq \mathbb{Z}_o^2$. In this case $\mathcal{I} + \mathcal{J} \subseteq \mathbb{Z}_o^2$ and arguing as before we have

$$\mathcal{I} + \mathcal{J} = (\text{conv}(\mathcal{I} + \mathcal{J})) \cap \mathbb{Z}_o^2. \quad (7.17)$$

□

Let $\varepsilon > 0$ be fixed and we consider subsets $\mathcal{I} \subset \varepsilon\mathbb{Z}^2$. With a slight abuse of notation, we say that \mathcal{I} is admissible if $\frac{1}{\varepsilon}\mathcal{I}$ is admissible in the sense of Def. 7.3.2. To each \mathcal{I} we associate a subset $E_{\mathcal{I}}$ of \mathbb{R}^2 defined (see Section 4.2) as the union of all ε -squares centered at $i \in \mathcal{I}$. We say that \mathcal{I} is the *set of centers* of $E_{\mathcal{I}}$.

We define the classes

$$\mathcal{A}_e^\varepsilon = \left\{ E \in \mathcal{D}_\varepsilon : E = E_{\mathcal{I}} \text{ for some admissible } \mathcal{I} \subseteq \varepsilon\mathbb{Z}_e^2 \right\}, \quad (7.18)$$

and analogously the class $\mathcal{A}_o^\varepsilon$ by requiring that $\mathcal{I} \subseteq \varepsilon\mathbb{Z}_o^2$.

For any distance d_φ on \mathbb{R}^2 (induced by a norm φ) and $\mathcal{I} \subset \varepsilon\mathbb{Z}^2$, we define the *discrete distance* from $\partial\mathcal{I}$ as

$$d_\varphi^\varepsilon(i, \partial\mathcal{I}) = \begin{cases} \inf\{d_\varphi(i, j) : j \in \mathcal{I}\} & \text{if } i \notin \mathcal{I} \\ \inf\{d_\varphi(i, j) : j \in \varepsilon\mathbb{Z}^2 \setminus \mathcal{I}\} & \text{if } i \in \mathcal{I}. \end{cases} \quad (7.19)$$

After the identification of \mathcal{I} with $E_{\mathcal{I}}$ as before, we define

$$d_\varphi^\varepsilon(i, \partial E_{\mathcal{I}}) = d_\varphi^\varepsilon(i, \partial\mathcal{I}).$$

The distance can be extended to all $\mathbb{R}^2 \setminus \partial E_{\mathcal{I}}$ by setting

$$d_\varphi^\varepsilon(x, \partial\mathcal{I}) = d_\varphi^\varepsilon(i, \partial\mathcal{I}) \quad \text{if } x \in Q_\varepsilon(i).$$

We note that if $E_{\mathcal{I}} = Q_{\varepsilon}(0)$, then

$$d_{\varphi}^{\varepsilon}(x, \partial \mathcal{I}) = \varphi^{\varepsilon}(x) = \varphi^{\varepsilon}(i) \quad \text{if } x \in Q_{\varepsilon}(i),$$

where

$$\varphi^{\varepsilon}(i) = \begin{cases} \varphi(i) & \text{if } i \neq 0 \\ \inf\{\varphi(j) : j \in \varepsilon\mathbb{Z}^2 \setminus \{0\}\} & \text{if } i = 0. \end{cases} \quad (7.20)$$

7.4 The general case

For any $\varepsilon, \tau, \lambda > 0$ we consider the energy $\mathcal{F}_{\varepsilon, \tau, \lambda} : \mathcal{D}_{\varepsilon} \times \mathcal{D}_{\varepsilon} \rightarrow \mathbb{R}$ defined as

$$\mathcal{F}_{\varepsilon, \tau, \lambda}(E, F) = -\frac{1}{\lambda} P_{\varepsilon}(E) + \frac{1}{\tau} \int_{E \Delta F} d_{\varphi}^{\varepsilon}(x, \partial F) dx, \quad (7.21)$$

where $P_{\varepsilon}(E) = \mathcal{H}^1(\partial E)$, which coincides with the energy P_{ε}^{α} (4.6) computed for $\alpha = 1$. As before, we choose $\tau = \gamma\varepsilon$ and $\lambda\varepsilon = \alpha$, so that (7.21) can be rewritten as

$$\mathcal{F}_{\varepsilon, \gamma, \alpha}(E, F) = -P_{\varepsilon}(E) + \frac{\alpha}{\gamma\varepsilon^2} \int_{E \Delta F} d_{\varphi}^{\varepsilon}(x, \partial F) dx. \quad (7.22)$$

Given the initial set $E_0^{\varepsilon} = Q_{\varepsilon}$, we define recursively a sequence $E_k^{\varepsilon, \gamma, \alpha}$ in $\mathcal{D}_{\varepsilon}$ by requiring the following:

- (i) $E_0^{\varepsilon, \gamma, \alpha} = E_0^{\varepsilon}$;
- (ii) $E_{k+1}^{\varepsilon, \gamma, \alpha}$ is a minimizer of the functional $\mathcal{F}_{\varepsilon, \alpha, \gamma}(\cdot, E_k^{\varepsilon, \gamma, \alpha})$.

The discrete flat flow associated to functionals $\mathcal{F}_{\varepsilon, \gamma, \alpha}$ is thus defined by

$$E^{\varepsilon, \gamma, \alpha}(t) = E_{\lfloor t/\tau \rfloor}^{\varepsilon, \gamma, \alpha}, \quad t \geq 0. \quad (7.23)$$

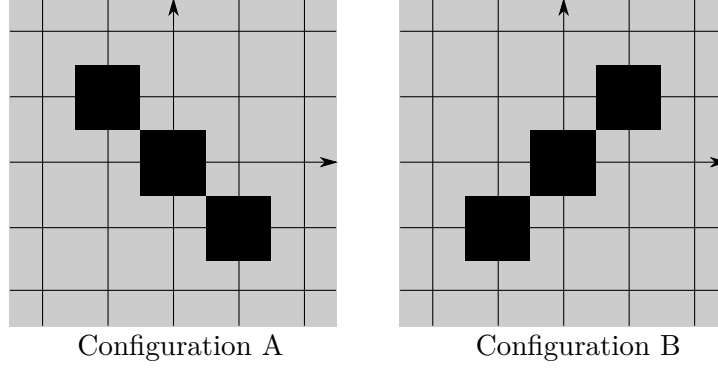
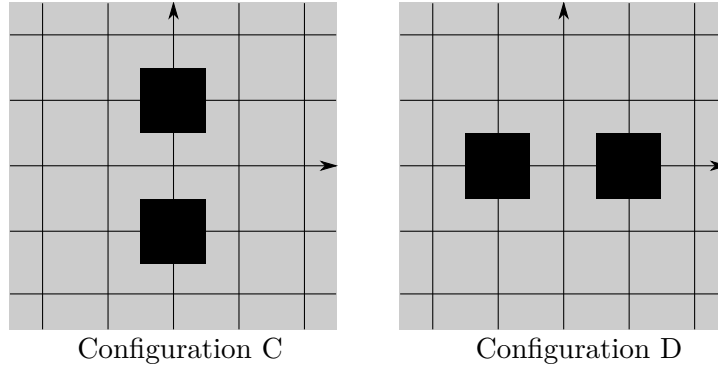
To simplify the notation, we omit the dependence on γ, α in $E_k^{\varepsilon, \gamma, \alpha}$, which will be denoted simply by E_k^{ε} .

We assume, as a technical hypothesis, the conjecture that each step of the discrete motion E_k^{ε} is a checkerboard convex and origin symmetric union of ε -squares.

Fundamental assumption. *Let $E_0^{\varepsilon} = Q_{\varepsilon}$. If F is a minimizer for the minimum problem for $\mathcal{F}_{\varepsilon, \gamma, \alpha}(\cdot, E_{k-1}^{\varepsilon})$, $k \geq 1$, then either $F \in \mathcal{A}_{\varepsilon}^{\varepsilon}$ or $F \in \mathcal{A}_0^{\varepsilon}$.*

7.4.1 The nucleation threshold

We first determine conditions on α, γ in order to have a non-trivial motion. The *nucleation threshold* is defined as the minimum value of $\frac{\gamma}{\alpha}$ above which it is energetically convenient to *nucleate*; that is, to have that $E_1^{\varepsilon} \neq E_0^{\varepsilon}$. To compute it, we write the variations of the energy (7.22) to obtain, starting from E_0^{ε} , each of the four minimal configurations pictured in Fig. 7.4 and Fig. 7.5, and impose them to be negative. In order to simplify the notation, we put $\varphi_{x,y}^{\varepsilon} := \varphi^{\varepsilon}(x, y)$. Configuration A and Configuration B are the minimal (not E_0^{ε}) subsets in $\mathcal{A}_{\varepsilon}^{\varepsilon}$, i.e., the union of E_0^{ε} and the two ε -squares centered at $i \in \varepsilon\mathbb{Z}_{\varepsilon}^2$ and whose discrete distances from $\partial E_0^{\varepsilon}$ are

Figure 7.4. Minimal configurations in $\mathcal{A}_\varepsilon^\varepsilon$.Figure 7.5. Minimal configurations in $\mathcal{A}_o^\varepsilon$.

minimal, that is $\varphi_{-\varepsilon,\varepsilon}^\varepsilon$ and $\varphi_{\varepsilon,\varepsilon}^\varepsilon$, respectively. Configuration C and Configuration D, instead, are the minimal subsets in $\mathcal{A}_o^\varepsilon$, i.e., the union of the two ε -squares centered at $i \in \varepsilon\mathbb{Z}_o^2$ whose discrete distances from ∂E_0^ε are $\varphi_{0,\varepsilon}^\varepsilon$ and $\varphi_{\varepsilon,0}^\varepsilon$, respectively.

The variation of the energy to obtain Configuration A is given by

$$-8\varepsilon + 2\frac{\alpha}{\gamma}\varphi_{-\varepsilon,\varepsilon}^\varepsilon, \quad (7.24)$$

which is negative if and only if $\frac{\gamma}{\alpha} \geq \frac{\varphi_{-1,1}^\varepsilon}{4}$. An analogous computation shows that the variation of the energy to obtain Configuration B is negative if and only if $\frac{\gamma}{\alpha} \geq \frac{\varphi_{1,1}^\varepsilon}{4}$. In the case of Configuration C, instead, the variation of the energy is

$$-4\varepsilon + \frac{\alpha}{\gamma}(2\varphi_{0,\varepsilon}^\varepsilon + \min\{\varphi_{0,\varepsilon}^\varepsilon, \varphi_{\varepsilon,0}^\varepsilon, \varphi_{\varepsilon,\varepsilon}^\varepsilon, \varphi_{-\varepsilon,\varepsilon}^\varepsilon\}), \quad (7.25)$$

which is negative if and only if $\frac{\gamma}{\alpha} \geq \frac{1}{4}[2\varphi_{0,1}^\varepsilon + \min\{\varphi_{0,1}^\varepsilon, \varphi_{1,0}^\varepsilon, \varphi_{1,1}^\varepsilon, \varphi_{-1,1}^\varepsilon\}]$; the same computation for Configuration D gives $\frac{\gamma}{\alpha} \geq \frac{1}{4}[2\varphi_{1,0}^\varepsilon + \min\{\varphi_{0,1}^\varepsilon, \varphi_{1,0}^\varepsilon, \varphi_{1,1}^\varepsilon, \varphi_{-1,1}^\varepsilon\}]$. Hence, the nucleation threshold depends on the norm φ^ε and can be estimated as

$$\frac{\gamma}{\alpha} \geq \frac{1}{4} \min \left\{ \varphi_{-1,1}^\varepsilon, \varphi_{1,1}^\varepsilon, 2 \min\{\varphi_{1,0}^\varepsilon, \varphi_{0,1}^\varepsilon\} + \min\{\varphi_{0,1}^\varepsilon, \varphi_{1,0}^\varepsilon, \varphi_{1,1}^\varepsilon, \varphi_{-1,1}^\varepsilon\} \right\}. \quad (7.26)$$

Remark 7.4.1. Note that if $d_\varphi^\varepsilon = d_\infty^\varepsilon$, then (7.26) reduces to (7.6) computed for $d = 2$.

7.4.2 Discrete nucleation

In this section, we study the discrete nucleation from the point $0 \in \varepsilon\mathbb{Z}^2$ (the set Q_ε), with fixed ε . By Fundamental assumption, it follows that in order to determine the first step of the evolution E_1^ε , we have to compare the minimizers of $\mathcal{F}_{\varepsilon,\gamma,\alpha}(\cdot, E_0^\varepsilon)$ among $\mathcal{A}_e^\varepsilon$ and $\mathcal{A}_o^\varepsilon$, that is the subsets of $\mathcal{A}_e^\varepsilon$ and $\mathcal{A}_o^\varepsilon$, respectively, given by the union of all the ε -squares $Q_\varepsilon(i)$ whose centers satisfy $\varphi^\varepsilon(i) < \frac{4\gamma}{\alpha}\varepsilon$.

More precisely, if we consider

$$\mathcal{I}_{1,\varepsilon} = \left\{ i \in \varepsilon\mathbb{Z}_e^2 : \varphi^\varepsilon(i) < \frac{4\gamma}{\alpha}\varepsilon \right\}, \quad (7.27)$$

then $\mathcal{F}_{\varepsilon,\gamma,\alpha}(E_{\mathcal{I}_{1,\varepsilon}}, E_0^\varepsilon) = \min_{E \in \mathcal{A}_e^\varepsilon} \mathcal{F}_{\varepsilon,\gamma,\alpha}(E, E_0^\varepsilon)$, while if

$$\tilde{\mathcal{I}}_{1,\varepsilon} = \left\{ i \in \varepsilon\mathbb{Z}_o^2 : \varphi^\varepsilon(i) < \frac{4\gamma}{\alpha}\varepsilon \right\}, \quad (7.28)$$

then $\mathcal{F}_{\varepsilon,\gamma,\alpha}(E_{\tilde{\mathcal{I}}_{1,\varepsilon}}, E_0^\varepsilon) = \min_{E \in \mathcal{A}_o^\varepsilon} \mathcal{F}_{\varepsilon,\gamma,\alpha}(E, E_0^\varepsilon)$.

Definition 7.4.2 (nucleus). We define the nucleus E_1^ε as follows:

- (i) $E_1^\varepsilon = E_{\mathcal{I}_{1,\varepsilon}}$ if $\mathcal{F}_{\varepsilon,\gamma,\alpha}(E_{\mathcal{I}_{1,\varepsilon}}, E_0^\varepsilon) < \mathcal{F}_{\varepsilon,\gamma,\alpha}(E_{\tilde{\mathcal{I}}_{1,\varepsilon}}, E_0^\varepsilon)$;
- (ii) $E_1^\varepsilon = E_{\tilde{\mathcal{I}}_{1,\varepsilon}}$ if $\mathcal{F}_{\varepsilon,\gamma,\alpha}(E_{\tilde{\mathcal{I}}_{1,\varepsilon}}, E_0^\varepsilon) < \mathcal{F}_{\varepsilon,\gamma,\alpha}(E_{\mathcal{I}_{1,\varepsilon}}, E_0^\varepsilon)$.

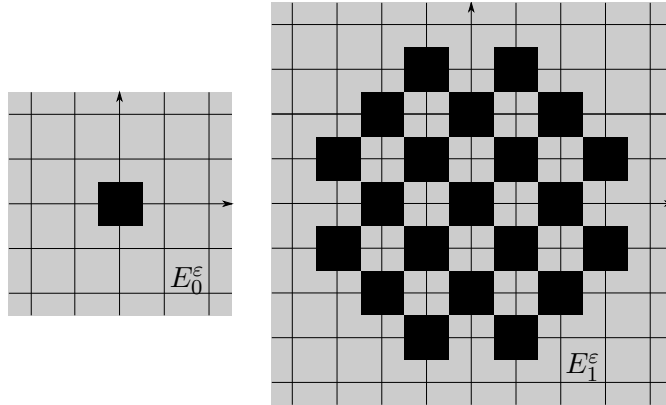


Figure 7.6. An example of nucleus E_1^ε .

Remark 7.4.3. If $\mathcal{F}_{\varepsilon,\gamma,\alpha}(E_{\mathcal{I}_{1,\varepsilon}}, E_0^\varepsilon) = \mathcal{F}_{\varepsilon,\gamma,\alpha}(E_{\tilde{\mathcal{I}}_{1,\varepsilon}}, E_0^\varepsilon)$, then we have a double choice for E_1^ε . To simplify the problem, we discard this case and assume from now on that E_1^ε is unique.

Proposition 7.4.4 (discrete nucleation). Assume that (7.26) holds, let $\varepsilon > 0$ be fixed and $E_0^\varepsilon = Q_\varepsilon$. Then the discrete evolution by minimization of the energy (7.22) is the set $E_k^\varepsilon = E_{\mathcal{I}_{k,\varepsilon}}$, $k \geq 2$, where $\mathcal{I}_{k,\varepsilon} \subseteq \varepsilon\mathbb{Z}^2$ is defined as follows:

- (i) if $E_1^\varepsilon = E_{\mathcal{I}_{1,\varepsilon}}$, then $\mathcal{I}_{k,\varepsilon} = \mathcal{I}_{1,\varepsilon}[k]$, and $\mathcal{I}_{1,\varepsilon}$ is given by (7.27);

- (ii) if $E_1^\varepsilon = E_{\tilde{\mathcal{I}}_{1,\varepsilon}}^\varepsilon$, then there exists $\bar{k} = \bar{k}(\gamma/\alpha) \geq 0$ such that $\mathcal{I}_{k,\varepsilon} = \tilde{\mathcal{I}}_{1,\varepsilon}[k]$ for all $0 \leq k \leq \bar{k}$, where $\tilde{\mathcal{I}}_{1,\varepsilon}$ is given by (7.28), while $\mathcal{I}_{k,\varepsilon} = \mathcal{I}_{\bar{k},\varepsilon} + \mathcal{I}_{1,\varepsilon}[k - \bar{k}]$ for all $k > \bar{k}$, with $\mathcal{I}_{1,\varepsilon}$ again given by (7.27).

Remark 7.4.5. In case (i), $E_k^\varepsilon \in \mathcal{A}_e^\varepsilon, \forall k \geq 1$ and $E_{k-1}^\varepsilon \subseteq E_k^\varepsilon$. In case (ii), instead, an analogous property holds only definitely, because E_k^ε oscillates between $\mathcal{A}_o^\varepsilon$ and $\mathcal{A}_e^\varepsilon$ for all $1 \leq k \leq \bar{k}$, while for $k > \bar{k}$ it stabilizes on the same class $\mathcal{A}_o^\varepsilon$ or $\mathcal{A}_e^\varepsilon$.

Proof. (i) The set $E_k^\varepsilon, k \geq 2$ is the union of E_{k-1}^ε and all the ε -squares whose centers $i \in \varepsilon\mathbb{Z}_e^2$ are such that

$$d_\varphi^\varepsilon(i, \partial E_{k-1}^\varepsilon) < \frac{4\gamma}{\alpha}\varepsilon. \quad (7.29)$$

Equivalently, if we define iteratively

$$\mathcal{I}_{k,\varepsilon} = \mathcal{I}_{k-1,\varepsilon} + \mathcal{I}_{1,\varepsilon}, \quad k \geq 2, \quad (7.30)$$

with $\mathcal{I}_{1,\varepsilon}$ given by (7.27), then

$$E_k^\varepsilon = E_{\mathcal{I}_{k,\varepsilon}}^\varepsilon. \quad (7.31)$$

In fact,

$$\sup\{d_\varphi^\varepsilon(i, j) : i \in \mathcal{I}_{k,\varepsilon}, j \in \mathcal{I}_{k-1,\varepsilon}\} \leq \sup\{\varphi^\varepsilon(i) : i \in \mathcal{I}_{1,\varepsilon}\} < \frac{4\gamma}{\alpha}\varepsilon.$$

By Lemma 7.3.7 it follows that $\mathcal{I}_{k,\varepsilon}$ is admissible and satisfies (a₁) of Definition 7.3.2; this implies that $E_k^\varepsilon \in \mathcal{A}_e^\varepsilon$. Note also that, by definition (7.30) and since $0 \in \mathcal{I}_{k-1,\varepsilon}, \forall k \geq 1$, we have that $\mathcal{I}_{k-1,\varepsilon} \subseteq \mathcal{I}_{k,\varepsilon}$ so that $E_{k-1}^\varepsilon \subseteq E_k^\varepsilon, \forall k \geq 1$.

- (ii) If k is odd, the set $E_k^\varepsilon, k \geq 2$ is the union of all ε -squares whose centers $i \in \varepsilon\mathbb{Z}_o^2$ are such that $d_\varphi^\varepsilon(i, \partial E_{k-1}^\varepsilon) < \frac{4\gamma}{\alpha}\varepsilon$, while if k is even, E_k^ε has the same properties as before with $i \in \varepsilon\mathbb{Z}_e^2$. Equivalently, we can define

$$\mathcal{I}_{k,\varepsilon} = \mathcal{I}_{k-1,\varepsilon} + \tilde{\mathcal{I}}_{1,\varepsilon}, \quad (7.32)$$

with $\mathcal{I}_{1,\varepsilon} := \tilde{\mathcal{I}}_{1,\varepsilon}$ given by (7.28). As before, we have

$$E_k^\varepsilon = E_{\mathcal{I}_{k,\varepsilon}}^\varepsilon. \quad (7.33)$$

We note that $E_{k-1}^\varepsilon \not\subseteq E_k^\varepsilon$ and, if k is even, $E_{k-1}^\varepsilon \in \mathcal{A}_o^\varepsilon, E_k^\varepsilon \in \mathcal{A}_e^\varepsilon$, while if k is odd, $E_{k-1}^\varepsilon \in \mathcal{A}_e^\varepsilon, E_k^\varepsilon \in \mathcal{A}_o^\varepsilon$.

However, the procedure defined by (7.32) can be iterated only for a finite number of steps, depending on $\frac{\gamma}{\alpha}$. In fact, the variation of the energy $\mathcal{F}_{\varepsilon,\gamma,\alpha}$ to pass from E_{k-1}^ε to E_k^ε is bounded from below by

$$-4(|\mathcal{I}_{k,\varepsilon}| - |\mathcal{I}_{k-1,\varepsilon}|) + \frac{\alpha}{\gamma} \left[\min\{\varphi_{1,0}^\varepsilon, \varphi_{0,1}^\varepsilon, \varphi_{-1,1}^\varepsilon, \varphi_{1,1}^\varepsilon\} (|\mathcal{I}_{k-1,\varepsilon}| + |\mathcal{I}_{k,\varepsilon}|) \right], \quad (7.34)$$

which is strictly positive for k sufficiently large, being $\mathcal{I}_{k-1,\varepsilon} \not\subseteq \mathcal{I}_{k,\varepsilon}, |\mathcal{I}_{k-1,\varepsilon}| \leq |\mathcal{I}_{k,\varepsilon}|$ and α/γ fixed.

Let \bar{k} be the smallest such k . For any $k > \bar{k}$, E_k^ε is the union of E_{k-1}^ε and all the ε -squares whose centers $i \in \varepsilon\mathbb{Z}_o^2$ if \bar{k} is odd, $i \in \varepsilon\mathbb{Z}_e^2$ if \bar{k} is even and

$$d_\varphi^\varepsilon(i, \partial E_{k-1}^\varepsilon) < \frac{4\gamma}{\alpha}\varepsilon. \quad (7.35)$$

As before, this is equivalent to define

$$\mathcal{I}_{k,\varepsilon} = \mathcal{I}_{k-1,\varepsilon} + \mathcal{I}_{1,\varepsilon}, \quad \forall k > \bar{k}, \quad (7.36)$$

where $\mathcal{I}_{1,\varepsilon}$ now is given by (7.27), and $E_k^\varepsilon = E_{\mathcal{I}_{k,\varepsilon}}$. Note that $E_{k-1}^\varepsilon \subseteq E_k^\varepsilon, \forall k \geq \bar{k}$ and $E_k^\varepsilon \in \mathcal{A}_o^\varepsilon$ if \bar{k} is odd, $E_k^\varepsilon \in \mathcal{A}_e^\varepsilon$ if \bar{k} is even. \square

Remark 7.4.6 (homothety of convex hulls). Let $\mathcal{P}_{k,\varepsilon}$ be the convex hull of $\mathcal{I}_{k,\varepsilon}$ defined iteratively at (i) of Proposition 7.4.4. Then, for all $k \geq 1$, $\mathcal{P}_{k,\varepsilon}$ and $\mathcal{P}_{1,\varepsilon}$ are homothetic with center 0.

For this, it will suffice to prove that $\mathcal{P}_{k,\varepsilon}$ is the k -dilate of $\mathcal{P}_{1,\varepsilon}$, that is

$$\mathcal{P}_{k,\varepsilon} = k\mathcal{P}_{1,\varepsilon}, \quad \text{for all } k \geq 1. \quad (7.37)$$

Clearly, (7.37) is true for $k = 1$. Let $k \geq 2$ and assume that

$$\mathcal{P}_{k-1,\varepsilon} = (k-1)\mathcal{P}_{1,\varepsilon}. \quad (7.38)$$

By Definition (7.30) and Proposition 7.3.6 it follows that

$$\begin{aligned} \mathcal{P}_{k,\varepsilon} &= \text{conv}(\mathcal{I}_{k,\varepsilon}) = \text{conv}(\mathcal{I}_{k-1,\varepsilon} + \mathcal{I}_{1,\varepsilon}) = \text{conv}(\mathcal{I}_{k-1,\varepsilon}) + \text{conv}(\mathcal{I}_{1,\varepsilon}) \\ &= \mathcal{P}_{k-1,\varepsilon} + \mathcal{P}_{1,\varepsilon}. \end{aligned} \quad (7.39)$$

Therefore, by (7.38) and again by Proposition 7.3.6 we finally obtain that

$$\mathcal{P}_{k,\varepsilon} = (k-1)\mathcal{P}_{1,\varepsilon} + \mathcal{P}_{1,\varepsilon} = k\mathcal{P}_{1,\varepsilon}. \quad (7.40)$$

In case (ii) of Proposition 7.4.4, instead, if $\mathcal{Q}_{k,\varepsilon} = \text{conv}(\mathcal{I}_{k,\varepsilon})$, where $\mathcal{I}_{k,\varepsilon}$ is defined by (7.36), we have

$$\mathcal{Q}_{k,\varepsilon} = \mathcal{Q}_{\bar{k},\varepsilon} + (k - \bar{k})\mathcal{P}_{1,\varepsilon}, \quad \text{for all } k \geq \bar{k}. \quad (7.41)$$

However, by boundedness of $\mathcal{Q}_{\bar{k},\varepsilon}$, there exists $\tilde{k} \geq \bar{k}$ such that $\mathcal{Q}_{\bar{k},\varepsilon} \subseteq \tilde{k}\mathcal{P}_{1,\varepsilon}$, from which we deduce that

$$\mathcal{Q}_{k,\varepsilon} \subseteq (k + \tilde{k} - \bar{k})\mathcal{P}_{1,\varepsilon}, \quad \text{for all } k \geq \bar{k}. \quad (7.42)$$

7.4.3 The limit motion

The following characterization of the limit motion holds.

Theorem 7.4.7 (limit motion). *Let α, γ be as in (7.5) and such that (7.26) be satisfied. Then we have two cases:*

(a) *let $E_k^\varepsilon = E_{\mathcal{I}_{k,\varepsilon}}$ be as in (i) of Proposition 7.4.4 and $F_k^\varepsilon = \mathcal{P}_{k,\varepsilon} = \text{conv}(\mathcal{I}_{k,\varepsilon})$, $F_\varepsilon(t) = \mathcal{P}_{\lfloor t/\tau \rfloor, \varepsilon}$, $t \geq 0$. Then, for all fixed t , the Kuratowsky limit of the family $F_\varepsilon(t)$ as $\varepsilon \rightarrow 0$ is a polygon $F(t)$ given by*

$$F(t) = \frac{1}{\gamma} t F_1 \quad (7.43)$$

where $F_1 = \frac{1}{\varepsilon} \text{conv}(\mathcal{I}_{1,\varepsilon})$, $\mathcal{I}_{1,\varepsilon}$ defined by (7.27).

(b) *let $E_k^\varepsilon = E_{\mathcal{I}_{k,\varepsilon}}$ be as in (ii) of Proposition 7.4.4 and $G_k^\varepsilon = \mathcal{Q}_{k,\varepsilon} = \text{conv}(\mathcal{I}_{k,\varepsilon})$, $G_\varepsilon(t) = \mathcal{Q}_{\lfloor t/\tau \rfloor, \varepsilon}$, $t \geq 0$. Then, for all fixed t , the Kuratowsky limit of the family $G_\varepsilon(t)$ as $\varepsilon \rightarrow 0$ is a polygon $G(t)$ satisfying the inclusion*

$$G(t) \subseteq F(t), \quad (7.44)$$

where $F(t)$ is the motion defined by (7.43).

Proof. (a) By Remark 7.4.6, we have

$$F_k^\varepsilon = k\varepsilon F_1. \quad (7.45)$$

We define

$$F_\varepsilon(t) = F_{\lfloor t/\gamma\varepsilon \rfloor}^\varepsilon = \left\lfloor \frac{t}{\gamma\varepsilon} \right\rfloor \varepsilon F_1, \quad (7.46)$$

which converges in the Kuratowski sense, as $\varepsilon \rightarrow 0$, to $F(t) = \frac{1}{\gamma} t F_1$.

(b) Again by Remark 7.4.6, we have

$$G_\varepsilon(t) = G_{\lfloor t/\tau \rfloor}^\varepsilon \subseteq \left(\left\lfloor \frac{t}{\gamma\varepsilon} \right\rfloor + \tilde{k} - \bar{k} \right) \varepsilon F_1, \quad (7.47)$$

from which passing to the limit as $\varepsilon \rightarrow 0$ in the Kuratowski sense we deduce that

$$G(t) \subseteq F(t). \quad (7.48)$$

□

Remark 7.4.8. As a trivial remark, we note that the motion in case (b) of Proposition 7.4.7 is slower than the motion obtained in case (a).

7.5 Some examples of nucleation

In this section we give some examples of nucleation for particular choices of the discrete distance d_φ^ε . More precisely, we characterize explicitly the discrete and the limit motion showing their dependence on the chosen metric.

7.5.1 The ℓ^1 -distance

We consider $d_\varphi^\varepsilon(x, y) = d_1^\varepsilon(x, y)$ defined as in (7.19) with $d_\varphi(x, y) = \|x - y\|_1$.

Remark 7.5.1 (pinning threshold). The minimal configuration is pictured in Fig. 7.8. The corresponding variation of the energy with respect to the initial set Q_ε is given by

$$-12\varepsilon + 5\frac{\alpha}{\gamma}\varepsilon,$$

which is negative if and only if

$$\frac{5}{12} \leq \frac{\gamma}{\alpha}. \quad (7.49)$$

We assume that (7.49) is verified and that $\frac{4\gamma}{\alpha} \notin \mathbb{N}$, otherwise we do not have uniqueness in the choice of the minimizers. To simplify the notation, we put $N_{\alpha,\gamma} = \left\lfloor \frac{4\gamma}{\alpha} \right\rfloor$. We then have two cases.

(a) if $N_{\alpha,\gamma}$ is even, then $E_1^\varepsilon \in \mathcal{A}_e^\varepsilon$. In this case, $\mathcal{I}_{1,\varepsilon}$ is given by

$$\mathcal{I}_{1,\varepsilon} = \left\{ i \in \varepsilon\mathbb{Z}_e^2 : \|i\|_1 \leq N_{\alpha,\gamma}\varepsilon \right\}, \quad (7.50)$$

and for $k \geq 1$,

$$\mathcal{I}_{k,\varepsilon} = \mathcal{I}_{1,\varepsilon}[k] = \left\{ i \in \varepsilon\mathbb{Z}_e^2 : \|i\|_1 \leq N_{\alpha,\gamma}k\varepsilon \right\}. \quad (7.51)$$

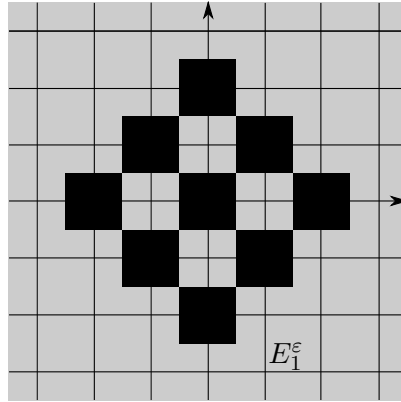


Figure 7.7. The set E_1^ε for $\frac{1}{2} < \frac{\gamma}{\alpha} < \frac{3}{4}$.

(b) if $N_{\alpha,\gamma}$ is odd, then $E_1^\varepsilon \in \mathcal{A}_o^\varepsilon$. The set of its centers is given by

$$\mathcal{I}_{1,\varepsilon} = \left\{ i \in \varepsilon\mathbb{Z}_o^2 : \|i\|_1 \leq N_{\alpha,\gamma}\varepsilon \right\}. \quad (7.52)$$

A direct computation shows that

$$\mathcal{I}_{k,\varepsilon} = \mathcal{I}_{1,\varepsilon}[k] = \begin{cases} \{i \in \varepsilon\mathbb{Z}_e^2 : \|i\|_1 \leq N_{\alpha,\gamma}k\varepsilon\} & \text{if } k \text{ is even} \\ \{i \in \varepsilon\mathbb{Z}_o^2 : \|i\|_1 \leq N_{\alpha,\gamma}k\varepsilon\} & \text{if } k \text{ is odd.} \end{cases} \quad (7.53)$$

Now we compute explicitly the variation of the energy to pass from E_k^ε to E_{k+1}^ε , k odd.

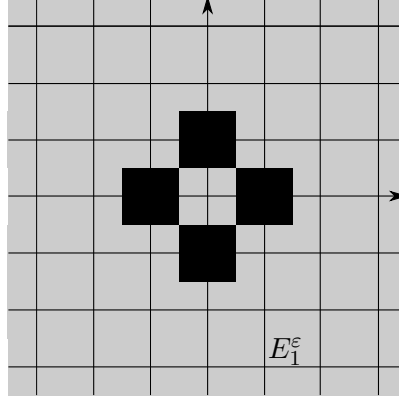


Figure 7.8. The set E_1^ε for $\frac{5}{12} < \frac{\gamma}{\alpha} < \frac{1}{2}$.

Note that

$$|\mathcal{I}_{k,\varepsilon}| = \sum \{4j : j = 1, \dots, N_{\alpha,\gamma}k, j \text{ odd}\} = N_{\alpha,\gamma}^2 k^2 + 2N_{\alpha,\gamma}k + 1, \quad (7.54)$$

while

$$|\mathcal{I}_{k+1,\varepsilon}| = \sum \{4j : j = 2, \dots, N_{\alpha,\gamma}(k+1), j \text{ even}\} = N_{\alpha,\gamma}^2 (k+1)^2 + 2N_{\alpha,\gamma}(k+1). \quad (7.55)$$

The variation of the perimeter term is then

$$-4(|\mathcal{I}_{k+1,\varepsilon}| - |\mathcal{I}_{k,\varepsilon}|) = -4[(2k+1)N_{\alpha,\gamma}^2 + 2N_{\alpha,\gamma} - 1], \quad (7.56)$$

while the variation of the bulk term is

$$\frac{\alpha}{\gamma} \left(|\mathcal{I}_{k,\varepsilon}| + N_{\alpha,\gamma}^2 k^2 + \left(N_{\alpha,\gamma}^3 + 2N_{\alpha,\gamma}^2 + N_{\alpha,\gamma} \right) k + \frac{2}{3}N_{\alpha,\gamma}^3 + 2N_{\alpha,\gamma}^2 + \frac{4}{3}N_{\alpha,\gamma} + 2 \right), \quad (7.57)$$

that is,

$$\frac{\alpha}{\gamma} \left(2N_{\alpha,\gamma}^2 k^2 + \left(N_{\alpha,\gamma}^3 + 2N_{\alpha,\gamma}^2 + 3N_{\alpha,\gamma} \right) k + \frac{2}{3}N_{\alpha,\gamma}^3 + 2N_{\alpha,\gamma}^2 + \frac{4}{3}N_{\alpha,\gamma} + 3 \right). \quad (7.58)$$

The total balance, given by adding (7.56) and (7.58), is then positive for k large.

The limit motion is characterized as follows (see Theorem 7.4.7).

Theorem 7.5.2. *Let $F_\varepsilon(t)$ be defined as in (a) of Theorem 7.4.7. Then, for all fixed t , the Kuratowsky limit of the family $F_\varepsilon(t)$ as $\varepsilon \rightarrow 0$ is a rhombus $F(t)$ of centre 0 and side length $\frac{1}{\gamma}\sqrt{2}\lfloor \frac{4\gamma}{\alpha} \rfloor t$.*

7.5.2 An example of asymmetric distance

We now give an example where the limit set is of dimension $d-1$; more precisely, a linearly growing segment. For this, we assume that $d=2$ and consider the (sufficiently) asymmetric norm

$$\varphi^\varepsilon(i) = \sqrt{\frac{33}{8}(i_1^2 + i_2^2) - \frac{31}{4}i_1i_2}, \quad i \in \varepsilon\mathbb{Z}^2. \quad (7.59)$$

We note that $\varphi^\varepsilon(\varepsilon, \varepsilon) = \frac{\sqrt{2}}{2}\varepsilon < \sqrt{\frac{33}{8}}\varepsilon = \varphi^\varepsilon(\varepsilon, 0) = \varphi^\varepsilon(0, \varepsilon)$ and we assume that

$$\frac{\sqrt{2}}{8} \leq \frac{\gamma}{\alpha} < \frac{1}{8}\sqrt{\frac{33}{2}}. \quad (7.60)$$

In this case,

$$\mathcal{I}_{1,\varepsilon} = \left\{ i \in \varepsilon\mathbb{Z}^2 : \varphi^\varepsilon(i) < \frac{4\gamma}{\alpha}\varepsilon \right\} = \{(-\varepsilon, -\varepsilon), (0, 0), (\varepsilon, \varepsilon)\},$$

and

$$\mathcal{I}_{k,\varepsilon} = \mathcal{I}_{1,\varepsilon}[k] = \{(j\varepsilon, j\varepsilon) : j = 0, \pm 1, \dots, \pm k\}, \quad k \geq 1. \quad (7.61)$$

We define $F_\varepsilon(t) = \text{conv}(\mathcal{I}_{\lfloor t/\gamma\varepsilon \rfloor, \varepsilon})$, where $E_k^\varepsilon = E_{\mathcal{I}_{k,\varepsilon}}$. In Fig. 7.9 some steps of the discrete evolution are represented.

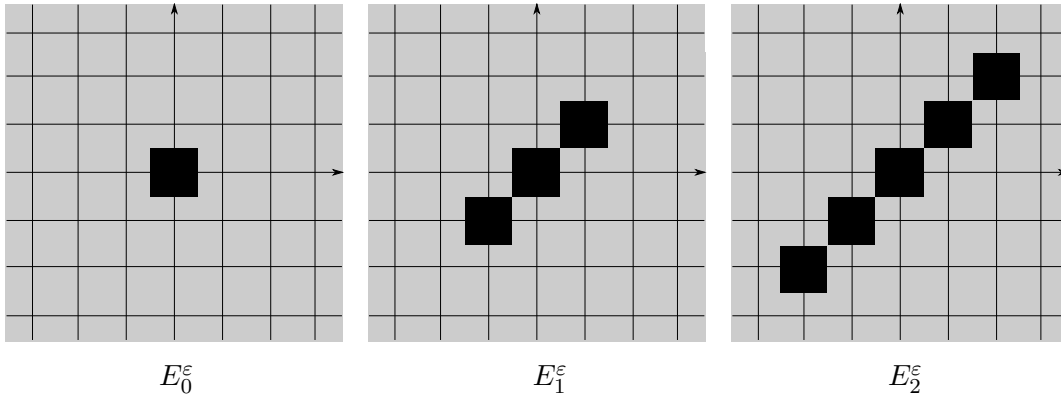


Figure 7.9. Some steps of the evolution.

The following limit evolution holds.

Proposition 7.5.3 (limit motion). *Let $\alpha, \gamma > 0$ be such that (7.60) is satisfied. Then, for all fixed t , the Kuratowsky limit of the family $F_\varepsilon(t)$ as $\varepsilon \rightarrow 0$ is a segment $F(t)$ such that $F(0) = \{0\}$ and whose length $L(t)$ satisfies*

$$L(t) = \frac{1}{\gamma}2\sqrt{2}t \quad (7.62)$$

for almost every $t \geq 0$.

Proof. We define $L_k^\varepsilon = \mathcal{H}^1(\text{conv}(\mathcal{I}_{k,\varepsilon}))$. We have that

$$L_{k+1}^\varepsilon = L_k^\varepsilon + 2\sqrt{2}\varepsilon, \quad (7.63)$$

with initial condition $L_0^\varepsilon = 0$. If we define $L_\varepsilon(t)$ as the linear interpolation in $[k\tau, (k+1)\tau]$ of the values L_k^ε , that is

$$L_\varepsilon(t) = \frac{L_{k+1}^\varepsilon - L_k^\varepsilon}{\tau}(t - (k+1)\tau) + L_{k+1}^\varepsilon = 2\sqrt{2}\frac{\varepsilon}{\tau}(t - (k+1)\tau) + L_{k+1}^\varepsilon, \quad (7.64)$$

then $L_\varepsilon(t)$ is an increasing continuous function of t and the sequence is uniformly Lipschitz on all intervals $[T, +\infty)$ such that $L_\varepsilon(T) \geq c > 0$. Hence, it converges,

up to a subsequence, as $\varepsilon \rightarrow 0$ to an increasing function $L(t)$. It follows that $F_\varepsilon(t)$ converges, as $\varepsilon \rightarrow 0$, in the Kuratowski sense to a limit segment $F(t)$.

To justify (7.62), we define $L_\varepsilon(t) = L_{\lfloor t/\gamma\varepsilon \rfloor}^\varepsilon$, which converges locally uniformly to $L(t)$ as $\varepsilon \rightarrow 0$. We have that

$$L_\varepsilon(t) = L_{\lfloor t/\gamma\varepsilon \rfloor}^\varepsilon = \left\lfloor \frac{t}{\gamma\varepsilon} \right\rfloor 2\sqrt{2}\varepsilon,$$

from which we obtain (7.62) passing to the limit as $\varepsilon \rightarrow 0$. □

Appendix A

Variational problems with percolation: rigid spin systems

In view of the possible definition of variational motion in random media (i.e., with randomly distributed inclusions) motivated by finding at least an estimate for the pinning threshold, we describe the results contained in the paper by myself [45] about random homogenization of energies associated to spin systems with unbounded interaction coefficients, by using percolation techniques.

A.1 The model problem and the percolation approach

In the context of Variational theories in Materials Science it is often necessary to model media with fine microstructure and to describe their properties via averaged effective energies. This is the main goal of Homogenization theory (see e.g. Braides and Defranceschi [13], Chechkin, Piatnitski and Shamaev [23]). In some cases periodic microstructure is not sufficient, so that random media have to be considered.

The model problem that we have in mind is that of a crystalline two-dimensional solid subject to fracture. We suppose that the relevant scale is that of the surface (fracture) energy so we may neglect the elastic energy of the lattice (this can be taken separately into account as in the paper by Braides and Piatnitski [16]). In this case, depending on the applied forces or boundary displacement of the sample, a fracture may appear, separating two regions where the displacement is constant. In the Griffith theory of Fracture (see Griffith [32]), the energy necessary for the creation of a crack is proportional to its area; in a discrete setting this is translated in the number of atomic bonds that are broken. In our model, at the atomistic level, there is a random distribution of ‘strong’ unbreakable bonds and ‘weak’ (ferromagnetic) breakable bonds. This model translates into a *rigid* spin problem, where the two values of the spin parametrize the two regions of constant displacement of the crystal. We note that in this problem the random distribution of rigid or weak bonds is considered as fixed and as characteristic of the crystalline material, so that we are interested in almost sure properties of the overall energies when the measure of the sample is large with respect to the atomic distance.

The way we will describe the overall behavior of this system is by scaling the

domain lattice by a small parameter ε and introducing the corresponding scaled energies, and then compute the variational limit (Γ -limit) of such energies, which is defined on the continuum and it can be considered as an effective energy.

The microscopic energy under examination can be written as

$$\sum_{ij} \sigma_{ij}^\omega (1 - u_i u_j), \quad (\text{A.1})$$

where $u_i \in \{\pm 1\}$ is a spin variable indexed on the lattice \mathbb{Z}^2 , the sum runs on nearest-neighbors (i.e. $|i - j| = 1$) in a given portion $\Omega \cap \mathbb{Z}^2$ of \mathbb{Z}^2 , the coefficients σ_{ij}^ω depend on the realization ω of an independent and identically distributed (i.i.d.) random variable and

$$\sigma_{ij}^\omega = \begin{cases} +\infty & \text{with probability } p \\ 1 & \text{with probability } 1 - p, \end{cases}$$

with $p \in [0, 1]$ fixed and the convention $+\infty \cdot 0 = 0$. In place of (A.1) we could consider the energies

$$- \sum_{ij} \sigma_{ij}^\omega u_i u_j, \quad (\text{A.2})$$

but in this case, just to avoid ambiguities in the sum, $\sigma_{ij}^\omega = +\infty$ forces $u_i = u_j$ and this gives a constraint for the problem.

In recent papers, Braides and Piatnitski [17, 18] treated the cases of *elliptic* random spin energies, that is with equi-bounded strictly positive random coefficients, and of *dilute* spin energies, with random coefficients given by

$$\tilde{\sigma}_{ij}^\omega = \begin{cases} 1 & \text{with probability } p \\ 0 & \text{with probability } 1 - p. \end{cases}$$

In order to describe the behavior as the size of Ω diverges we introduce a scaled problem, as is customary in the passage from lattice systems to continuous variational problems, in which, on the contrary, Ω is kept fixed, but scaled energies are defined as follows. A small parameter $\varepsilon > 0$ is introduced, the lattice is scaled accordingly to $\varepsilon\mathbb{Z}^2$, and the energies (A.1) are scaled (after multiplying by 2) to

$$E_\varepsilon^\omega(u) := \sum_{ij} \varepsilon \sigma_{ij}^\omega (u_i - u_j)^2. \quad (\text{A.3})$$

Note that uniform states (which are pointwise minimizers of the “integrand”) have zero energy; moreover, the “surface scaling” ε is driven by the knowledge that for $p = 0$ (i.e., for ferromagnetic interactions) the Γ -limit with that scaling is not trivial (as shown e.g. by Alicandro, Braides and Cicalese [1]). After this scaling, the sum is taken on nearest neighbors in $\Omega \cap \varepsilon\mathbb{Z}^2$, and the normalization allows also to consider $\Omega = \mathbb{R}^2$ (in this case the domain of the energy is composed of all u which are constant outside a bounded set).

The coarse graining of these energies corresponds to a general approach in the theory of Γ -convergence for lattice system where the discrete functions $u = \{u_i\}$ are

identified with their piecewise-constant extensions, and the scaled lattice energies with energies on the continuum whose asymptotic behavior is described by taking L^1 -limits in the u variable and applying a mesoscopic homogenization process to the energies. A general theory for interfacial energies by Ambrosio and Braides [5] suggests the identification of limit energies with functionals of the form

$$\int_{\Omega \cap \partial\{u=1\}} \varphi(x, \nu) d\mathcal{H}^1,$$

with ν the normal to $\partial\{u=1\}$.

Our analysis will be carried out by using results from Percolation theory. Percolation is a model for random media (see Grimmett [33] and Kesten [37]). We are interested in *bond percolation* on the square lattice \mathbb{Z}^2 : we view \mathbb{Z}^2 as a graph with edges between neighboring vertices, and all edges are, independently of each other, chosen to be ‘strong’ with probability p and ‘weak’ with probability $1-p$. A weak path is a sequence of consecutive weak edges, a weak cluster is a maximal connected component of the collection of weak edges. Percolation exhibits a phase transition: there exists a critical value of probability p_c , the *percolation threshold*, such that if $p < p_c$ then with probability one there exists a unique infinite weak cluster, while if $p > p_c$ then all the weak clusters are finite almost surely. For bond percolation on \mathbb{Z}^2 , the percolation threshold is given by $p_c = \frac{1}{2}$.

Actually, the structure of the Γ -limit of the energies (A.3) depends on probability through the percolation threshold. Above the percolation threshold the Γ -limit is $+\infty$ on the functions not identically equal to 1 or -1. Below the percolation threshold, instead, the coarse graining leads first to showing that indeed we may define a limit magnetization u taking values in $\{\pm 1\}$. This u is obtained as a L^1 -limit on the scaled infinite weak cluster, thus neglecting the values u_i on nodes i isolated from that cluster. The surface tension is obtained by optimizing the almost sure contribution of the interfaces, and showing that it can be expressed as a first-passage percolation problem, so that the limit is of the form

$$\int_{\Omega \cap \partial\{u=1\}} \lambda_p(\nu) d\mathcal{H}^1. \quad (\text{A.4})$$

The Γ -lim inf inequality is obtained by a blow-up argument. We perform a construction based on the Channel property (Theorem A.3.2) which allows to modify the test sets in order to get a ‘weak’ boundary, avoiding bonds with infinite energy. This is useful also for the construction of a recovery sequence.

This type of variational percolation results can be linked to the paper by Braides and Piatnitski [16] where discrete fracture of a membrane is studied and linked to large deviations for the chemical distance in supercritical Bernoulli percolation. The value $\lambda_p(\nu)$ is defined through the asymptotic behavior of the chemical distance (that is, the distance on the infinite weak cluster) between a pair of points aligned with ν . The general framework for first-passage percolation and chemical distance can be found in Grimmett and Kesten [34], Kesten [35]. The result of this paper is that in the subcritical case, a crack in the crystal may appear following a minimal path on the infinite weak cluster and the microscopical pattern of the lattice (this fact justifies the anisotropy of the fracture energy (A.4)). In

the supercritical case, instead, the solid almost surely is rigid and there is no fracture.

Overview of the chapter. In Section A.2 we fix notation and present the setting of the problem, describing the energies that we will consider. Section A.3 contains some results from percolation theory necessary for the computations. Section A.4 contains the proof of the main result: in the subcritical regime (that is, for $p < p_c$), the energies Γ -converge to a deterministic anisotropic perimeter whose density is obtained by means of an asymptotic first-passage percolation formula related to the chemical distance on the lattice; in the supercritical regime (that is, for $p > p_c$), the Γ -limit is identically $+\infty$ on the functions u not identically equal to 1 or -1. In Section A.5 we show that the homogenization of rigid spin systems is actually a limit case of the elliptic random homogenization of spin systems; that is, the behavior of a rigid spin system is approximated by that of an elliptic spin system with one of the interaction coefficients very large. The proof of this new “continuity” property of the surface tension (Proposition A.5.5) essentially relies on a percolation result (Lemma A.5.1).

A.2 Notation and setting of the problem

If A is a measurable subset of \mathbb{R}^2 , we denote its 2-dimensional Lebesgue measure indifferently by $\mathcal{L}^2(A)$ or $|A|$. \mathcal{H}^k denotes the k -dimensional Hausdorff measure. $B_\rho(x)$ is the open ball of center x and radius ρ and S^1 is the boundary of $B_1(0)$. If $\nu \in S^1$, $Q_\rho^\nu(x)$ is the square centered at x , of side length ρ and one side orthogonal to ν , that is

$$Q_\rho^\nu(x) = \{y \in \mathbb{R}^2 : |\langle y - x, \nu \rangle| \leq \rho/2, |\langle y - x, \nu^\perp \rangle| \leq \rho/2\},$$

where $\nu^\perp = (-\nu_2, \nu_1)$ denotes the clockwise rotation by $\pi/2$ of ν .

We use the notation for *bond-percolation* problems as in Braides and Piatnitski [16], Section 2.4. In this percolation model, we assign the label “strong” or “weak” to a bond with probability p and $1 - p$, respectively, the choice being independent on distinct bonds.

Denote by $\hat{\mathbb{Z}}^2$ the *dual grid* of \mathbb{Z}^2 , that is the set of the middle points of the segments $[i, j]$, $i, j \in \mathbb{Z}^2$, $|i - j| = 1$, of the standard integer grid \mathbb{Z}^2 . The notation $i(\hat{z}), j(\hat{z})$ is used for the endpoints of the segment containing \hat{z} . We may identify each point $\hat{z} \in \hat{\mathbb{Z}}^2$ with the corresponding closed segment $[i(\hat{z}), j(\hat{z})]$, so that points in $\hat{\mathbb{Z}}^2$ are identified with bonds in \mathbb{Z}^2 .

Let $(\Sigma, \mathcal{F}, \mathbf{P})$ be a probability space, and let $\{\xi_{\hat{z}}, \hat{z} \in \hat{\mathbb{Z}}^2\}$ be a family of independent identically distributed random variables such that

$$\xi_{\hat{z}} = \begin{cases} 1 & \text{ (“strong”) with probability } p \\ 0 & \text{ (“weak”) with probability } 1 - p, \end{cases}$$

and $p \in [0, 1]$ is fixed. Let $\omega \in \Sigma$ be a realization of this i.i.d. random variable in \mathbb{Z}^2 and introduce the coefficients

$$\sigma_{\hat{z}}^\omega = \begin{cases} +\infty & \text{if } \xi_{\hat{z}}(\omega) = 1 \\ 1 & \text{otherwise.} \end{cases}$$

We write $\sigma_{\hat{z}}^\omega = \sigma_{ij}^\omega$, after identifying each \hat{z} with a pair of nearest-neighbors in \mathbb{Z}^2 .

For each ω we consider the energies

$$E_\varepsilon^\omega(u) = \frac{1}{8} \sum_{i,j \in \Omega_\varepsilon} \varepsilon \sigma_{ij}^\omega (u_i - u_j)^2, \quad (\text{with the convention } \infty \cdot 0 = 0) \quad (\text{A.5})$$

defined on $u : \Omega_\varepsilon \rightarrow \{\pm 1\}$, where we use the notation $\Omega_\varepsilon = \frac{1}{\varepsilon} \Omega \cap \mathbb{Z}^2$ and Ω is an open subset of \mathbb{R}^2 with Lipschitz boundary. The factor 8 is a normalization factor due to the fact that each bond is accounted twice and $(u_i - u_j)^2 \in \{0, 4\}$.

Each function $u : \Omega_\varepsilon \rightarrow \{\pm 1\}$ is identified with the piecewise-constant function (which, with a slight abuse of notation, we also denote by u) such that $u(x) = u_i$ on each coordinate square of center εi and side length ε contained in Ω and 1 otherwise, no matter what this value is. In this way all u can be considered as functions in $L^1(\Omega)$, and more precisely in $BV(\Omega; \{\pm 1\})$.

The case $p = 0$ corresponds to a *ferromagnetic spin system*, which can be described approximately as $\varepsilon \rightarrow 0$ by the anisotropic perimeter energy (see [1])

$$F_0(u) = \int_{\partial^* \{u=1\} \cap \Omega} \|\nu_u\|_1 d\mathcal{H}^1$$

defined on $u \in BV(\Omega; \{\pm 1\})$, where $\partial^* \{u=1\}$ denotes the measure-theoretical reduced boundary of the set of finite perimeter $\{u=1\}$, ν_u its inner normal (see Section 1.3) and $\|\cdot\|_1$ the ℓ^1 -norm defined by $\|x\|_1 = |x_1| + |x_2|$, $x = (x_1, x_2)$.

In this passage from discrete to continuous we identify each function $u : \Omega_\varepsilon \rightarrow \{\pm 1\}$ with the set $A = \bigcup \{\varepsilon i + \varepsilon Q : i \in \Omega_\varepsilon : u_i = 1\}$ or the function $u \in BV(\Omega; \{\pm 1\})$ given by $u = 2\chi_A - 1$, where $Q = \left[-\frac{1}{2}, \frac{1}{2}\right) \times \left[-\frac{1}{2}, \frac{1}{2}\right)$ denotes the coordinate semi-open unit square in \mathbb{R}^2 centered at 0.

A.3 Some results from percolation theory

We recall some results from percolation theory (see e.g., Braides and Piatnitski [16], and Grimmett [33], Kesten [37] for general references on percolation theory).

We introduce a terminology for *weak points*, that is those points $\hat{z} \in \hat{\mathbb{Z}}^2$ such that $\xi_{\hat{z}} = 0$. Keeping in mind the identification of \hat{z} with $[i(\hat{z}), j(\hat{z})]$ stated in the previous section, we denote the corresponding bond also by \hat{z} , and we refer to \hat{z} as a *weak bond* or point, indifferently. We say that two weak points \hat{z} and \hat{z}' are *adjacent* if the corresponding two segments have an endpoint in common. A sequence of weak bonds $\gamma = \{\hat{z}_1, \dots, \hat{z}_k\}$ is said to be a *weak path* if any two consecutive points of this sequence are adjacent. In what follows we identify a weak path with the subset of \mathbb{R}^2 composed of the union of the corresponding segments; the *length* of the weak path γ is the number of its connections, and we denote it by $|\gamma|$. A subset A of $\hat{\mathbb{Z}}^2$ of weak points is said to be *connected* if for every two points \hat{z}', \hat{z}'' of A there exists a weak path as above such that $\forall j \in \{1, 2, \dots, k\}, \hat{z}_j \in A, \hat{z}_1 = \hat{z}', \hat{z}_k = \hat{z}''$. A maximum connected component of adjacent weak points is called a *weak cluster*.

A first result deals with the existence of infinite weak clusters and it shows that there is a critical probability ($p_c = \frac{1}{2}$ in two dimensions for the square lattice) which separates two different behaviors of the bond-percolation system.

Theorem A.3.1 (percolation threshold). *For any $p > p_c = 1/2$ (supercritical regime) all the weak clusters are almost surely finite, while for any $p < 1/2$ (subcritical regime) with probability one there is exactly one infinite weak cluster \mathcal{W}^ω .*

From now on we will refer to \mathcal{W}^ω simply as *the weak cluster*. Let $\nu = (\nu_1, \nu_2) \in S^1$ and $0 < \delta < 1$. We denote by T_ν^δ the rectangle

$$T_\nu^\delta = \{x \in \mathbb{R}^2 : |\langle x, \nu \rangle| \leq \delta/2, 0 \leq \langle x, \nu^\perp \rangle \leq 1\}.$$

A path joining the smaller sides of the rectangle will be called a *channel* (or *left-right crossing*). A weak path with this property will be called a *weak channel*. The following result gives a lower bound on the number of weak channels almost surely crossing sufficiently large rectangles (or squares) in the subcritical regime.

Theorem A.3.2 (Channel property). *Let $p < 1/2$, ω denote a realization and $M > 0$. Then there exist constants $c(p) > 0$ and $c_1(p) > 0$ such that almost surely for any δ , $0 < \delta \leq 1$ there is a number $N_0 = N_0(\omega, \delta)$ such that for all $N > N_0$ and for any T_ν^δ and $|x_0| \leq M$ the rectangle $N(T_\nu^\delta + x_0)$ contains at least $c(p)N\delta$ disjoint weak channels which connect the smaller sides of the rectangle. Moreover, the length of each such a channel does not exceed $c_1(p)N$.*

A realization $\omega \in \Sigma$ is said to be *typical* if the statement of the Theorem A.3.2 holds for such an ω . Now we introduce some terminology also for *strong bonds*, that is those points $\hat{z} \in \hat{\mathbb{Z}}^2$ such that $\xi_{\hat{z}} = 1$. We consider the shifted lattice $Z_b = \mathbb{Z}^2 + \left(\frac{1}{2}, \frac{1}{2}\right)$ and notice that the set of middle points of its bonds coincides with $\hat{\mathbb{Z}}^2$. Thus, to each point $\hat{z} \in \hat{\mathbb{Z}}^2$ we can associate the corresponding bond in Z_b . If \hat{z} is identified with the corresponding segment with endpoints in Z_b , then we may define the notion of *adjacent points* as for weak bonds. The notions of *strong channel* and *strong cluster* are modified accordingly. For $p > 1/2$ there is almost surely a unique infinite strong cluster and the channel property stated above holds for the strong channels as well.

To simplify the notation, from now on we will denote by x (in place of \hat{x}) a generic point in $\hat{\mathbb{Z}}^2$. If $p < 1/2$ and two points $x, y \in \hat{\mathbb{Z}}^2$ belong to the weak cluster, then by definition of cluster there is at least a path γ in the cluster joining x and y . To describe the metric properties of the weak cluster we introduce a random distance.

Definition A.3.3 (chemical distance). *Let $x, y \in \hat{\mathbb{Z}}^2$ and ω be a realization of the random variable. The chemical distance $D^\omega(x, y)$ between x and y in the realization ω is defined as*

$$D^\omega(x, y) = \min_{\gamma} |\gamma|, \tag{A.6}$$

where $|\gamma|$ is the length of the path γ and the minimum is taken on the set of paths joining x and y and that are weak in the realization ω .

Remark A.3.4. The chemical distance is defined only if x and y are in the same cluster; otherwise, by convention, $D^\omega(x, y) = +\infty$.

When it is finite, the random distance $D^\omega(x, y)$ is thus the minimal number of weak bonds needed to link x and y in the realization ω (also x and y are taken into account), and is thus not smaller than $\|x - y\|_1$. When $p < \frac{1}{2}$, $D^\omega(0, x)$ on the weak cluster can be seen as a *travel time* between 0 and x in a first-passage percolation model (see Garet and Marchand [30], Kesten [36]), where the passage times of the edges are independent identically distributed random variables with common distribution $p\delta_{+\infty} + (1 - p)\delta_1$. The following Lemma deals with the existence of an asymptotic time constant in a given direction.

Lemma A.3.5. *Assume that $0 \in \mathcal{W}^\omega$. For any $\tau \in \mathbb{R}^2$ the following limit exists almost surely and does not depend on ω*

$$\lambda_p(\tau) = \lim_{\substack{m \rightarrow +\infty \\ 0 \longleftrightarrow \lfloor m\tau \rfloor}} \frac{1}{m} D^\omega(0, \lfloor m\tau \rfloor), \quad (\text{A.7})$$

where $\lfloor m\tau \rfloor = (\lfloor m\tau \rfloor_1, \lfloor m\tau \rfloor_2)$, $\lfloor m\tau \rfloor_k = \lfloor m\tau_k \rfloor$ is the integer part of the k -th component of $m\tau$ and $0 \longleftrightarrow \lfloor m\tau \rfloor$ means that 0 and $\lfloor m\tau \rfloor$ are linked by a path in the weak cluster. Moreover, λ_p defines a norm on \mathbb{R}^2 .

Proof. See Garet and Marchand [29], Corollary 3.3. □

The same asymptotic result holds for sequences of points in the weak cluster ‘asymptotically aligned’ with τ , that is x_m, y_m such that $y_m - x_m = m\tau + o(m)$ as $m \rightarrow \infty$. The proof of this fact relies essentially on the following large deviation result for the chemical distance (see Garet and Marchand [30]):

Theorem A.3.6. *Let $p < 1/2$ and λ_p be the norm on \mathbb{R}^2 given by Lemma A.3.5. Then*

$$\forall \varepsilon > 0, \quad \limsup_{m \rightarrow +\infty} \frac{\log \mathbf{P}[0 \longleftrightarrow \lfloor m\tau \rfloor, D^\omega(0, \lfloor m\tau \rfloor)/\lambda_p(\tau) \notin (1 - \varepsilon, 1 + \varepsilon)]}{m} < 0. \quad (\text{A.8})$$

Proposition A.3.7. *Let $(x_m), (y_m)$ be two sequences of points in $\hat{\mathbb{Z}}^2$ contained in the weak cluster such that*

$$\sup_m \left\{ \frac{|x_m|}{m} + \frac{|y_m|}{m} \right\} \leq C < +\infty \quad \text{and} \quad y_m - x_m = m\tau + o(m), \quad (\text{A.9})$$

where $\tau \in \mathbb{R}^2$, C is a positive constant and $o(m)/m \rightarrow 0$ as $m \rightarrow +\infty$. Then the following limit exists almost surely and does not depend on ω

$$\lambda_p(\tau) = \lim_{m \rightarrow +\infty} \frac{1}{m} D^\omega(x_m, y_m). \quad (\text{A.10})$$

Proof. We denote by $\tilde{\lambda}_p(\tau)$ the right hand side of equation (A.10). We prove (A.10) in the case that $y_m = \lfloor mx + m\tau \rfloor$ and $x_m = \lfloor mx \rfloor$, $x \neq 0$. The stationarity of the i.i.d. Bernoulli process ensures that the probability law of $D^\omega(\lfloor mx \rfloor, \lfloor mx + m\tau \rfloor)$ is the same of $D^\omega(0, \lfloor m\tau \rfloor)$.

Therefore, by (A.8) we have that

$$\forall \varepsilon > 0, \quad \limsup_{m \rightarrow +\infty} \frac{\log \mathbf{P} \left[\lfloor mx \rfloor \longleftrightarrow \lfloor mx + m\tau \rfloor, \frac{D^\omega(\lfloor mx \rfloor, \lfloor mx + m\tau \rfloor)}{\lambda_p(\tau)} \notin (1 - \varepsilon, 1 + \varepsilon) \right]}{m} < 0.$$

By Borel-Cantelli Lemma we obtain that $\forall \varepsilon > 0$,

$$\limsup_{\substack{m \rightarrow +\infty \\ \lfloor mx \rfloor \longleftrightarrow \lfloor mx + m\tau \rfloor}} \frac{1}{m} D^\omega(\lfloor mx \rfloor, \lfloor mx + m\tau \rfloor) \in [(1 - \varepsilon)\lambda_p(\tau), (1 + \varepsilon)\lambda_p(\tau)]$$

\mathbf{P} -almost surely, that is,

$$\lim_{\substack{m \rightarrow +\infty \\ \lfloor mx \rfloor \longleftrightarrow \lfloor mx + m\tau \rfloor}} \frac{1}{m} D^\omega(\lfloor mx \rfloor, \lfloor mx + m\tau \rfloor) = \lambda_p(\tau)$$

\mathbf{P} -almost surely. By a compactness argument, we have that $\tilde{\lambda}_p(\tau) \leq \lambda_p(\tau)$. Indeed, if x_m, y_m are as in (A.9), then there exist a subsequence $m_j \rightarrow +\infty$ and \tilde{x}, \tilde{y} such that $\frac{x_{m_j}}{m_j} \rightarrow \tilde{x}$, $\frac{y_{m_j}}{m_j} \rightarrow \tilde{y}$, with $\tilde{y} = \tilde{x} + \tau$. Therefore, in the computation of the limit in (A.10) we can choose $x_m = \lfloor m\tilde{x} \rfloor$ and $y_m = \lfloor m\tilde{x} + m\tau \rfloor$.

Now, if we consider two points x_m, y_m on the weak cluster satisfying (A.9), we can find x such that x_m and $\lfloor mx \rfloor$, y_m and $\lfloor mx + m\tau \rfloor$ almost surely are linked by weak paths whose length is at most $o(m)$. Hence,

$$D^\omega(\lfloor mx \rfloor, \lfloor mx + m\tau \rfloor) \leq D^\omega(x_m, y_m) + o(m)$$

and from this it follows that $\lambda_p(\tau) \leq \tilde{\lambda}_p(\tau)$. \square

Remark A.3.8. If $\nu \in \mathbb{R}^2$ is a unit vector and $\tau = \nu^\perp$, then by symmetry $\lambda_p(\nu) = \lambda_p(\tau)$.

A.4 The rigid percolation theorem

We first remark that the energies E_ε^ω defined by (A.5) are equi-coercive with respect to the strong L^1 -convergence. The proof is immediate as in the elliptic case, while for dilute spin energies this result requires a more difficult argument (see Braides and Piatnitski [18], Section 3.1).

Lemma A.4.1 (equi-coerciveness of E_ε^ω). *Let Ω be a bounded Lipschitz open set. For any ω in a set $\tilde{\Sigma} \subseteq \Sigma$ with $\mathbf{P}(\tilde{\Sigma}) = 1$, if (u_{ε_k}) is a sequence such that $\sup_k E_{\varepsilon_k}^\omega(u_{\varepsilon_k}) < +\infty$, then there exists a function $u \in BV(\Omega; \{\pm 1\})$ and a subsequence, still denoted by (u_{ε_k}) , such that $u_{\varepsilon_k} \rightarrow u$ in $L^1(\Omega)$.*

Proof. Equi-boundedness of the energies forces the coefficients σ_{ij}^ω to be equal to 1 almost surely if $(u_{\varepsilon_k})_i \neq (u_{\varepsilon_k})_j$, so that the equi-coerciveness follows from that of ferromagnetic energies (see e.g. Braides and Piatnitski [17], Section 2). \square

The main result is the following.

Theorem A.4.2 (Rigid percolation theorem). *Let Ω be a bounded Lipschitz open set and E_ε^ω be the energies defined by (A.5). Then we have two regimes:*

- (a) *If $p < 1/2$ (subcritical regime), then \mathbf{P} -almost surely there exists the Γ -limit of E_ε^ω with respect to the $L^1(\Omega)$ -convergence on $BV(\Omega; \{\pm 1\})$, it is deterministic, and is given by*

$$F_p(u) = \int_{\Omega \cap \partial^* \{u=1\}} \lambda_p(\nu) d\mathcal{H}^1, \quad (\text{A.11})$$

for $u \in BV(\Omega; \{\pm 1\})$. In (A.11) λ_p is defined by (A.7), (A.10) and ν is the unit normal vector at $\partial^ \{u = 1\}$.*

- (b) *If $p > 1/2$ (supercritical regime), then \mathbf{P} -almost surely there exists the Γ -limit of E_ε^ω and it coincides with $F(u) \equiv +\infty$ on the whole $L^1(\Omega)$ except for u constant identically ± 1 .*

Proof. (a) We begin with the proof of the lower bound (liminf inequality), and fix a typical realization ω and a family $u_\varepsilon \rightarrow u$ in $L^1(\Omega)$ with $u \in BV(\Omega; \{\pm 1\})$ such that $\liminf_{\varepsilon \rightarrow 0} E_\varepsilon^\omega(u_\varepsilon) < \infty$. We can assume, up to a subsequence, that such a liminf is actually a limit.

For all ε we consider the set in the dual lattice $\varepsilon\hat{\mathbb{Z}}^2$ of $\varepsilon\mathbb{Z}^2$ defined by

$$S_\varepsilon = \left\{ \varepsilon k : k = \frac{i+j}{2}, i, j \in \Omega_\varepsilon, |i-j| = 1, u_\varepsilon(\varepsilon i) = 1, u_\varepsilon(\varepsilon j) = -1 \right\}$$

and the measure

$$\mu_\varepsilon = \sum_{\varepsilon k \in S_\varepsilon} \varepsilon \sigma_k^\omega \delta_{\varepsilon k}.$$

Note that $E_\varepsilon^\omega(u_\varepsilon) = \mu_\varepsilon(\Omega)$, so that the family of measures $\{\mu_\varepsilon\}$ is equi-bounded. Hence, up to further subsequences, we can assume that $\mu_\varepsilon \rightharpoonup^* \mu$, where μ is a finite measure.

Let $A = \{u = 1\}$ and $A_\varepsilon = \{u_\varepsilon = 1\}$. With fixed $h \in \mathbb{N}$, we consider the collection \mathcal{Q}_h of squares $Q_\rho^\nu(x)$ such that the following conditions are satisfied:

- (i) $x \in \partial^* A$ and $\nu = \nu(x)$;
- (ii) $\left| (Q_\rho^\nu(x) \cap A) \triangle \Pi^\nu(x) \right| \leq \frac{1}{h} \rho^2$, where $\Pi^\nu(x) = \{y \in \mathbb{R}^2 : \langle y - x, \nu \rangle \geq 0\}$;
- (iii) $\left| \frac{\mu(Q_\rho^\nu(x))}{\rho} - \frac{d\mu}{d\mathcal{H}^1 \llcorner \partial^* A}(x) \right| \leq \frac{1}{h}$;

$$(iv) \left| \frac{1}{\rho} \int_{Q_\rho^\nu(x) \cap \partial^* A} \lambda_p(\nu(y)) d\mathcal{H}^1(y) - \lambda_p(\nu(x)) \right| \leq \frac{1}{h};$$

$$(v) \mu(Q_\rho^\nu(x)) = \mu(\overline{Q_\rho^\nu(x)}).$$

For fixed $x \in \partial^* A$ and for ρ small enough (ii) is satisfied by definition of reduced boundary (see Section 1.3), (iii) follows from the Besicovitch Derivation Theorem provided that

$$\frac{d\mu}{d\mathcal{H}^1 \llcorner \partial^* A}(x) < +\infty;$$

(iv) holds by the same reason (x is a Lebesgue point of λ_p), and (v) is satisfied for almost all $\rho > 0$ since μ is a finite measure (and so $\mu(\partial Q_\rho^\nu(x)) = 0$).

We deduce that \mathcal{Q}_h is a fine covering of the set

$$\partial^* A_\mu = \left\{ x \in \partial^* A : \frac{d\mu}{d\mathcal{H}^1 \llcorner \partial^* A}(x) < +\infty \right\},$$

so that (by Morse's lemma, see Morse [40]) there exists a countable family of disjoint closed squares $\{\overline{Q_{\rho_j}^{\nu_j}}(x_j)\}$ still covering $\partial^* A_\mu$. Note that

$$\mathcal{H}^1(\partial^* A \setminus \partial^* A_\mu) = 0$$

because of the existence of the derivative of the measure μ with respect to $\mathcal{H}^1 \llcorner \partial^* A$.

We now fix one of such squares $Q_\rho^\nu(x)$. We would like to use the sets $\frac{1}{\varepsilon}A_\varepsilon$ as test sets to estimate from below the part of μ concentrated on $\partial^* A$. Since these sets could not have correct boundary data, we modify them on the boundary. As in the case of spin energies with bounded coefficients (see Braides and Piatnitski [17, 18]), we could truncate the sets with the hyperplane $\partial\Pi^\nu = \{\langle y - x, \nu \rangle = 0\}$, but it may have infinite energy (possibly containing some strong bond), so we approximate it with a weak path γ_ω .

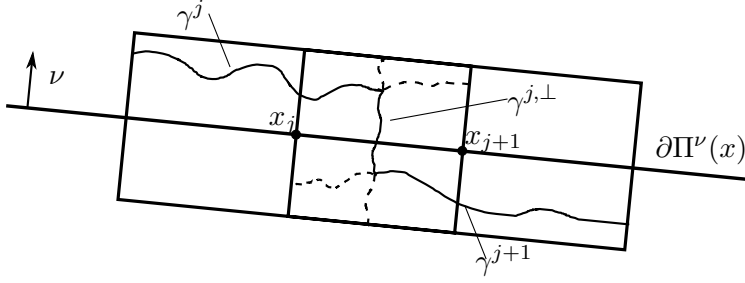
We subdivide the construction of test sets into steps.

Step 1: Construction of the weak path γ_ω . Let $0 < \delta \leq 1$. We cover the set $\partial\Pi^\nu(x) \cap Q_\rho^\nu(x)$ by considering the points

$$x_j = x + j\rho\delta\nu^\perp, \quad |j| = 0, 1, \dots, \left\lfloor \frac{1}{2\delta} \right\rfloor + 1, \quad (A.12)$$

and the rectangles R_j centered at x_j , with side-lengths $\rho\delta$ and $2\rho\delta$ and the small sides parallel to ν . The rectangles R_j and R_{j+1} have in common a square of side-length $\rho\delta$ and we denote it by $Q_{\rho\delta}^j$. From the channel property (Theorem A.3.2) for ε small enough we can find a weak channel γ^j (the highest) in R_j and a weak channel γ^{j+1} (the lowest) in R_{j+1} whose length is at most $2c_1(p)\rho\delta/\varepsilon$. Applying the same property to $Q_{\rho\delta}^j$ we can find a weak channel $\gamma^{j,\perp}$ connecting the two opposite sides of $Q_{\rho\delta}^j$ orthogonal to ν , whose length is at most $c_2(p)\rho\delta/\varepsilon$. The union $\gamma^j \cup \gamma^{j,\perp} \cup \gamma^{j+1}$ contains a weak path $\tilde{\gamma}^{j,j+1}$ connecting the smaller sides of the rectangle $R_j \cup R_{j+1}$ (see Fig. A.1).

We can repeat this construction for R_{j+1}, R_{j+2} and $Q_{\rho\delta}^{j+1}$ choosing γ^{j+1} , the highest weak channel γ^{j+2} in R^{j+2} and $\gamma^{j+1,\perp}$ in $Q_{\rho\delta}^{j+1}$ to define the weak path $\tilde{\gamma}^{j+1,j+2}$. If

Figure A.1. Construction of $\tilde{\gamma}^{j,j+1}$.

we repeat iteratively this procedure for any couple of rectangles R_j, R_{j+1} , j as in (A.12), the desired γ_ω will be obtained by gluing all the paths $\tilde{\gamma}^{j,j+1}$.

Step 2: Estimates. Note that γ_ω disconnects $Q_\rho^\nu(x)$ and we denote by Q_ω^+ the connected component of $Q_\rho^\nu(x)$ containing $Q_\rho^\nu(x) \cap \{ \langle y - x, \nu \rangle \geq \rho\delta/2 \}$. We have that

$$\left| (Q_\rho^\nu(x) \cap \Pi^\nu(x)) \triangle Q_\omega^+ \right| \leq \rho^2 \delta. \quad (\text{A.13})$$

By (ii) and (A.13), choosing ε small enough and using the fact that $|A_\varepsilon \triangle A| \rightarrow 0$, we obtain

$$\begin{aligned} \left| (Q_\rho^\nu(x) \cap A_\varepsilon) \triangle Q_\omega^+ \right| &\leq \left| (Q_\rho^\nu(x) \cap A) \triangle \Pi^\nu(x) \right| + \left| Q_\rho^\nu(x) \cap (A_\varepsilon \triangle A) \right| + \\ &\quad + \left| (Q_\rho^\nu(x) \cap \Pi^\nu(x)) \triangle Q_\omega^+ \right| \leq \rho^2 \left(\frac{2}{h} + \delta \right). \end{aligned} \quad (\text{A.14})$$

For simplicity of notation we can assume that $x = 0$ and $\nu = e_2$. With fixed $\eta < 1/2$, from (A.14) it follows that

$$\mathcal{A} := \left| \left((Q_\rho^\nu(x) \cap A_\varepsilon) \triangle Q_\omega^+ \right) \cap \left\{ y : \rho \frac{\eta}{2} \leq \text{dist}(y, \partial Q_\rho^\nu(x)) \leq \rho\eta \right\} \right| \leq \rho^2 \left(\frac{2}{h} + \delta \right). \quad (\text{A.15})$$

Step 3: Construction of an optimal weak circuit. We subdivide the annulus between the two concentric squares (with side-lengths $\rho(1 - \eta)$ and $\rho(1 - 2\eta)$ respectively) in four rectangles $R_i (i = 1, \dots, 4)$ with side-lengths $\rho(1 - \eta)$ and $\rho\eta/2$ (they have in common, two by two, a little square of side-length $\rho\eta/2$). From the channel property (Theorem A.3.2), for ε small enough in each of these rectangles we can find at least $c(p)\rho\eta/2\varepsilon$ disjoint weak channels K_i connecting the smaller sides of the rectangle, and with length at most $c_1(p)\rho(1 - \eta)/\varepsilon$. Since $\mathcal{A} \geq \sum_{K_i} (|K_i| \cap \mathcal{A})$, from the mean value theorem in each rectangle R_i there exists a weak channel \tilde{K}_i such that

$$|\tilde{K}_i \cap \mathcal{A}| \leq \frac{\mathcal{A}}{\#(K_i)} \leq \frac{\rho^2(2/h + \delta)}{4c(p)\rho\eta/2\varepsilon} = \frac{\rho\varepsilon}{2c(p)\eta} \left(\frac{2}{h} + \delta \right).$$

Therefore, considering the weak circuit K contained in $\bigcup_{i=1}^4 \tilde{K}_i$, we have that

$$\mathcal{H}^1 \left(\left((Q_\rho^\nu(x) \cap A_\varepsilon) \triangle Q_\omega^+ \right) \cap K \right) \leq \frac{2\rho\varepsilon}{c(p)\eta} \left(\frac{2}{h} + \delta \right). \quad (\text{A.16})$$

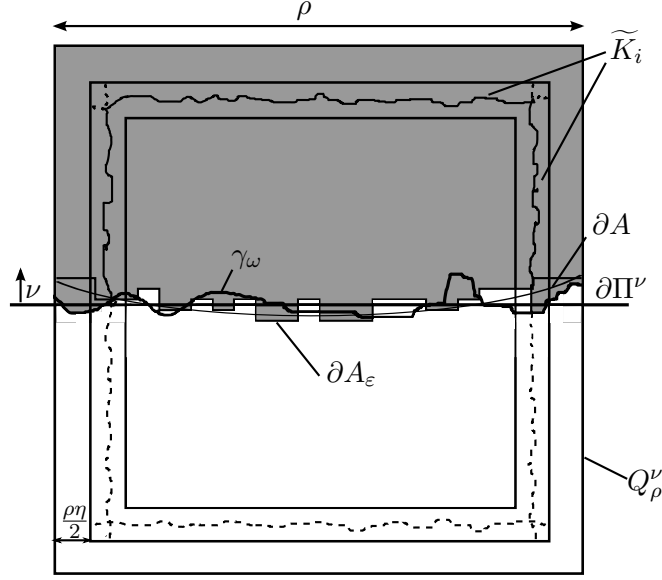


Figure A.2. Construction of a test set.

Step 4: Definition of the test sets. Now we define the subset $A_\varepsilon^1 \subset Q_\rho^\nu(x)$ as (see Fig. A.2)

$$A_\varepsilon^1 = \begin{cases} A_\varepsilon, & \text{in the set containing 0 and whose boundary is } K \\ Q_\omega^+, & \text{otherwise.} \end{cases} \quad (\text{A.17})$$

Note that

$$\mathcal{H}^1 \left((\partial A_\varepsilon^1 \setminus \partial A_\varepsilon) \cap Q_\rho^\nu(x) \right) \leq \frac{2\rho\varepsilon}{c(p)\eta} \left(\frac{2}{h} + \delta \right) + \tilde{c}(p)\rho\delta/2\varepsilon. \quad (\text{A.18})$$

We can find points $x_\varepsilon, y_\varepsilon \in \hat{\mathbb{Z}}^2$ such that $\varepsilon x_\varepsilon, \varepsilon y_\varepsilon \in \partial A_\varepsilon^1$ and $|\varepsilon x_\varepsilon + \frac{\rho}{2}e_1| \leq 2\varepsilon, |\varepsilon y_\varepsilon - \frac{\rho}{2}e_1| \leq 2\varepsilon$, and a weak path K^ε in $\frac{1}{\varepsilon}(\partial A_\varepsilon^1 \cap Q_\rho^\nu(x)) \cap \hat{\mathbb{Z}}^2$ connecting x_ε at y_ε . By the estimate (A.18) we have

$$\begin{aligned} \mu_\varepsilon(Q_\rho^\nu(x)) &\geq \varepsilon|K^\varepsilon| - \left(\frac{2\rho\varepsilon^2}{c(p)\eta} \left(\frac{2}{h} + \delta \right) + \tilde{c}(p)\rho\delta/2 \right) \\ &\geq \varepsilon D^\omega(x_\varepsilon, y_\varepsilon) - \left(\frac{2\rho\varepsilon^2}{c(p)\eta} \left(\frac{2}{h} + \delta \right) + \tilde{c}(p)\rho\delta/2 \right). \end{aligned}$$

Since $|(y_\varepsilon - x_\varepsilon) - \frac{\rho}{\varepsilon}e_1| \leq 4$, choosing $m = \rho/\varepsilon$ in the definition of λ_p (equation (A.10)) and for fixed η, δ and h we obtain

$$\liminf_{\varepsilon \rightarrow 0} \mu_\varepsilon(Q_\rho^\nu(x)) \geq \rho\lambda_p(e_1) - \tilde{c}(p)\rho\delta/2 = \rho\lambda_p(e_2) - \tilde{c}(p)\rho\delta/2 = \rho\lambda_p(\nu) - \tilde{c}(p)\rho\delta/2.$$

By the (iv) above we then have

$$\liminf_{\varepsilon \rightarrow 0} \mu_\varepsilon(Q_\rho^\nu(x)) \geq \int_{Q_\rho^\nu(x) \cap \partial^* A} \lambda_p(\nu(y)) d\mathcal{H}^1(y) - \left(\frac{\rho}{h} + \tilde{c}(p) \frac{\rho^2\delta}{2} \right)$$

and finally

$$\begin{aligned}
\liminf_{\varepsilon \rightarrow 0} \mu_\varepsilon(\Omega) &\geq \sum_j \liminf_{\varepsilon \rightarrow 0} \mu_\varepsilon(Q_{\rho_j}^{\nu_j}(x_j) \cap \partial^* A) \\
&\geq \sum_j \int_{Q_{\rho_j}^{\nu_j}(x_j) \cap \partial^* A} \lambda_p(\nu(y)) d\mathcal{H}^1(y) - C \left(\frac{\rho}{h} + \tilde{c}(p) \frac{\rho^2 \delta}{2} \right) \\
&= \int_{\Omega \cap \partial^* A} \lambda_p(\nu(y)) d\mathcal{H}^1(y) - C \left(\frac{\rho}{h} + \tilde{c}(p) \frac{\rho^2 \delta}{2} \right);
\end{aligned}$$

the lim inf inequality then follows by the arbitrariness of ρ, δ and h .

The construction of a recovery sequence giving the upper bound (limsup inequality) can be performed just for *polyhedral sets*, since they are dense in energy in the class of sets of finite perimeter. We only give the construction when the set is of the form $\Pi^\nu(x) \cap \Omega$ since it is easily generalized to each face of a polyhedral boundary. We can localize the construction to the faces of a polyhedral set because the limit energy does not concentrate at its corners: this follows by the chosen scaling. It is no restriction to suppose that $\Pi^\nu(x) = \Pi^\nu(0) =: \Pi^\nu$, that ν is a *rational direction* (that is, there exists a positive real number S such that $S\nu \in \mathbb{Z}^2$), and that

$$\mathcal{H}^1(\partial\Omega \cap \partial\Pi^\nu) = 0, \quad (\text{A.19})$$

since also with these restrictions we obtain a dense class of sets. We will compute the Γ -limsup for $u = 2\chi_{\Pi^\nu} - 1$.

Let $M > 0$ be large enough so that $\Omega \subset\subset Q_M^\nu(0)$, we set $\tau = \nu^\perp$ and we fix $\eta > 0$ such that $\eta < M/2$. There exists a path γ_ε in the weak cluster of the dual lattice $\hat{\mathbb{Z}}^2$ contained in the stripe $\{x : |\langle x, \nu \rangle| \leq \eta/\varepsilon\}$ and with the two endpoints lying at distance at most 2ε from the two sides $\{x : |\langle x, \tau \rangle| = \pm M/2\}$. The existence of γ_ε can be proved with the same construction performed for γ_ω in the proof of the Γ -lim inf inequality. After identifying γ_ε with a curve in \mathbb{R}^2 , for ε small enough it disconnects $\frac{1}{\varepsilon}\Omega$. We can therefore consider Ω_ε^+ , the maximal connected component $\frac{1}{\varepsilon}\Omega \setminus \gamma_\varepsilon$ containing $\Omega \cup \{x : \langle x, \nu \rangle \geq \eta/\varepsilon\}$, and define

$$u_\varepsilon^\eta(\varepsilon i) = \begin{cases} 1 & \text{if } i \in \mathbb{Z}^2 \cap \Omega_\varepsilon^+ \\ -1 & \text{otherwise.} \end{cases}$$

Note that

$$E_\varepsilon^\omega(u_\varepsilon^\eta) \leq \varepsilon |\gamma_\varepsilon| \leq \lambda_p(\tau) \mathcal{H}^1(\partial\Pi^\nu \cap \Omega) + O(\eta).$$

By a diagonal argument, for any fixed $\eta > 0$ we can construct a subsequence (still denoted by u_ε^η) converging in $L^1(\Omega)$ as $\varepsilon \rightarrow 0$ to u^η , where u^η is a function such that $\|u^\eta - u\|_{L^1(\Omega)} \rightarrow 0$ as $\eta \rightarrow 0$. We have

$$\limsup_{\varepsilon \rightarrow 0^+} E_\varepsilon^\omega(u_\varepsilon^\eta) \leq \lambda_p(\tau) \mathcal{H}^1(\partial\Pi^\nu \cap \Omega) + O(\eta), \quad \forall \eta > 0,$$

and letting $\eta \rightarrow 0$ we obtain

$$\Gamma\text{-}\limsup_{\varepsilon \rightarrow 0^+} E_\varepsilon^\omega(u) \leq \lambda_p(\tau) \mathcal{H}^1(\partial\Pi^\nu \cap \Omega) = \lambda_p(\nu) \mathcal{H}^1(\partial\Pi^\nu \cap \Omega).$$

Eventually, we obtain the desired inequality recalling that $\mathcal{H}^1(\partial\Pi^\nu\cap\bar{\Omega}) = \mathcal{H}^1(\partial\Pi^\nu\cap\Omega)$ by (A.19).

(b) It will suffice to show that $E'(u) := \Gamma\text{-}\liminf_{\varepsilon \rightarrow 0} E_\varepsilon^\omega(u) = +\infty$ if $u \neq -1$ or $u \neq 1$ identically. We reason by contradiction and assume that there exists a non-constant function $u \in BV(\Omega; \{\pm 1\})$ such that $E'(u) < +\infty$. Fixed a point $x \in S(u)$ and a square $Q_\rho^\nu(x)$ of side-length $\rho > 0$ sufficiently large, by channel property (see Theorem A.3.2 and subsequent remarks) almost surely there exists (at least) a strong channel connecting two opposite sides of the square. Therefore, if u_ε is a sequence converging to u , there must be at least one pair i, j of nearest neighbors in the strong cluster such that $(u_\varepsilon)_i \neq (u_\varepsilon)_j$ so that $E_\varepsilon^\omega(u_\varepsilon) = +\infty$. This implies that $E'(u) = +\infty$. □

A.5 A continuity result

The number $\lambda_p(\nu)$ defined by equation (A.10) describes the average distance on the weak cluster in the direction ν (and, by Remark A.3.8, also in the orthogonal direction). Its value cannot be decreased by using ‘small portions’ of strong connections, as expressed by the following result.

Lemma A.5.1. *Let $\eta > 0$ be fixed. Then there are $\delta \in (0, 1)$ and $\rho > 0$ such that almost surely there exists N_0 such that for all $N \geq N_0$ and all channels of length L connecting the two shorter sides of NT_ν^δ and with $L < (\lambda_p(\nu) - \eta)N$ we have $\#(\text{strong links}) \geq \rho(\eta)N$.*

The proof of this technical Lemma is contained in Braides and Piatnitski [16] and it is used to prove that, in the subcritical case, the overall behavior of a discrete membrane with randomly distributed defects is characterized by a fracture type energy, and the surface interaction is described by the asymptotical chemical distance λ_p .

We would like to exploit Lemma A.5.1 to prove that an elliptic random spin system with coefficients 1 and $\beta > 0$, in the limit as β goes to $+\infty$ (i.e. for β very large), has the same behavior of a rigid system (that is, with $\beta = +\infty$). More precisely, if $\varphi_p(\beta, \nu)$ is the surface tension coming from the elliptic problem, then

$$\lim_{\beta \rightarrow +\infty} \varphi_p(\beta, \nu) = \lambda_p(\nu) = \varphi_p(+\infty, \nu).$$

The expression $\lambda_p(\nu) = \varphi_p(+\infty, \nu)$ means that λ_p is the surface tension computed for $\beta = +\infty$. Such a continuity result seems to be interesting, because in general it does not hold outside this random setting, as shown by the following simple example.

Example A.5.2. Consider the energies

$$F_\varepsilon^\beta(u) = \sum_{ij} \varepsilon c_{ij}^\beta (u_i - u_j)^2, \tag{A.20}$$

where

$$c_{ij}^\beta = \begin{cases} \beta & \text{if } i_1 = j_1 = 0 \\ 1 & \text{otherwise.} \end{cases} \quad (\text{A.21})$$

It is well known from the theory of homogenization of elliptic spin systems that there exists the Γ -limit

$$\Gamma\text{-}\lim_{\varepsilon \rightarrow 0} F_\varepsilon^\beta(u) = F^\beta(u) = \int_{\Omega \cap \partial^* \{u=1\}} \varphi_\beta(\nu) d\mathcal{H}^1 = \int_{\Omega \cap \partial^* \{u=1\}} \|\nu\|_1 d\mathcal{H}^1; \quad (\text{A.22})$$

note that the sequences $\{c_{ij}^\beta\}$ and $\{\varphi_\beta\}$ (and consequently $\{F^\beta\}$) are (trivially) increasing in β and we can put $c_{ij}^\infty = \sup_{\beta > 0} c_{ij}^\beta$, $\tilde{\varphi} = \sup_{\beta > 0} \varphi_\beta$ and

$$\tilde{F}(u) = \sup_{\beta > 0} F^\beta(u) = \int_{\Omega \cap \partial^* \{u=1\}} \tilde{\varphi}(\nu) d\mathcal{H}^1 = \int_{\Omega \cap \partial^* \{u=1\}} \|\nu\|_1 d\mathcal{H}^1.$$

Now if we consider the energies

$$F_\varepsilon^\infty(u) = \sum_{ij} \varepsilon c_{ij}^\infty (u_i - u_j)^2, \quad (\text{A.23})$$

where

$$c_{ij}^\infty = \begin{cases} +\infty & \text{if } i_1 = j_1 = 0 \\ 1 & \text{otherwise.} \end{cases} \quad (\text{A.24})$$

(with the usual convention $+\infty \cdot 0 = 0$) then we have that

$$F^\infty(u) = \Gamma\text{-}\lim_{\varepsilon \rightarrow 0} F_\varepsilon^\infty(u) = \int_{\Omega \cap \partial^* \{u=1\} \cap \{x_1 > 0\}} \|\nu\|_1 d\mathcal{H}^1 + \int_{\Omega \cap \partial^* \{u=1\} \cap \{x_1 < 0\}} \|\nu\|_1 d\mathcal{H}^1.$$

Therefore, $\tilde{F}(u) \neq F^\infty(u)$.

We recall the main results about homogenization of random spin systems (see Braides and Piatnitski [17]). Given a probability space $(\Sigma, \mathcal{F}, \mathbf{P})$, we consider an ergodic stationary discrete random process $\sigma_{\hat{z}}^\omega, \hat{z} \in \hat{\mathbb{Z}}^2$.

We are going to compute the Γ -limit of the energies

$$E_\varepsilon^\omega(u) := \sum_{ij} \varepsilon \sigma_{ij}^\omega (u_i - u_j)^2$$

(with the usual identification $\sigma_{ij}^\omega = \sigma_{\hat{z}}^\omega$). For any $x, y \in \mathbb{Z}^2$ and $\omega \in \Sigma$ we define

$$\psi^\omega(x, y) = \min \left\{ \sum_{n=1}^K \sigma_{i_n i_{n-1}}^\omega : i_0 = x, i_K = y, K \in \mathbb{N} \right\}, \quad (\text{A.25})$$

where the minimum is taken over all paths joining x and y . The following statement holds (we can compare it with Lemma A.3.5).

Proposition A.5.3. *For any $\tau \in \mathbb{R}^2$ the following limit exists \mathbf{P} -almost surely and does not depend on ω*

$$\psi_0(\tau) = \lim_m \frac{1}{m} \psi^\omega(0, \lfloor m\tau \rfloor), \quad (\text{A.26})$$

where $\lfloor m\tau \rfloor_k = \lfloor m\tau_k \rfloor$ is the integer part of the k -th component of $m\tau$. For any $x \in \mathbb{R}^2$ and $\tau \in \mathbb{R}^2$ the limit relation

$$\lim_{m \rightarrow +\infty} \frac{1}{m} \psi^\omega(\lfloor mx \rfloor, \lfloor mx + m\tau \rfloor) = \psi_0(\tau) \quad (\text{A.27})$$

holds \mathbf{P} -almost surely.

At this point we can recall the main convergence theorem.

Theorem A.5.4 (elliptic random homogenization). *Let σ_{ij}^ω satisfy the hypothesis of ellipticity $0 < \alpha \leq \sigma_{ij}^\omega \leq \beta < +\infty$ for all i, j . Then the $\Gamma\text{-}\lim_{\varepsilon \rightarrow 0} E_\varepsilon^\omega$ exists \mathbf{P} -almost surely, is deterministic and is given by*

$$F^\omega(u) = \int_{\Omega \cap \partial^* \{u=1\}} \varphi_p(\nu) d\mathcal{H}^1. \quad (\text{A.28})$$

where

$$\varphi_p(\nu) = \psi_0(\nu^\perp). \quad (\text{A.29})$$

A particular case of the preceding random problem is obtained by considering the i.i.d. Bernoulli bond-percolation model with coefficients

$$\sigma_z^\omega = \begin{cases} \beta > 0 & \text{with probability } p \\ 1 & \text{with probability } 1 - p. \end{cases} \quad (\text{A.30})$$

With this choice of coefficients we find that the function φ_p of Theorem A.5.4 now depends also on β , $\varphi_p = \varphi_{p,\beta}$. We will prove that the case of rigid spin is the limit as $\beta \rightarrow +\infty$ of the problem defined by coefficients (A.30), in the sense expressed by the following theorem.

Theorem A.5.5 (continuity). *Let $\varphi_{p,\beta}$ be defined by Theorem A.5.4 when the coefficients σ_z^ω are given by (A.30), and λ_p be defined by Proposition A.3.7. Then, for all $\nu \in \mathbb{R}^2$, we have two cases:*

(i) *If $p < 1/2$, then $\lim_{\beta \rightarrow +\infty} \varphi_{p,\beta}(\nu) = \lambda_p(\nu)$;*

(ii) *If $p > 1/2$, then $\lim_{\beta \rightarrow +\infty} \varphi_{p,\beta}(\nu) = +\infty$.*

Proof. (i) Let $p < 1/2$. First remark that, with fixed $\nu \in \mathbb{R}^2$ and for all $\beta > 0$, we have

$$\varphi_{p,\beta}(\nu) \leq \lambda_p(\nu),$$

because the minimum in the definition of λ_p (see equation (A.3.5)) is taken in a smaller set of paths.

Therefore, λ_p being independent of β ,

$$\lim_{\beta \rightarrow +\infty} \varphi_{p,\beta}(\nu) \leq \lambda_p(\nu).$$

Now suppose that there exists $\eta > 0$ such that $\lim_{\beta \rightarrow +\infty} \varphi_{p,\beta}(\nu) \leq \lambda_p(\nu) - \eta$; we would like to show that this assumption leads to a contradiction.

First of all, $\varphi_{p,\beta}$ being increasing in β , we have that

$$\varphi_{p,\beta}(\nu) \leq \lambda_p(\nu) - \eta, \quad \forall \beta > 0. \quad (\text{A.31})$$

With fixed β , by (A.27) there exists $\bar{n} \in \mathbb{N}$ almost surely such that, for all $n \geq \bar{n}$

$$\psi^\omega([nx], [nx + n\tau]) \leq (\lambda_p(\nu) - \eta')n, \quad (\text{A.32})$$

where $\tau = \nu^\perp$, η' is a constant and $x \in \mathbb{R}^2$. Suppose that $\psi^\omega([nx], [nx + n\tau]) = \sum_{m=1}^K \tilde{\sigma}_{i_m i_{m-1}}^\omega$ with $i_0 = [nx]$, $i_K = [nx + n\tau]$ and let γ be the corresponding path.

By means of Lemma A.5.1, we can find $\delta \in (0, 1)$, a constant $C = C(\eta') > 0$ such that if $n' \geq n$ is such that the channel γ connects the shorter sides of $n'T_\nu^\delta$, then from the fact that

$$|\gamma| \leq \sum_{m=1}^K \tilde{\sigma}_{i_m i_{m-1}}^\omega \leq (\lambda_p(\nu) - \eta')n', \quad (\text{A.33})$$

it follows that

$$\#(\text{strong links in } \gamma) \geq Cn'. \quad (\text{A.34})$$

Now

$$\beta Cn' \leq \sum_{m=0}^K \tilde{\sigma}_{i_m i_{m-1}}^\omega \leq (\lambda_p(\nu) - \eta')n', \quad (\text{A.35})$$

and letting $\beta \rightarrow +\infty$ we obtain a contradiction.

(ii) If $p > 1/2$, we can reason as in Theorem A.4.2(b), because the percentage of β is fixed by channel property. In particular, for large m , the paths linking $[mx]$ and $[mx + m\tau]$ in equations (A.25), (A.26) and (A.27) contain at least a β -bond. \square

Bibliography

- [1] R. Alicandro, A. Braides and M. Cicalese, Phase and anti-phase boundaries in binary discrete systems: a variational viewpoint. *Netw. Heterog. Media* **1** (2006), 85–107.
- [2] F. Almgren and J. E. Taylor, Flat flow is motion by crystalline curvature for curves with crystalline energies. *J. Diff. Geom.* **42** 1 (1995), 1–22.
- [3] F. Almgren, J. E. Taylor and L. Wang, Curvature driven flows: a variational approach. *SIAM J. Control Optim.* **50** (1993), 387–438.
- [4] L. Ambrosio, Minimizing movements. *Rend. Accad. Naz. Sci. XL Mem. Mat. Appl.* **19** (5)(1995), 191–246.
- [5] L. Ambrosio and A. Braides, Functionals defined on partitions of sets of finite perimeter, II: semicontinuity, relaxation and homogenization, *J. Math. Pures. Appl.* **69** (1990), 307–333.
- [6] L. Ambrosio, N. Fusco and D. Pallara, *Functions of Bounded Variation and Free Discontinuity Problems*, Oxford University Press, Oxford (2000).
- [7] L. Ambrosio, N. Gigli and G. Savaré, Gradient flows in metric spaces and in the space of probability measures, *Lectures in Mathematics ETH Zürich*. Birkhäuser, Basel, 2005.
- [8] K. Bhattacharya and B. Craciun, Effective motion of a curvature-sensitive interface through a heterogeneous medium. *Interfaces Free Bound.* **6** (2004), 151–173.
- [9] A. Braides, *Approximation of Free-Discontinuity Problems*, Lecture Notes in Mathematics **1694**, Springer Verlag, Berlin, 1998.
- [10] A. Braides. *Γ -convergence for Beginners*. Oxford University Press, Oxford, 2002.
- [11] A. Braides, *Local Minimization, Variational Evolution and Γ -convergence*. Lecture Notes in Mathematics **2094**, Springer Verlag, Berlin, 2013.
- [12] A. Braides, A. Causin and M. Solci. Interfacial energies on quasicrystals. *IMA J. Appl. Math.* (2012) **77**, 816–836.
- [13] A. Braides and A. Defranceschi, *Homogenization of Multiple Integrals*. Oxford University Press, Oxford, 1998.

- [14] A. Braides, M.S. Gelli and M. Novaga, Motion and pinning of discrete interfaces. *Arch. Ration. Mech. Anal.* **95** (2010), 469–498.
- [15] A. Braides, M. Maslennikov, L. Sigalotti, Homogenization by blow-up. *Applicable Analysis* **87** (2008), 1341–1356.
- [16] A. Braides and A. Piatnitski, Overall properties of a discrete membrane with randomly distributed defects. *Arch. Ration. Mech. Anal.* **189** (2008), 301–323.
- [17] A. Braides and A. Piatnitski, Homogenization of surface and length energies for spin systems. *J. Funct. Anal.*, **264** (2013), 1296–1328.
- [18] A. Braides and A. Piatnitski. Variational problems with percolation: dilute spin systems at zero temperature *J. Stat. Phys.* **149** (2012), 846–864
- [19] A. Braides and G. Scilla. Motion of discrete interfaces in periodic media, *Interfaces Free Bound.* **15** (2013), 451–476.
- [20] A. Braides and G. Scilla. Nucleation and backward motion of anisotropic discrete interfaces, In preparation.
- [21] A. Braides and G. Scilla. Nucleation and backward motion of discrete interfaces, *C. R. Acad. Sci. Paris* **351** (2013), 803–806.
- [22] A. Braides and M. Solci. Interfacial energies on Penrose lattices. *M3AS* **21** (2011), 1193–1210
- [23] G. A. Chechkin, A.L. Piatnitski, and A. S. Shamaev, *Homogenization. Methods and applications*. Translations of Mathematical Monographs 234. American Mathematical Society, Providence, RI, 2007.
- [24] C. Conca, J. San Martín, L. Smaranda and M. Vanninathan, On Burnett coefficients in periodic media in low contrast regime. *J. Math. Phys.* **49** (2008).
- [25] G. Dal Maso, *An Introduction to Γ -convergence*, Birkhäuser, Boston, 1993.
- [26] E. De Giorgi, New problems on minimizing movements. In *E. De Giorgi. Selected Papers*. Springer, Berlin, 2006.
- [27] N. Dirr and N. K. Yip, Pinning and de-pinning phenomena in front propagation in heterogeneous media. *Interfaces Free Bound.* **8** (2006), 79–109.
- [28] G. Francfort and J.-J. Marigo. Stable damage evolution in a brittle continuous medium. *Eur. J. Mech. A/Solids*, **12** (1993), 149–189.
- [29] O. Garet and R. Marchand, Asymptotic shape for the chemical distance and first-passage percolation on the infinite Bernoulli cluster. *ESAIM Probab. Statist.* **8** (2004), 169–199.
- [30] O. Garet and R. Marchand, Large deviations for the chemical distance in supercritical Bernoulli percolation. *Annals of probability* **35** (2007), 833–866.

- [31] K. B. Glasner, Homogenization of contact line dynamics. *Interfaces Free Bound.* **8** (2006), 523–542.
- [32] A. A. Griffith, The phenomenon of rupture and flow in solids. *Phil. Trans. R. Soc. Lond A* **221** (1920), 163–198.
- [33] G. Grimmett. *Percolation*. Springer, Berlin, 1999.
- [34] G. Grimmett and H. Kesten, First-passage percolation, network flows and electrical resistances. *Z. Wahrsch. Verw. Geb.* **66** (1984), 335–366.
- [35] H. Kesten, *Aspects of first-passage percolation*. École d’été de probabilités de Saint-Fleur, XIV-1984, Lecture notes in Math., vol. 180 (Ed. Hennequin P. L.) Springer, Heidelberg, 1986, pp. 125–262.
- [36] H. Kesten, *First-passage percolation. From classical to modern probability*, 93–143, Progr. Probab., **54**, Birkhäuser, Basel, 2003.
- [37] H. Kesten, *Percolation Theory for Mathematicians*. Progress in Probability and Statistics, 2. Birkhäuser, Boston, 1982.
- [38] K. Kuratowski, *Topology, Vol. 1*. Academic Press, New York (1966).
- [39] P. L. Lions and P. E. Souganidis, Homogenization of degenerate second-order PDE in periodic and almost-periodic environments and applications. *Ann. Inst. H. Poincaré Anal. Non Linéaire* **22** (2005), 667–677.
- [40] A. P. Morse, Perfect blankets, *Trans. Amer. Math. Soc.* **6** (1947), 418–442.
- [41] E. Presutti, *Scaling Limits in Statistical Mechanics and Microstructures in Continuum Mechanics*. Springer-Verlag, Berlin, 2009.
- [42] R. T. Rockafellar, *Convex Analysis*, Princeton University Press, 1970.
- [43] R. Schneider, *Convex bodies: The Brunn-Minkowski Theory*, Cambridge University Press (1993).
- [44] G. Scilla, Motion of discrete interfaces in ‘low-contrast’ periodic media, Preprint 2013. <http://cvgmt.sns.it/paper/2170/>
- [45] G. Scilla, Variational problems with percolation: rigid spin systems, *Adv. Math. Sci. Appl.* **23** 1 (2013), 187–207.
- [46] M. Solci, Double-porosity homogenization for perimeter functionals. *Math. Methods Appl. Sci.* **32** (2009), 1971–2002.
- [47] J.E. Taylor. Motion of curves by crystalline curvature, including triple junctions and boundary points, *Differential Geometry, Proceedings of Symposia in Pure Math.* **51** (part 1) (1993), 417–438.